UNIVERSIDAD DE ANTIOQUIA

METHODOLOGY FOR SIZING HYBRID POWER GENERATION SYSTEMS (SOLAR-DIESEL), BATTERY BACKED IN NON INTERCONNECTED ZONES USING PSO

Autor(es)

Oswaldo Antonio Arráez Cancelliere

Universidad de Antioquia

Facultad de Ingeniería, Departamento de Ingeniería Eléctrica

Medellín, Colombia

2019

METHODOLOGY FOR SIZING HYBRID POWER GENERATION SYSTEMS (SOLAR-DIESEL), BATTERY BACKED IN NON INTERCONNECTED ZONES USING PSO

Oswaldo Antonio Arráez Cancelliere

Trabajo de grado como requisito para optar al título de:
Maestría en Ingeniería – Énfasis Energética.

Director(a)

Nicolas Muñoz Galeano y PhD. Ingeniería Electrónica.

Universidad de Antioquia
Facultad de Ingeniería, Departamento de Ingeniería Eléctrica
Medellín, Colombia
2019

UNIVERSIDAD DE ANTIOQUIA

ABSTRACT

Faculty of Engineering
Department of Electrical Engineering

Master of Engineering

METHODOLOGY FOR SIZING HYBRID POWER GENERATION SYSTEMS (SOLAR-DIESEL), BATTERY BACKED IN NON INTERCONNECTED ZONES USING PSO

By: Oswaldo Antonio Arráez Cancelliere

Nowadays the access to electrical energy has become fundamental for the development of any region. Nonetheless, in developing countries there still many communities without a proper access to this service. There are plenty of reasons that make difficult the electrification of rural areas, however Hybrid Renewable Energy (HRE) systems have become an attractive option to solve these problems and provide with energy rural areas. Among HRE systems, the Solar-Diesel is often employed because the abundance of the solar resource. Battery banks are used due to the low reliability of photovoltaic energy system makes necessary the storage of energy. In this work, only HRE system based on solar-diesel with batteries are considered.

Due to the stochastic nature of the variable associated to an HRE system and the lack of information and technical knowledge on off-grid areas, the design process of these systems could be difficult. For this reason, it is developed a methodology that helps the sizing process of these systems to obtain the most reliable and economic solution. In this work, a sizing methodology including a PSO algorithm is developed based minimizing the levelized cost of energy and including, on the objective function, the annual cost of energy not supplied. Also, the sub-model for estimation of the solar resource and the load demand on the location are described and developed. A dispatch strategy that prioritize the use of renewable energy is explained and applied on the simulation of the HRE system. Three study cases are analyzed and discussed. Lastly, comparison with the software HOMER is performed and discussed.

It is expected that this work assists the sizing and design process of HRE systems for off-grid locations minimizing the cost of energy and maximizing the reliability of these systems.

Key words

Hybrid energy Systems, Stand Alone system, Off-grid areas, PSO, Photovoltaic energy, rural electrification, Power Dispatch strategy, HOMER.

ACKNOWLEDGEMENTS

Ante todo, quiero agradecer a mis padres, he contado con su apoyo incondicional en todas las etapas de mi vida, en gran parte gracias a ellos soy lo que soy y son de ellos cada uno de mis logros.

Agradezco a mi Diana por su amor y palabras de aliento cuando fueron necesarias. Siempre tuvo la disposición para mantenerme a flote en este proceso y prestar su ayuda cuando más fue necesaria. Gracias por otro logro más juntos, uno de muchos que espero alcanzar a tu lado.

Agradezco a mi familia, incluido mis suegros y en especial, a mi hermana Cinthya, que presto su ayuda activamente durante el desarrollo de este trabajo.

Agradezco sinceramente a mi tutor, profesor Nicolás Muñoz Galeano, por su paciencia, excelente disposición para sacar las cosas adelante, su apoyo, no solo durante el desarrollo de este trabajo de maestría, sino en toda mi permanecía en la Universidad de Antioquia, pero, sobre todo, agradezco su amistad.

Agradezco también a los compañeros del grupo GIMEL al profesor Fernando Villada, a Walter, a Jesús por su excelente disposición para conversar temas asociados a este trabajo.

Quiero agradecer a todo el equipo de la empresa Gaia Tecnología e Innovación S.A.S, por el tiempo, la paciencia y el apoyo durante del desarrollo de este trabajo.

Quiero agradecer a la Profesora Eva Monagas, gran parte de mis conocimientos en metodología de investigación se lo debo a sus enseñanzas, incluso en la distancia se que puedo contar con su apoyo.

Finalmente, quiero mostrar mi gratitud con la Universidad de Antioquia por el apoyo económico otorgado a través del estímulo Estudiante Instructor me permitió cursar mis estudios de Maestría.

NOMENCLATURE

Symbol	Description	Units
ϕ	Latitude degrees north reference in decimal format	-
δ	Declination angle	[°]
d_n	Day number counted from the beginning of the year	-
ω	Solar hour angle	[°]
T_{solar}	Solar Time	h
T_{local}	Local clock	h
L_{st}	Standard meridian for the local time zone	h
L_{loc}	Longitude of the location East positive	
ΔT_{gmt}	Local time zone	h
EoT	Stands for Equation of Time	
$\boldsymbol{\theta_{zs}}$	Solar zenith	$^\circ\, degrees$
$\boldsymbol{\gamma_s}$	Solar altitude	$^\circ\, degrees$
ω_s	Sunrise angle	$^\circ\, degrees$
T_d	Length of the day	h
$\boldsymbol{\psi_s}$	Solar azimuth	$^\circ\, degrees$
$\boldsymbol{\theta_i}$	Angle of incidence	$^\circ\, degrees$
β	Tilt of the inclined plane [0-90°]	$^\circ\, degrees$
α	Surface azimuth angle [0S 90W]	$^\circ\, degrees$
$\boldsymbol{B_0}$	Solar constant	W/m^2
$\boldsymbol{B_0(0)}$	Extraterrestrial irradiance over the horizontal surface	Wh/m^2
$B_{0d}(0)$	Extraterrestrial irradiance over the day	Wh/m^2
$B_{0dm}(0)$	Average daily extraterrestrial irradiation in a month	Wh/m^2
$\boldsymbol{K_{Tm}}$	Clearness Index	
$G_{dm}(0)$	Average daily horizontal global irradiation of a month	Wh/m^2
$\boldsymbol{K_d}$	Diffuse Fraction index	
$G(0)$	Hourly global horizontal irradiation	Wh/m^2
$D(0)$	Diffuse horizontal irradiation	Wh/m^2
$B(0)$	Direct horizontal irradiation	Wh/m^2
$G(\beta,\alpha)$	Global irradiance on the plane of the array	Wh/m^2
$B(\beta,\alpha)$	Direct irradiance on the plane of the array	Wh/m^2
$D(\beta,\alpha)$	Diffuse irradiance on the plane of the array	Wh/m^2
$AL(\beta,\alpha)$	Albedo irradiance on the plane of the array	Wh/m^2
r_B	Beam transposition factor	-
r_D	Diffuse transposition factor	-
r_{AL}	Albedo transposition factor	-
ρ	Ground reflection factor	-
k_{hay}	Anisotropy index	-
i	Description of the electrical appliance	-
N_i	Number of electrical appliances	-
P_i	Nominal power of each electrical appliance	W
h_i	Daily overall time each appliance is in use	h/day
w_i	Period during the day when each appliance can be used	-
$E_i(h)$	Energy demanded on hour	kWh
$E_{L,d}(h)$	Daily energy demanded	kWh/day
$\alpha_{unc,i}$	Uncertainty Factor	%
j	User class	-
N_j	Number of user class	-
N_{ij}	Number of electrical appliances for user class	-
P_{ij}	Nominal power of each electrical appliance and each user class	W
w_{ij}	Period during the day when each appliance can be used for each user class	-
$E_{AV,day}$	Average energy demanded in a day	kWh/day
α_{power}	Percentage of daily demand	%
P_{pv}	Power generated by PV system per hour	kWh
$T_{amb,m}$	Monthly average ambient temperature	$°C$
T_{cell}	Temperature of the cell	$°C$
f_{pv}	De-rating factor of the solar module	
N_{pv}	Number of PV module	
$P_{pv_{stc}}$	Rated power of the solar module in Standard Test Conditions	Wp
α_p	Temperature coefficient of maximum power	$\%/°C$
G_{stc}	Global irradiance in Standard Test Condition	W/m^2
T_{stc}	Temperature of the cell Standard Test Condition	$°C$
$NOCT$	Nominal operation cell temperature	$°C$
$E_{bat,max\_d}(t)$	Maximum amount of energy that the battery bank can be discharged in one-time step	kWh
$E_{bat,max\_c}(t)$	Maximum amount of energy that the battery can be charged in one-time step	kWh
E_{max}	Maximum flow of energy to charge or discharge the battery bank	kWh
$SOC(t)$	State of charge of the battery bank at time step t	kWh
SOC_{min}	Minimum state of charge of the battery	kWh
SOC_{max}	Maximum state of charge of the battery	kWh
$E_{bat,n}$	Nominal capacity of the battery bank at a given capacity rate	kWh

Symbol	Description	Units
DOD_{max}	Maximum deep of discharge of the battery bank	%
C_{rate}	Capacity rate	-
σ	Self-discharge coefficient	-
η_{bat_c}	Charge efficiency of the battery	-
η_{bat_d}	Discharge efficiency of the battery	-
$E_{bat}(t)$	Energy that the battery bank provides or is charged at time-step t	kWh
N_{b_s}	Number of batteries in series	
N_{b_p}	Number of batteries in parallel	
$E_{bcell,nom}$	Nominal capacity of one battery cell	kWh
$V_{dc_{sist}}$	DC voltage system	V
$V_{dc_{bc}}$	Nominal voltage of each battery cell	-
N_{br}	Total number of batteries	-
FC_{DG}	Fuel consumption of the diesel generator	l
f_0	Fuel Curve intercept coefficient	l/kW
f_1	Fuel curve slope coefficient	l/kW
P_{DG}	Output power of the diesel generator	kW
w_{DG}	Rated power of the diesel generator	kW
$N_{DG,max}$	Maximum number of DG units	-
$N_{on}(t)$	Minimum number of DG units of nominal power	-
$P_L(t)$	Load energy demanded in one time-step.	kWh
δ_{min}	Minimum load ratio	%
ENS	Energy not supplied	kWh
PFT	Power failure time	h
$\Delta_L(t)$	Deficit of power to supply the load	kWh
η_{INV}	Inverter efficiency	-
$EW(t)$	Energy wasted	kWh
$P_{pv}(t)$	Photovoltaic energy generated in one time-step.	kWh
ACS	Annualized Cost of the system	USD
COE	Cost of Energy	USD/kWh
$O\&M_i$	Annualized Operation and maintenance costs	USD
CC_i	Capital cost of each component	USD
RC_i	Annualized replacement cost of each component	USD
CRF	Capital Recovery Factor	-
N_c	Number of components	-
i_r	Real interest rate	%
R	Life time of the project	$years$
i_n	Nominal interest rate	%
i_f	Annual inflation rate	%
c_i	Cost per unit installed for each component	USD/kW
γ_i	De-rate factors of the initial capital cost invested	-
$K_i(i_r, L_i, y_i)$	Single payment present worth	-
L_i	Useful life time of the component	$years$
y	Number of replacements of the component during the project`s life time.	-
ρ_i	Percentage of annual operation and maintenance cost for each component	%
f_c	Fuel cost	USD/l
$LPSP$	Loss of power supply probability	%
C_{loss}	Cost of electricity not supply	USD/kWh
AC_{loss}	Annualized cost of energy not supplied	USD
t	Effective corporate tax income rate	%
$T1$	Maximum number of years to apply the investment tax credit	$years$
$T2$	Useful life of the power generating facility	$years$
d	Depreciation factor	-
Δ	Tax reduction factor	
s_i	Current position of particles	-
v_i	Velocity of particles	-
R_i	Uniformly distributed random numbers in the ranges (0,1)	-
N_{pv_l}	Lower bound number of PV module	-
w_{DG_l}	Lower bound nominal power of Diesel	kW
$N_{b_{p_l}}$	Lower bound number of Battery cell in parallel	-
E_{bcell,nom_l}	Lower bound nominal capacities of battery cell kWh	kWh
N_{pv_u}	Upper bound number of PV modules	
w_{DG_u}	Upper bound nominal power of Diesel unit in kW	kW
$N_{b_{p_u}}$	Upper bound number of Battery cell in parallel	-
E_{bcell,nom_u}	Upper bound nominal capacity of battery cell kWh	kWh
$Iter_{max}$	Maximum number of iterations	-
$nPop$	Population Size	-
w	Inertia Coefficient	-
w_{max}	Inertia Coefficient max	-
w_{min}	Inertia Coefficient min	-
c_1	Personal Acceleration Coefficient	-
c_2	Social Acceleration Coefficient	-

TABLE OF CONTENTS

TABLE OF FIGURES

LIST OF TABLES

CHAPTER I

PROBLEM STATEMENT

1.1. PROBLEM STATEMENT

Due to the technological and industrial worldwide progress, the growing industry and society need of power generation for development and increment of life quality; it is of unquestionable importance to increase sustainable access to electrical energy. In developing countries, there are still many locations without power supply. For example, Colombia in 2012, it had a coverage rate of electricity service of 96.1%, remaining 470,244 houses without electricity access [1]. The lowest level of demand coverage is on the south-east area of the country, in Amazonas and Vichada department with percentage under 60%. Other departments as Choco, Cauca and Guajira have an 80.9% 86.82% and 77.83% respectively. Particularly, Guajira has an elevated level of solar resource.

The national government seeks to resolve this situation; being reflected in Article 17 of the National Development Plan 2014-2018 which indicates that special conditions will be set to increase coverage [2]. Also in the same plan, the Government allocates resources for “Green growth”, which means a sustainable growth to allow the reduction of carbon emissions [2]. This shows the importance of developing off-grid solutions for sustainable and friendly environmental power generation systems, which lead to improvement in life quality and production processes in these areas.

According to the Indicative Expansion Electricity Coverage Plan (PIEC – Plan Indicativo de Expansión de Cobertura) 2013-2017 by Mining and Energy Planning Unit (UPME – Unidad de Planeación Minero Energética) the 15.74% of house without access to the interconnected system of electricity generation in Colombia is preferable isolated power generation. This is due to the

high costs of connecting these areas to the National Interconnected System (SIN – Sistema Interconectado Nacional) [1]. Until a few years ago, power generation in these areas had been achieved mainly by the implementation of fossil generators, raising the continuing necessity to purchase fuels such diesel [3]. However, this situation has been changing due to the development of other alternative technologies t not conventional energy sources (Fuentes No Convencionales de Energía - FNCE). These technologies have matured and overcome a number of implementation barriers (regulatory, economic, technical and technological) [4] that today allow them to stand as a cost-efficient option with a minimal environmental impact against these thermal groups.

Power generation through fossil generators offers a continuous and reliable source of energy making it a very popular option for electrification in Non-Interconnected Zones (ZNI - Zonas No Interconectadas). This alternative presents an initial investment cost relatively low compared to other sources of power generation. However, fossil power generators are sized to meet peak demand and have a mediocre performance when the load is quite below to its rated capacity. Additionally, operating and maintenance costs are high; the cost of energy is subject to changes according the national and international fuel markets. In addition, logistical challenges associated with fuel supply in remote areas can cause a significant increase in generation costs [5]. A solution for these disadvantages is the implementation of hybrid generation systems which includes fossil and other energy source. For warm and high average daily radiation levels [6], as Colombia´s case, photovoltaic solar energy with battery backup represents an attractive complementary source to diesel generation systems. This solution allows the reduction of generation costs and increased system reliability[7], [8].

Hybrid systems have shown lower generation costs and greater reliability than dependent systems of a single source of energy [5], [7]–[11]. Each element of the system has to be properly sized to achieve a techno-economic profitability. Therefore, the penetration of renewable energy sources in the energy market depends mainly on the applied sizing methodology to optimize its design [12].

The optimization of these systems could be complex, since many variables are naturally stochastic and linked to the selected location. Examples of these variables are temperature, solar resource and load profile of the location [13]. Moreover, the optimization technique to be used will depend on the selected objective function, which can be oriented in seeking financial gain, increase system reliability and reduce the environmental impact [14].

Then, it is necessary to develop a methodology for optimization design of hybrid systems that allow the integration of photovoltaic and diesel generation systems, with or without energy storage, allowing reducing energy costs and maintaining a high reliability in energy supply in off-grid areas. The methodology to develop will required to obtain a set of input information linked to the project site, as meteorological and load profile data, and technical and economic information of the main equipment of the hybrid system. Then, an optimization process is necessary to determinate the most convenient kind of hybrid system (Diesel Only, PV with energy storage, Diesel-PV-with energy storage or Diesel-PV without energy storage) and the best combination of Diesel Power, PV power and battery bank capacity. The economic and reliability parameters that support the solution obtain is expected to be presented with the solution.

1.2. OBJECTIVES

1.2.1. MAIN OBJECTIVE

To develop a methodology for sizing hybrid power generation systems (solar-diesel), battery-backed in non-interconnected zones, which minimizes the total cost of the solution and maximize the reliability of supply using PSO.

1.2.2. SECONDARY OBJECTIVES

1. To gather information on solar resource available in Colombia, costs of system elements (solar, diesel and batteries), average installation costs and energy demand in ZNI.
2. To develop energy production models of diesel and photovoltaic systems, taking into account a system of power storage through a battery bank.
3. To build a model that allows assessment of implementation, operation and maintenance and energy not supplied costs of the system, considering the individual costs of each technology.
4. To develop a PSO model for sizing hybrid power generation systems (solar-diesel) with batteries in off-grid areas.
5. To validate the proposed methodology comparing the results obtained with those yielded by other computational design tools for hybrid power generation systems.

1.3. IMPACT AND PRODUCTS

In developing countries, rural electrification in areas with limited or no access to grid connection is one of the most challenging issues for governments. These areas are partially integrated with the electrical grid. This poor electricity distribution is mainly due to geographical inaccessibility, rugged terrains, lack of electrical infrastructure, and high required economic investment for installing large grid connected power lines over long distances to provide electricity for regions with a low population [5]. On the other hand, rapid depletion of fossil fuel resources on a global scale and progressive increase in energy demand and fuel price are other motives to reduce the reliance on fossil fuels. Hybrid Renewable Energy System can be a suitable option for such remote areas.

The methodology, to develop in this research, will assist the sizing and design process of an HRE system for an off-grid area minimizing the cost of energy and maximizing the reliability of the system. The economic incentives offer by the government to encourage the use of not conventional renewable energy sources are considered in the model. Then, the contribution of this research could be appreciated in the following areas:

- **Social:** In the development of non-interconnected areas through electrification using hybrid energy system with photovoltaic energy and diesel.
- **Environmental:** In those areas where, according to this methodology, there is an economic benefit in the use of photovoltaic system, by reducing the carbon emission of diesel plant. An estimate of the carbon emission reduction will be calculated based on the amount of energy produced by photovoltaic system in contrast with the fossil source.
- **Economic:** Allowing to minimize the cost of energy in off-grid areas from the design process.
- **Academic:** Contributing with the group GIMEL in Universidad de Antioquia, in its line “Rational use of Energy”. Specifically, on the analysis of energetic scenarios replacing non-renewable energy sources for renewable energy sources.

CHAPTER II

STATE OF ART

This section presents the results of the bibliographic review carried out on hybrid renewable energy systems and the state of art on the sizing methodologies and optimization techniques used on the design of these systems.

2.1. STATE OF ART

In literature, several reviews about hybrid renewable energy system and optimization techniques used for their design can be found. In (Siddaiah & Saini, 2016) [15], the authors made a review about different mathematical models proposed to optimize the design of hybrid renewable energy systems in function of economic and reliability aspects. First, the review presents the different models used to simulate Hybrid Renewable Energy (HRE), systems with and without Diesel Generators (DGs). Then, modeling and optimization techniques are summarized forming three groups: (1) Classical/conventional techniques, (2) Artificial Intelligent Techniques and (3) Hybrid techniques. The classical techniques are analytical in nature and use differential calculus to optimize the energy model. The artificial intelligent techniques use heuristic based optimization algorithm to address the sizing problem in a HRE. Examples of these techniques are: knowledge based system; Genetic Algorithm (GA); Particle Swarm Optimization (PSO); Evolutionary Particle Swarm Optimization (EPSO), Ant Colony Optimization, among others. These techniques are the most applied in optimization problems in HRE systems. Hybrid techniques combine two or more optimization techniques to reach the solution.

Another review in (Luna-Rubio et al, 2012) [12] divides the sizing methodologies according to the optimization technique used. Methodologies are divided in four groups: (1) Probabilistic, (2) Analytical, (3) Iterative, and (4) Hybrid. Probabilistic Methods optimize one or two system performance indicators in order to size the components of the system, it is highly dependent of the data input used. In Analytical Methods, the HRE system is represented by computational models and the best configuration of the system is determined in function of one or more performance index indicators. This method does not offer an accurate solution in multi-objective problems. Iterative Methods use a recursive algorithm to reach the best configuration of the system according to the design specifications, being useful for multi-objective optimization. Hybrid methodologies combine two or more methodologies improving the convergence time in the optimization process. In the author's opinion, the iterative and hybrid methodologies are the best suited to solve a multi-objective sizing problem in a hybrid microgrid.

Also in (Prakash & Khatod, 2016) [16], a review optimization techniques for distributed generation systems is presented. Five optimization techniques are classified in five groups: (1) Analytical Techniques (2) Classical Optimization Techniques (3) Artificial Intelligent (Meta-heuristic) Techniques (4) Miscellaneous Techniques (5) Other Techniques for Future Use. This review also presents different methodologies according the objective function. This author concludes that analytical and classical methods are not computational efficient for large and complex systems. In contrast, meta-heuristic and hybrid methods reach a solution in a more efficiently way, including also conditions of uncertainties in the load profile and the meteorological data commonly found in off-grid areas.

In this research, the review of the sizing methodologies for HRE systems in off-grid areas will be divided in two groups: (1) according to the objective function and, (2) according to the optimization method used.

2.1.1 ACCORDING TO OBJECTIVE FUNCTION

In (Mandelli et al, 2016) [17], it is proposed a sizing methodology for off-grid PV System in developing countries where traditional sources of energy (ex. Batteries, small diesel generators) are already in use. The methodology introduces the concept of Levelized Cost of Supplied and Lost Energy (LCoSLE) which, in contrast of the traditional Levelized Cost of Energy, includes the Value of Loss of Energy related costs in the equation. The objective in this methodology is to minimize the

LCoSLE. In this way, it is possible to optimize economically the sizing of the main component of the Photovoltaic system in a rural zone using an input data the load profile of the target location. In the author's opinion, this methodology is more appropriated for sizing in rural areas of developing countries than traditional approaches that use as target the reliability of the system. Also, in this work is presented the concept of Value of Lost of Load (VLL). A similar concept is employed on the reliability model used in this work.

In (Haghighat et al, 2016) [18], the author analyze seven configurations using wind, solar and diesel as source of energy for three communities in Colombia. The software tool HOMER is used to perform a techno-economic feasibility of the proposed hybrid systems, taking into account Net Present Cost (NPC), Initial Capital Cost (ICC), and the Levelized Cost of Energy (LCOE) as economic indicators. Three locations are analyzed proving Solar-Diesel combination as preferred due to the environmental and economically benefits in the long run. Nevertheless, if the capital cost would be considered as the only criteria among the proposed configuration, the diesel based system would be selected as optimal. This methodology is limited by the restrictions imposed by the software HOMER. Also, the result may vary if the reliability of the system is considered on the model. On addition, recent fiscal incentives granted by the Colombian government for not conventional energy source systems are not considered by the author.

2.1.2 ACCORDING TO OPTIMIZATION METHOD USED

In (Ashok, S., 2007) [19], the author seeks for the optimal solution for electrification in rural areas using a hybrid system. Several renewable energy sources such as wind energy, solar photovoltaic, micro-hydro, also with diesel generator as backup, are considered. The solution yields optimal combination with unit sizing of each component in the system to minimizing the Annual Operating Cost (AOC). The combination with lowest cost, minimal use of diesel generators and service reliability is selected as optimal. The optimization model is solved by a Quasi-Newton algorithm, which is a numerical iterative algorithm with nonlinear constrains. This kind of algorithm could require a large amount of memory and could thus be disadvantageous in the cases of large complicated systems.

In 2015 (Maleki et al, 2015)[20], the authors compare the performance of seven evolutionary algorithms for optimum sizing of a PV/ WT/battery hybrid system to continuously satisfy the load demand with the minimal Total Annual Cost (TAC). The evaluated algorithms were: (1) Particle

Swarm Optimization (PSO), Tabu Search (TS) and Simulated Annealing (SA), Improved Particle Swarm Optimization (IPSO), Improved Harmony Search (IHS), Improved Harmony Search-based Simulated Annealing (IHSBSA), and Artificial Bee Swarm Optimization (ABSO). The experimental data used in the comparison is from South of Iran, and Matlab software is used to code and execute the heuristic algorithms. As result, the author finds that ABSO yields better results than other algorithms in terms of TAC. Also, it is concluded that PV/Wind/Battery systems are the most cost-effective to supply 100% of the demand. If a Loss of Power Supply Probability (LPSP) of 5% is considered, the PV/Battery systems are the most-effective system.

In (Shadmand et al, 2014) [21], the authors show a sizing methodology using a Multi-Objective Genetic Algorithm (MOGA) to guarantees a reliable energy supply, minimizing demand not met, with lowest investment, minimizing total annual cost (TAC). The model is evaluated with and without uncertainties on the demand and meteorological data on the model. These uncertainties are resolved using a Monte Carlo (MC) Technique. The analysis shows that these uncertainties affects significantly on the value of investment. The results are showed using a Pareto Front in which a tradeoff between reliability and investment can be observed. The development done it in [21] is similar to the objective of our research, nonetheless the economic model may vary in order to consider other variables as the government incentives and the optimization algorithm used to solve the problem could change with the intention of find more efficiently a solution for the problem.

A recent example of a hybrid optimization method is showed by (Maleki et al, 2016) [22]. A hybrid evolutionary method is used to determine the optimal number of modules, wind turbines and batteries for a specific region in Iran minimizing the Total Annual Cost (TAC) of the system. This methodology uses a Particle Swarm Optimization (PSO) algorithm combined with a Monte Carlo (MC) technique to reach the solution. This methodology proves to be useful in areas where the meteorological and demand data is scarce.

In the last decade, a numerous amount of optimization techniques has been used to obtain an optimal solution of the sizing problematic on HRE. The results among the different approaches may vary depending on the characteristics of the model employed to simulate the behavior of the different elements of the system and the economic and reliability model used as base on the optimization process. In Table 1, it is summarized the articles reviewed for this state of art.

The main objective of this work is to develop an optimization methodology for sizing HRE system in off-grid areas of developing countries. In contrast to other works, each step of the methodology, since a location is selected will be described in detail. Also, special condition will be considered on the development of the economic and reliable model to adjust it to the reality of Colombia, for example the National and international physical distribution cost or the incentive proposed for the law 1715 for electrification using non-conventional energy sources.

TABLE 1. REVIEW OF SIZING METHODOLOGIES IN HRE SYSTEMS.

#	Ref	Year	Optimization Technique	Parameter to Optimize	Criteria	Observations	Contribution
1	[17]	2016	Numerical Method – Matlab	LCoSLE	Economic Reliability	This methodology is only based on data coming from characterizing the local situation and hence also the results are more related to the targeted context.	The concept of VLL was useful for the definition of the reliability model employed on this work.
2	[18]	2016	HOMER	NPC ICC LCOE	Economic Environmental	Solar-Diesel combination is preferred due to the environmental and economically benefits in the long run in the three areas of Colombia analyzed. It is limited by the restrictions imposed by the software HOMER.	Reference cost for hybrid energy system in Colombia were useful for the definition of the problem. Also, the illustrated configuration of hybrid system on HOMER.
3	[19]	2007	Analytical - Quasi-Newton algorithm	AOC	Economic Reliability	This algorithm requires a large amount of memory thus is disadvantageous for large system.	The flowchart of the optimization process was useful to design the sub-model required on this work.
4	[20]	2015	PSO ABSO TS IHSBSA SA HIS IPSO	TAC	Economic Reliability	ABSO yields better results than other algorithms in terms of TAC.	This work presents a description of the PSO algorithm used to solve sizing hybrid energy system. This description was useful for the PSO model developed on this work. Also, allows to compare the complexity of different metaheuristic algorithms used on this line of work.
5	[21]	2014	MOGA MC	TAC DNM	Economic Reliability	Uncertainties affects significantly on the value of investment. The economic incentives provided by government are not considered.	Calculation availability and economic indicator was useful for the development of the economic and reliability sub-model used in this work. Also, remark the necessity of include uncertainties effects on future work.
6	[22]	2016	PSO MC	TAC	Economic	Useful in areas where the meteorological and demand data is scarce.	The description of the battery sub-model and the PSO sub-model was helpful on the developed of the sub-model used on this work.

CHAPTER III

METHODOLOGICAL FRAMEWORK

This section describes the sequence of steps to follow to accomplish the objectives of this research. The techniques to acquire the required data will also be described. For last, the techniques to analyze and describe the result will be presented.

3.1.- TYPE OF RESEARCH.

According (Hernandez, et al, 2006) [23], our research can be classified as a quantitative experimental research. These use a scientific method to find the relationships among a group of variables. In our case, we will find the relationship between the size of each source of energy on a hybrid energy system solar-diesel with batteries, which will be represented as the amount and capacity of solar modules, inverters, batteries and diesel plants, and the cost and reliability of the system. Other variables will be also considered such as the meteorological data on the site (average irradiation and temperature), the load profile, the temperature effect and the price trends of main elements of the hybrid system.

3.2 METHODOLOGICAL STEPS

This section seeks to describe in detail the phases required to achieve the objectives of this research.

Step 1: To gather information on solar resource and temperature, costs of system elements (solar, diesel and batteries), average installation costs and energy demand in ZNI.

1. Build a model to generate a long-year hour resolution array of global irradiance over an arbitrary inclined surface from the daily average monthly global horizontal irradiation and the geographical location.
2. Estimate the load profile of the selected locations. Three approaches are described to generate the long-year hour resolution electrical demand for a user or community. This information will be used on the model to develop.
3. Build a table with the price of each element on the Hybrid Renewable Energy System. Each element of the hybrid energy system based on Solar/diesel/battery will be described. Then, a table with the price of each element on the system will be presented. The information to construct this table will be collected from local distributors.
4. Estimate the installation and maintenance cost in an off-grid area. For this, renewable energies installations companies in Colombia will be consulted to obtain an average installation cost for hybrid renewable energy systems. This information will be presented in a table. The name of consulted companies will be remained anonymous for this research.

Step 2: To develop energy production models of diesel and photovoltaic systems, considering a system of power storage through a battery bank.

1. Describe the mathematical model of a photovoltaic system with battery backup. The equations and constrains related to the production of energy of solar panels and the storage capacity of the battery will be presented.
2. Describe the mathematical model of diesel plant. In the same way, the equations and constrains that describe the production of energy of a diesel plant will be described.
3. Describe the mathematical model of a Diesel/photovoltaic hybrid system without battery backup. The equations and constrains to be considered in this scenario will be described.
4. Describe the mathematical model of a diesel/photovoltaic hybrid system with battery backup. The equations and constrains to be considered in this scenario will be described.

5. Describe the energy dispatch strategies used on hybrid renewable energy systems.

Step 3: To build a model that allows assessment of implementation, operation, maintenance and energy not supplied costs of the system, considering the individual costs of each technology.

1. Describe the equations that describe the economic model of a photovoltaic system with battery backup for an off-grid area. These equations will be obtained in function of the data of the price of each element, installation and maintenance cost gather on step one. Among the indicator to be considered on the model will be the Levelized Cost of Energy (LCOE) and the Annualized cost of the system (ACS).
2. Describe the equations that describe the economic model of a Diesel generation system for an off-grid area. In this model must be considered the installation and maintenance cost and the replacement cost.
3. Describe the equations that describe the economic model of a hybrid renewable energy system based on photovoltaic/diesel with battery storage in an off-grid area. These equations will be obtained with the principle of superposition using the equations gotten from 1 and 2.
4. Describe the equation related to the reliability model associated to the concept to cost of energy not supplied.

Step 4: To develop a mathematical model of PSO algorithm for sizing hybrid power generation systems (solar-diesel) with batteries in off-grid areas.

1. Review different optimization techniques used in literature to solve similar problems.
2. Set the objective functions, parameters and constrains according the results on step 2 and 3 for a hybrid renewable energy system.
3. Develop an algorithm to find an optimal solution for the optimization problem. This algorithm will be presented in a block diagram.
4. Write the programming code and run the algorithm. The result must be the number of solar modules, batteries, diesel plants for each location, together with the economic and reliability indicators associated to the solution. This result will be presented in a table.
5. Analyze the results obtained. Present the results in a table and describe the results obtained for each location.

Step 5: To validate the proposed methodology comparing the results obtained with those yielded by other computational design tools for hybrid power generation systems.

1. Select computational design tools for hybrid power generation systems to run the problem.
2. Use the data gather in step 1 as input for the selected tool and run the analysis.
3. Describe and compare the results obtained. Both results will be presented in a table.

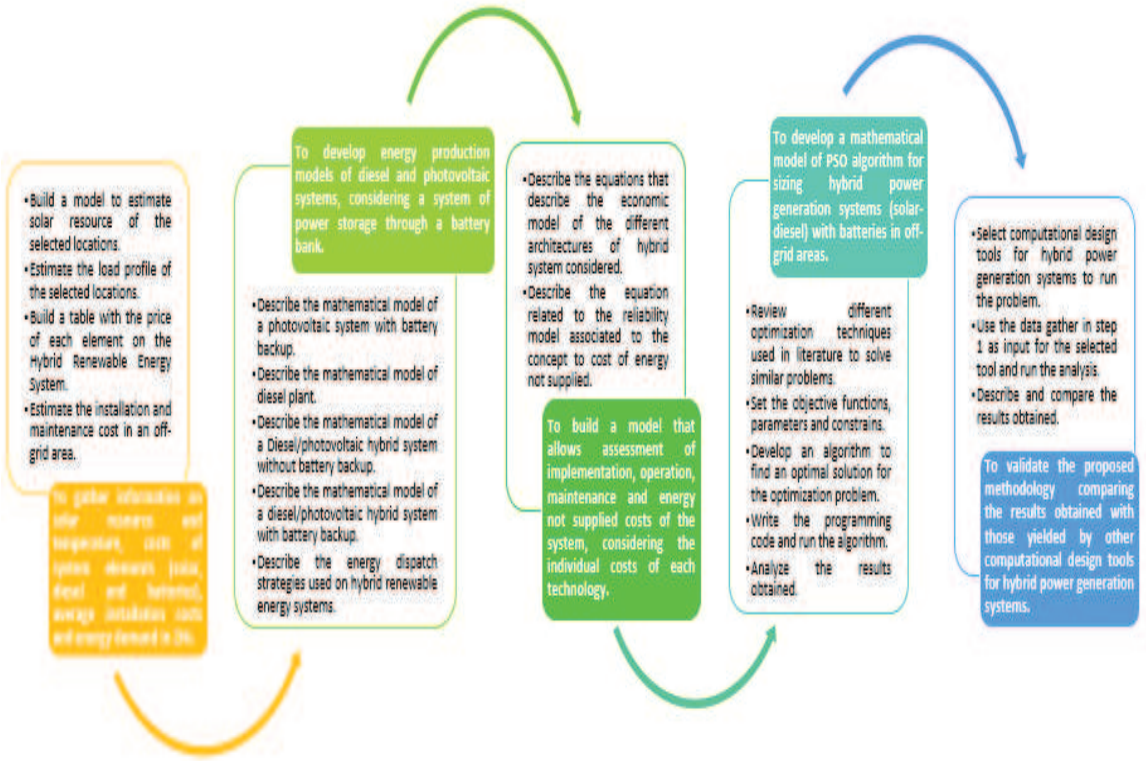

FIGURE 1. METHODOLOGICAL STEPS DIAGRAM

CHAPTER IV

ANALYSIS AND RESULTS

Firstly, it is presented a legal framework focused on topics of non-conventional energy sources and off-grid areas in Colombia. Secondly, technical and economic inputs of the model are described. Thirdly, an energy production model of elements of the system is presented. Then, economic and reliability parameters to analyze hybrid energy systems are discussed. Lastly, the PSO technique is generally described and then applied as optimization model for sizing methodology of HRE integrated by diesel and solar generation and battery storage.

4.1. LEGAL FRAMEWORK

Rapid increases in cumulative and generation PV-capacity can be explained in three ways: first, by the intrinsic benefits of PV technology; second, by the reduction of PV systems' production costs; and lastly, as policy is seeking alternative power generation technologies to face different issues as electrical coverage on off-grid areas, environmental problems, geopolitical instability and price volatility of fossil fuels [24]. Until comprehensive policy changes are implemented, renewable energies will never realize their full potential [25].

In this section, the most relevant laws and decrees which regulate and promote the use of renewable energies in Colombia are described. Also, it is highlighting the regulation regarding to the use of renewable energies in non-interconnected areas. Table 2 shows the legal framework for Colombia. This framework is made to contextualize the legal

situation of non-conventional energy sources and fiscal incentives granted by the government to support the development of these kind of solution in the country.

The most relevant law promoting the use of renewable energy is the law 1715. This law establishes incentives to promote the research, and implementation of non-conventional energy sources therefore represents a major effort to diversify the energy mix of the country integrating environmentally sustainable energy sources.

TABLE 2. COLOMBIAN LEGAL FRAMEWORK REGARDING RENEWABLE ENERGIES AND RURAL ELECTRIFICATION

DATE	TYPE	NUMBER	RELEVANCE
11/7/1994	Law	143	On Article 71, which promotes the substitution of fossil energy source for alternative energy systems in non-interconnected areas
3/10/2001	Law	697	Which promotes the rational and efficient use of renewable energy sources
24/12/2001	Resolution	180359	Which regulates the Financial Support Fund for the Energization of Non-Interconnected Zones (FAZNI - Fondo de Apoyo Financiero para la Energización de las Zonas no Interconectadas).
24/7/2007	Law	1151	Which issues the National Development Plan 2006-2010. Article 65-66, promotes the electrical coverage on off-grid areas using non-conventional energy sources.
26/10/2007	Resolution	CREG 091-2007	Which regulates the methodology to establish the generation, transmission and distribution costs on non-interconnected areas.
26/12/2007	Resolution	2138	Which issues the procedure to provide subsidies to the electrical sector on non-interconnected areas.
16/6/2011	Law	1450	Which issues the National Development Plan 2010-2014. Article 105 promotes the investigation, development and implementation of environmentally sustainable energy sources, as solar energy, to reduce the carbon footprint of the country.
23/1/2014	Resolution	CREG 004-2016	Which modifies the resolution CREG 091-22017 to establish the methodology to determinate the generation, transmission and distribution costs on non-interconnected areas.
7/3/2014	Resolution	CREG 027-2014	Which establishes guidelines to provide domiciliary electrical service on non-interconnected areas.
13/5/2014	Law	1715	Which regulates the integration of non-conventional energy sources to the national energy system. This law introduces the financial incentives to promote the use of renewable energies.
9/6/2015	Law	1753	Which issues the National Development Plan 2014-2018, promotes the electrical coverage on off-grid areas using non-conventional energy sources.
11/8/2015	Decree	1623	Which establishes policy guidelines for the expansion of coverage of the electric power service in the National Interconnected System and in Non-Interconnected Areas.
26/5/2017	Decree	884	Which regulates the implementation of a National Plan for Rural Electrification (PNER- Plan Nacional de Electrificación Rural) within the framework of the peace agreement and the end of the armed conflict and promotes the use of Non-conventional energy sources for the electrification of rural areas.

4.2. TECHNICAL INPUTS OF THE HRES

This section describes the inputs necessary to design Solar-Diesel-Battery systems on the context of this work.

4.2.1. IRRADIANCE DATA

The quality of solar resource data is critical for economic and technical assessment of solar power installation. Understanding uncertainty and managing weather-related risk is essential for successful planning and operating of solar electricity assets. High quality solar resource and meteorological data can be obtained by two approaches: high-accuracy instruments installed at a meteorological station, and complex solar meteorological models which are validated using high-quality ground instruments [26].

The input information available for PV designer is usually restricted to the 12 monthly mean values of global horizontal irradiation (GHI) and average temperature, which characterize solar climate of locations. However, to calculate the energy production of a photovoltaic system, it is necessary global irradiation over the plane of the PV array. The assessment of radiation arriving on an inclined surface, using as input global horizontal data, raises two main problems: to separate the GHI into their direct and diffuse components (decomposition); and, from them, to estimate the radiation components falling on an inclined surface (transposition) [27]. To solve these problems, it is important to describe the following parameters:

- **Declination angle (δ):** It is the angle between the equatorial plane and a straight line drawn between the center of the Earth and the Centre of the sun. It may be considered as approximately constant over the course of any one day. It can be calculated using Eq. 4.1 where d_n is the day number counted from the beginning of the year [28].

$$\delta = 23.45° \times sin\left[\frac{360\times(d_n+284)}{365}\right] \quad (4.1)$$

- **Solar hour angle (ω):** It is the difference between noon and the selected moment of the day in terms of a 360° rotation in 24h. $\omega = 0$ at the midday of each day and is counted as negative in the morning and positive in the afternoon. The solar hour angle is given as:

$$\omega = 15 * (T_{solar}(h) - 12) \quad (4.2)$$

$$T_{solar}(h) = T_{local}(h) + \frac{4(L_{st} - L_{loc}) + EoT}{60} \quad (4.3)$$

$$EoT\ (min) = 9.87 \sin 2B - 7.53 \cos B - 1.5 \sin B \quad (4.4)$$

$$B_n = \frac{360}{365}(d_n - 81) \quad (4.5)$$

$$L_{st} = 15 * \Delta T_{gmt} \quad (4.46)$$

Where T_{solar} and T_{local} are the solar time and the local clock time respectively; L_{st} and L_{loc} are the standard meridian for the local time zone and the longitude of the location (East positive, West Negative); ΔT_{gmt} is the local time zone (e.g. Bogotá ,-5); and EoT stands for Equation of Time which is the time difference between the apparent solar time for people and the real mean solar time and takes into account the perturbation of the earth's rotation [28].

- **Solar zenith (θ_{zs}) and solar altitude (γ_s):** Solar zenith is the angle between the vertical and the incident solar beam, it can also be described as the angle of incidence of beam radiation on a horizontal surface [27]. The complement of the zenith angle is called the solar altitude, γ_s. These angles can be calculated using Eq. 4.7 and are function of the declination angle (δ), the latitude (ϕ) (north positive, south negative), and the true solar time (ω).

$$\cos\theta_{zs} = \sin\delta \sin\phi + \cos\delta \cos\phi \cos\omega = \sin\gamma_s \quad (4.7)$$

$$\gamma_s = 90 - \theta_{zs} \quad (4.8)$$

Equation 4.7 can be used to find the sunrise angle (ω_s) since at sunrise $\gamma_s = 0$. Hence

$$\omega_s = -\cos^{-1}(-\tan\delta \tan\phi) \quad (4.9)$$

In accordance with the sign convention, ω_s is always negative. The sunset angle is equal to $-\omega_s$ and the length of the day is equal to:

$$T_d(hour) = \frac{2 * abs(\omega_s)}{15°} \quad (4.10)$$

- **Solar azimuth (ψ_s):** It is the angle between the meridians of the locations and the sun. it can also be described as the angular displacement from noon of the projection of beam radiation on the horizontal plane. The solar azimuth is given by:

$$\cos\psi_s = \left(\frac{\sin\gamma_s * \sin\phi - \sin\delta}{\cos\gamma_s \cos\phi}\right) \quad (4.11)$$

In the Northern Hemisphere, solar azimuth is referenced to true south not magnetic south and is defined as positive toward the west, that is, in the evening, and negative toward the east, that is, in the morning [27]. In Fig. 2: solar zenith, solar altitude and solar azimuth are described.

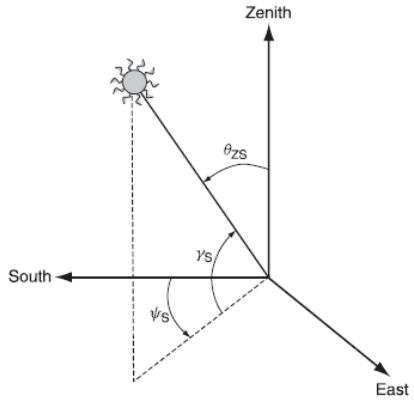

FIGURE 2 POSITION OF THE SUN RELATIVE TO A FIXED POINT ON THE EARTH DEFINING THE SOLAR AZIMUTH (ψ_s), THE SOLAR ZENITH (θ_{zs}) AND THE SOLAR ALTITUDE (γ_s).*[27]*

- **Angle of incidence (θ_i)**: Most practical applications require the position of the sun relative to an inclined plane to be determined. The angle of solar incidence between the sun's rays and the normal to the surface is given by

$$\cos(\theta_i) = \sin(\delta)\sin(\emptyset)\cos(\beta) - [sign(\emptyset)]\sin(\delta)\cos(\emptyset)\sin(\beta)\cos(\alpha) + \cos(\delta)\cos(\emptyset)\cos(\beta)\cos(\omega) + [sign(\emptyset)]\cos(\delta)\sin(\emptyset)\sin(\beta)\cos(\alpha)\cos(\omega) + \cos(\delta)\sin(\alpha)\sin(\omega)\sin(\beta) \quad (4.12)$$

Where, β is the tilt of the inclined plane (the angle formed with the horizontal) and α is the surface azimuth angle conventionally measured clockwise from the south (See Fig. 3) [29]. The $sign()$ function is 1 when the latitude is greater than 0 and is -1 otherwise.

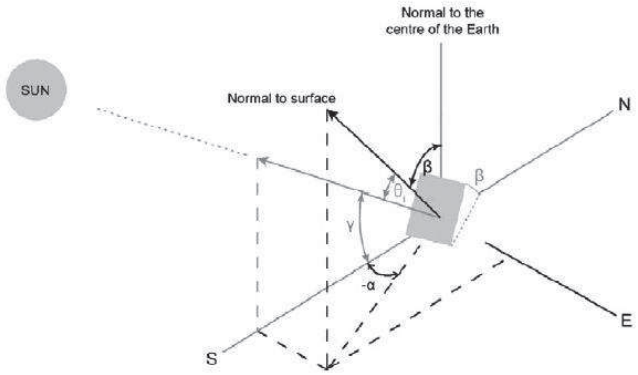

FIGURE 3. DEFINITION OF ANGLES USED AS COORDINATES FOR AN ELEMENT OF SKY RADIATION TO AN INCLINED PLANE OF TILT β AND ORIENTED TO α. *[29]*

- **Solar constant (B_0):** It is the amount of solar radiation received at the top of the atmosphere on a normal plane at the mean Earth-sun distance [27]. A good approximation of this value is

$$B_0 = 1367\ W/m^2 \tag{4.13}$$

- **Extraterrestrial irradiance over the horizontal surface ($B_0(0)$)**: Extraterrestrial radiation over a horizontal surface varies over the day and it is given by

$$B_0(0) = B_0 * \left[1 + 0.033 \cos\left(\frac{360}{365} d_n\right)\right] \cos\theta_{zs} \tag{4.14}$$

If Eq. 4.14 is integrated over the day is obtained

$$B_{0d}(0) = \frac{24}{\pi} B_0 * \left[1 + 0.033 \cos\left(\frac{360}{365} d_n\right)\right] \left[\cos\phi \cos\delta \sin\omega_s + \frac{\pi}{180}\ \omega_s \sin\phi \sin\delta\right] \tag{4.15}$$

Hence, average daily extraterrestrial irradiation in a month over a surface is obtained by

$$B_{0dm}(0) = \frac{1}{d_{n2} - d_{n1} + 1} \sum_{d_{n1}}^{d_{n2}} B_{0d}(0) \tag{4.16}$$

The value calculated in Eq. 4.16 is important to estimate the clearness index (K_{Tm}) [27].

- **Clearness Index (K_{Tm}):** It is the relation between the solar radiation at the Earth's surface and the extraterrestrial radiation over the horizontal plane. The clearness index K_{Tm} for each month is given by

$$K_{Tm} = \frac{G_{dm}(0)}{B_{0dm}(0)} \quad (4.17)$$

Where, $G_{dm}(0)$ is the average daily horizontal global irradiation of a month, which is usually an input value [27].

- **Diffuse Fraction index (K_d):** It is the relation between the diffuse radiation over the horizontal plane and the global radiation over the horizontal plane. This index is widely used on decomposition models to separate the global radiation into its direct and diffuse components.

$$K_{dm} = \frac{D_{dm}(0)}{G_{dm}(0)} \quad (4.18)$$

The modeling process for calculating the effective in-plane hourly irradiation when starting from monthly average of horizontal daily irradiation and using monthly average daily irradiance profiles is shown on Fig 4 [30].

The daily irradiance profile can be defined in terms of irradiance divided by daily irradiation and on assuming that the profile of the extraterrestrial horizontal solar radiation translates directly into the profile of the diffuse component, while an empirical correction is needed for global radiation [31]. The following equations describe the model to calculate the daily irradiance profile starting from daily average monthly values:

$$G(0) = r'_G \times G_{dm}(0) \quad (4.19)$$

$$D(0) = r'_D \times D_{dm}(0) \quad (4.20)$$

$$B(0) = G(0) - D(0) \quad (4.21)$$

With

$$r'_D = \frac{B_0(0)}{B_{0d}(0)} = \frac{\pi}{T} \times \left(\frac{\cos\omega - \cos\omega_s}{\frac{\pi}{180} \times \omega_s \times \cos\omega_s - \sin\omega_s} \right) \quad (4.22)$$

$$r'_G = r'_D \times (a + b \times \cos\omega) \quad (4.23)$$

$$a = 0.409 - 0.5016 \times \sin(\omega_s + 60) \quad (4.24)$$

$$b = 0.6609 + 0.4767 \times \sin(\omega_s + 60) \quad (4.25)$$

Where ω and ω_s are expressed in degrees and *T* is the day length usually expressed in hours (24 hours). The index r_D and r_G have units of T^{-1}, they can be used to calculate irradiation during short periods centered on the considered instant ω. Subscripts "*d*" and "*m*" mean the daily and monthly average of daily values respectively.

The diffuse component of the average daily irradiation, $D_{dm}(0)$, is derived from a decomposition model consisting of an empirical relationship between the clearness index, K_{Tm}, and the diffuse fraction, K_{dm}. In (R. Moreton et al, 2017) [30], the author reviews and compares four decomposition models for monthly average of horizontal daily irradiation: a linear relationship proposed by Page [32]; two polynomial equations defined by Collares [31] and Erbs [33] and a local correlation proposed by for Madrid by Macagnan [34]. The author stands out the Page decomposition model in combination with Perez transposition model [34] as a good performance combination used for passing from global horizontal irradiation to effective in-plane irradiance when is started from monthly average of daily irradiations values.

The decomposition model proposed by Page [32] consist of a liner equation that correlated the diffuse fraction index and the clearness index using data from then locations situated between 40°N and 40°S and is given by

$$K_{dm} = 1 - 1.13K_{Tm} \quad (4.26)$$

Once the global horizontal irradiance is separated into direct and diffuse components and the daily irradiance profile is obtained, it is necessary to calculate the effective irradiance on the plane of the array. The irradiance over the plane with a tilt β, in degrees, and oriented to angle α, conventionally measured clockwise from the south, can be obtained by

$$G(\beta, \alpha) = B(\beta, \alpha) + D(\beta, \alpha) + AL(\beta, \alpha) \quad (4.27)$$

Where symbols G, B, D, AL represent, respectively, global, direct, diffuse and albedo components. The irradiance components over the plane are given by

$$B(\beta,\alpha) = B(0) * r_B \quad (4.28)$$

$$D(\beta,\alpha) = D(0) * r_D \quad (4.29)$$

$$AL(\beta,\alpha) = G(0) * r_{AL} \quad (4.30)$$

The beam transposition factor is calculated straightforward from simple geometric considerations [35]:

$$r_B = \frac{\max(0,\cos\theta_i)}{\cos\boldsymbol{\theta_{zs}}} \quad (4.31)$$

Assuming isotropic albedo radiation, the corresponding transposition factor is given by

$$r_{AL} = \rho\frac{1-\cos\beta}{2} \quad (4.32)$$

Where, ρ is the ground reflection factor. The albedo radiation is scarcely relevant and rarely measured. A general reflection value of 0.2 is considered since this has been extendedly used on practice [35].

The diffuse transposition factor depends on the assumption made for the sky radiance distribution. In (R. Moreton et al, 2017) [30], 8 transposition models are reviewed, obtaining the best results using Perez model. Similar results are obtained in [36] where four transposition models are compared and validated with 2 year data measured at site and the most accurate results were obtained by Hay and Davies transposition model and Perez transposition model. In this work, Liu and Jordan isotropic sky model is used due its simplicity of implementation and good results reported [37].

On the transposition model proposed by Liu and Jordan, the diffuse radiation is given by an isotropic component coming from the entire celestial hemisphere. The diffuse transposition factor is given by

$$r_D = \frac{1+\cos\beta}{2} \quad (4.33)$$

In summary, the global irradiation over the tilted plane is calculated by

$$G(\beta,\alpha) = B(0) * r_B + D(0) * r_D + G(0) * r_{AL} \quad (4.34)$$

Figure 4 describes the process to generate the hourly irradiance on an arbitrary inclined surface.

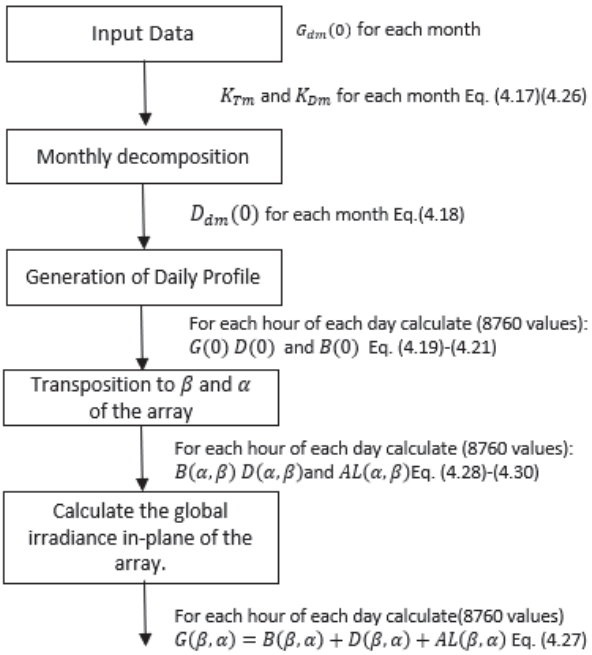

FIGURE 4.

DIAGRAM EXPLAINING THE CALCULATION OF THE DAILY IRRADIATION ON AN INCLINED SURFACE.

A MATLAB routine was developed to generate an hour resolution year array of the global irradiance over the plane from the twelve data points corresponding to the daily average global horizontal irradiation of the closest point to the location, the tilt angle of the surface β, the surface azimuth angle α, measured clockwise from the south, and the geographical coordinates of the location.

4.2.2. LOAD PROFILE ESTIMATION

Daily load profiles represent an essential input for off-grid systems capacity planning methods and lifetime techno-economic analysis. In rural areas of developing countries, it is complicated to obtain this profile by the well-known lack of information about users' electric consumptions. The approach to calculate the daily load profile depends on the scope of the design. For example, it is different to calculate a daily load profile to an off-grid system to provide energy to a single home than generate a daily load profile for an entire off-grid rural community. In this section, three approaches to calculate the daily load profile are presented.

The first approach is suited to small systems with one user or application. The second approach derives from the first and it is used to estimate the daily profile on a rural community. The last approach uses as input the load profile data of a similar rural community to estimate the daily load profile of a new community.

First approach: Daily load profile for a single user from a survey

For a single user, the daily load profile can be built from a simple survey including: description of the electrical appliance (i), the number of electrical appliance (N_i), nominal power of each electrical appliance (P_i), duration time in hours in which each appliance is "on" (h_i) and the window(s) of time in which the appliance is "on" during the day (w_i). Multiple operation windows can be defined during the day. Different daily profile can be generated for the same user according to seasonal change, working days weekend, etc. In Table 3, an example of an off-grid house user is presented as example. Figure 5 shows the daily load profile of the example in Table 3.

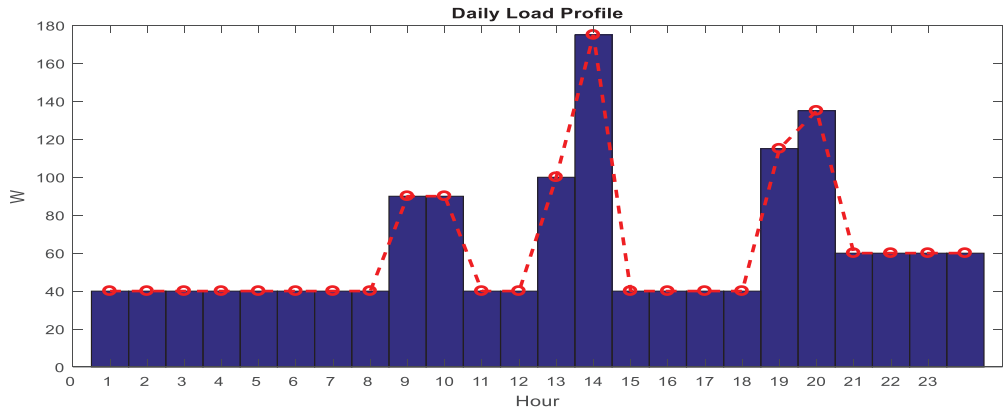

FIGURE 5. DAILY LOAD PROFILE DIAGRAM FOR EXAMPLE 1.

TABLE 3. EXAMPLE OF LOAD ON A RURAL HOUSE

Appliance (i)	N_i	Nominal Power (P_i) [W]	Daily use (h_i) [h/day]	$w_{i,1}$		$w_{i,2}$		$w_{i,3}$		Daily energy [Wh/day]
i	N_i	P_i	h_i	h_{start}	h_{stop}	h_{start}	h_{stop}	h_{start}	h_{stop}	E_L
Lamps	2	10	4	19	23	-	-	-	-	80
TV	1	75	3	13	14	18	20	-	-	225
Radio	1	50	2	8	10	-	-	-	-	100
Fan	1	60	2	12	14	-	-	-	-	120
+Fridge	1	40	24	0	23	-	-	-	-	960
Total daily energy [kWh/day]										1,485
Total monthly energy [kWh/month]										44,55

(Source: Own preparation)

The Excel file "Dailyprofile1" (included as attached file) can be used to survey the electrical load information of the user. The power demanded is calculated each hour of the year using this information. A routine to generate the hour-to-hour year-long array of energy demand is developed using MATLAB software. The demanded energy each hour is calculated by

$$E_L(h) = \sum_i^{appliance}(N_i * P_i * w_i(h)) \quad (4.35)$$

Where, $E_L(h)$ is the energy demanded on hour h as the power is assumed constant during that hour. N_i and P_i are the number and nominal power of the electrical appliance type i and $w_i(h)$ is a binary function which is one when the appliance type i is "on" and it is zero otherwise. The peak power is calculated when $E_L(h)$ is maximum during the day. The daily energy demanded is given by

$$E_{L,d}(h) = \sum_0^{23} E_L(h) \quad (4.36)$$

This approach represents a simple procedure that can be applied to formulate daily load profile for rural areas. Nevertheless, the daily load profile generated by this approach has a certain degree of uncertainties and relays on the veracity of the input data which tend to be inaccurate mainly in

setting the functioning windows. Another disadvantage of this approach is that realistically the daily load profile varies on size and shape from day to day.

To consider the uncertainties on the input data, a perturbation factor can be applied in each time-step calculation of the energy demand according to an uncertainty factor, $\alpha_{unc,i}$. This factor reflects the uncertainty of the information given in each appliance. Table 4 introduces the uncertainty factor on the input data survey.

TABLE 4. EXAMPLE OF LOAD ON A RURAL HOUSE WITH UNCERTAINTIES

Electrical Appliance	Qty	Nominal Power [W]	Daily use [h/day]	Functioning Windows 1 $w_{i,1}$		Functioning Windows 2 $w_{i,2}$		Functioning Windows 3 $w_{i,3}$		Uncertainty Factor [%]	Daily energy [Wh/day]
i	N_i	P_i	h_i	h_{start}	h_{stop}	h_{start}	h_{stop}	h_{start}	h_{stop}	α_{unc}	$E_{L,d,i}$
Lamps	2	10	4	19	23	-	-	-	-	20	80
TV	1	75	3	13	14	18	20	-	-	30	225
Radio	1	50	2	8	10	-	-	-	-	10	100
Fan	1	60	2	12	14	-	-	-	-	15	120
+Fridge	1	40	24	0	23	-	-	-	-	20	960

(Source: Own preparation)

The Eq. 4.35 is replaced by

$$E_L(h) = \sum_i^{appliance}(N_i * P_i * w_i(h) * (1 + normrnd(0, \alpha_{unc,i})) \qquad (4.37)$$

Where the function "normrnd" generates a random number from a normal distribution with a mean of zero and a standard deviation equal to the uncertainty factor. In this way, a more realistic daily profile is obtained for each day of the year. Figure 6 shows the daily load profile considering the uncertainties for a day and for a week of the year.

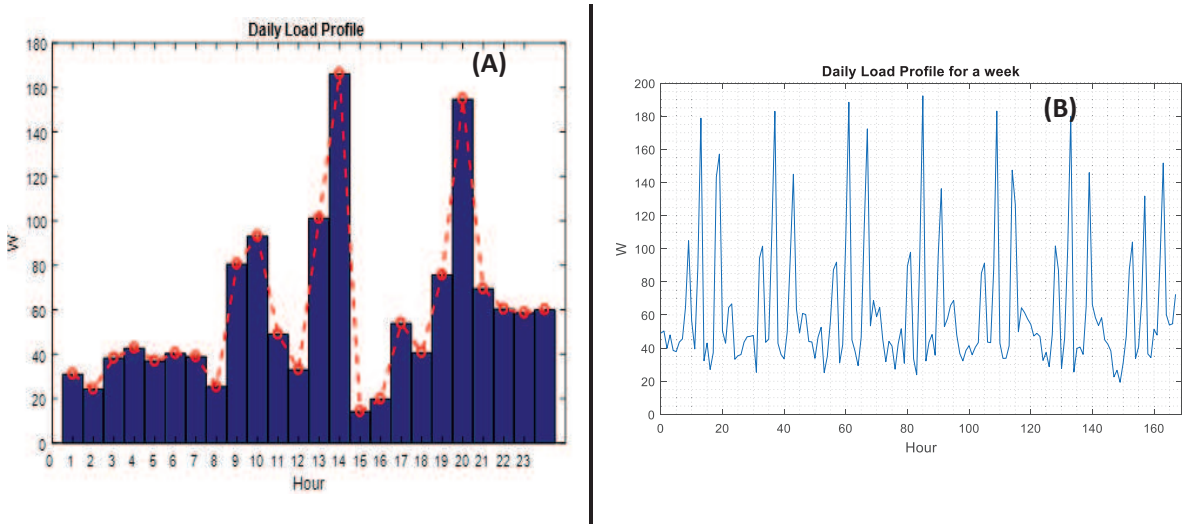

FIGURE 6.

(A) DAILY LOAD PROFILE DIAGRAM WITH UNCERTAINTIES (B) DAILY LOAD PROFILE FOR A WEEK.

A similar solution that considers the uncertainties on the generation of a daily load profile in rural areas is employed by (Mandelli et al, 2016) [38] in which two random parameters are introduced to vary the daily use and the functioning windows of each appliance. Also, in HOMER Energy software [39], a daily and time-step perturbation factors are used to add variability after the year-long array of load data is generated.

Second approach: Daily load profile for a community from a survey

The daily load profile for a community can be estimated in a similar way of a single user. The community is divided in groups of users (class) with similar electrical necessities and behaviors, for example: household 1, household 2, school, church. An electrical load survey is applied to each class to gather the same information necessary for a single user, considering the uncertainty factor $\alpha_{unc,ij}$. The subscripts "$_i$" and "$_j$" are used to denote the electrical appliance and user class respectively. As example, Table 5 shows the necessary information to build a daily load profile for a small community.

The Excel file "Dailyprofile2" (included as attached file) can be used to survey the electrical load information of each user. A routine to generate the hour-to-hour year-long array of energy demand is developed using MATLAB. Eq. 4.38 calculates energy demanded for each hour of the year.

$$E_L(h) = \sum_j^{user\ class} N_j * \left(\sum_i^{appliance} N_{ij} * P_{ij} * w_{ij}(h) * (1 + normrnd(0, \alpha_{unc,ij})\right) \quad (4.38)$$

TABLE 5.EXAMPLE OF LOAD RURAL COMMUNITY WITH UNCERTAINTIES

User class	Qty	Electrical Appliance	Qty	Nominal Power [W]	Daily use [h/day]	Functioning Windows 1 $w_{i,1}$		Functioning Windows 2 $w_{i,2}$		Functioning Windows 3 $w_{i,3}$		Uncertainty Factor [%]
j	N_j	i	N_i	P_i	h_i	h_{start}	h_{stop}	h_{start}	h_{stop}	h_{start}	h_{stop}	α_{unc}
Household _1	10	Lamps	2	10	4	19	23	-	-	-	-	20
		TV	1	75	3	13	14	18	20	-	-	30
		Radio	1	50	2	8	10	-	-	-	-	10
		Fan	1	60	2	12	14	-	-	-	-	15
		Fridge	1	40	24	0	24	-	-	-	-	20
Household _2	15	Lamps	2	10	4	6	8	17	20	-	-	15
		TV	1	75	3	18	20	-	-	-	-	30

		Fridge	1	40	24	0	24	-	-	-	-	0
School	3	Lamps	16	10	6	8	14	-	-	-	-	20
		Lamps	4	20	4	3	8	14	23	-	-	20
		TV	1	75	3	13	14	18	20	-	-	10
		PC	1	150	2	8	10	-	-	-	-	10
		Fridge	1	40	24	0	24	-	-	-	-	0

The Figure 7 shows the daily load profile graphic for the given example.

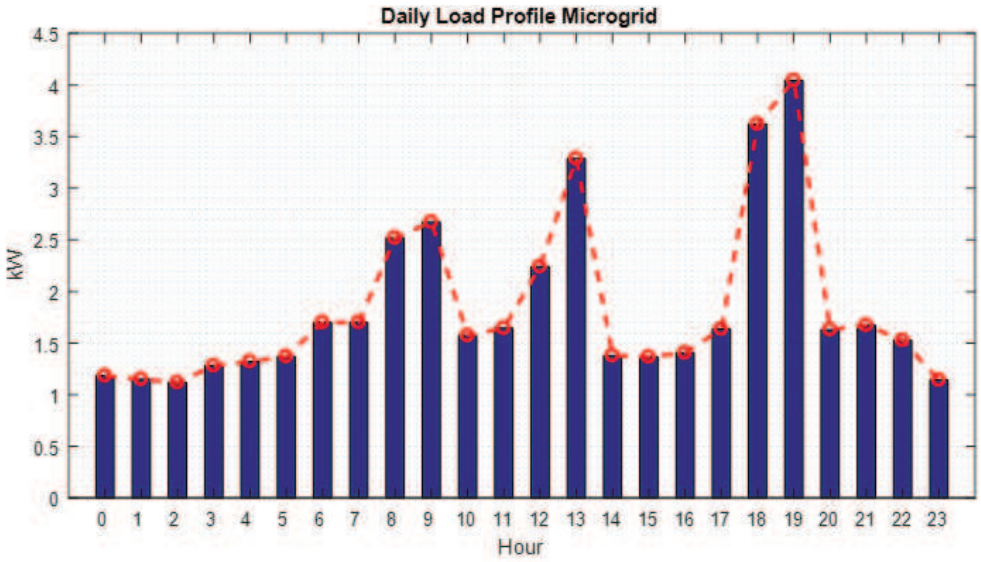

FIGURE 7. DAILY LOAD PROFILE FOR A COMMUNITY WITH UNCERTAINTIES

This approach tends to overestimate the peak of power due to it is assumed that the functioning windows of each appliance of the same group of users are on at the same time.

Third approach: Daily load profile for a community from measured electrical demand

The third approach is used when the electrical demand of the user or community is known. This case is common in communities where the electrical demand is already supplied; for example, with diesel generators, it is desired to evaluate the impact of change to a hybrid renewable energy system. The required power each hour is expressed in percentage of the yearly average daily energy demand. Table 6 shows, as example, the approximated average daily load profile of Vigia del Fuerte, a rural community in Colombia [40]. In this example, an uncertainty factor of 10% is assumed for each hour.

Like the first and second approach, it is introduced a random value to add day to day variability on the hour resolution year-long array generated. The random number is drawn from a normal distribution with a mean of zero and a standard deviation equal to the uncertainty factor α_{unc}. This method is used on HOMER Energy software in addition of a daily perturbation factor [39].

TABLE 6. DAILY LOAD PROFILE

Hour	Power [%]	Uncertainty factor [%]
h	α_{power}	α_{unc}
0	3.54	10
1	3.42	10
2	3.31	10
3	3.12	10
4	3.07	10
5	3.07	10
6	2.95	10
7	2.95	10
8	3.78	10
9	4.13	10
10	4.25	10
11	4.49	10
12	4.89	10
13	4.79	10
14	4.70	10
15	4.58	10
16	4.49	10
17	4.25	10
18	5.31	10
19	5.90	10
20	5.43	10
21	5.19	10
22	4.49	10
23	3.90	10
Yearly average daily energy demand [kWh], $E_{AV,day}$		3880

The demanded energy for each hour of the year is calculated using (Eq. 4.39). The power is assumed as constant for each time-step of an hour.

$$E_L(h) = E_{AV,day} * \frac{\alpha_{power}}{100}(1 + normrnd(0, \alpha_{unc,i}) \quad (4.39)$$

A MATLAB routine is developed to generate the hour resolution long-year electrical demand array. It is assumed that the same daily behavior for the entire year. Like the first and second approach, the same daily profile is used for each day of the year.

4.3. MATHEMATICAL ENERGY PRODUCTION MODELS

This section presents the equations to model the energy production of the photovoltaic array, the energy production of the diesel generator and the behavior of the state of charge (SOC) of the battery bank. Also, a power dispatch strategy is defined in order to set constrains on the sizing methodology developed. Figure 8 shows the schematic diagram of a hybrid solar/battery/diesel generation system.

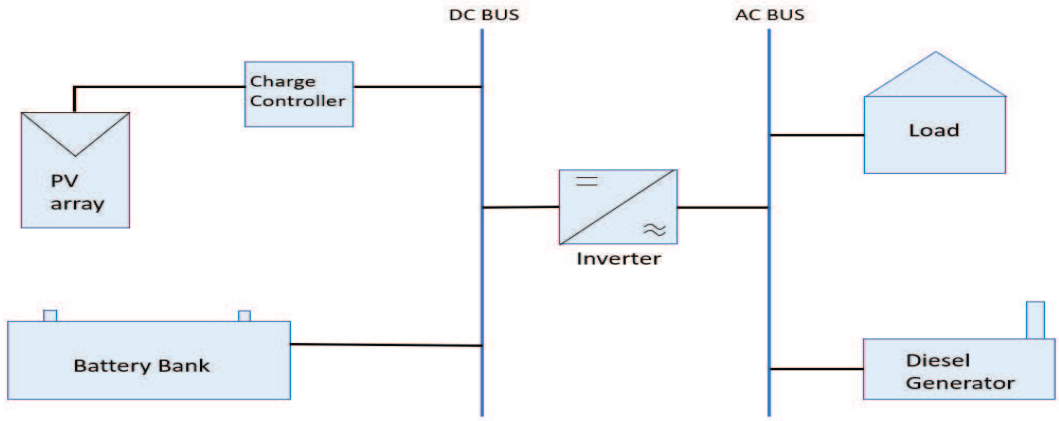

FIGURE 8. SCHEMATIC DIAGRAM OF A HYBRID SOLAR/BATTERY/DIESEL GENERATION SYSTEM

These systems can be divided in three groups depending on where the PV power is injected: DC-coupled and AC-coupled and hybrid coupled [41].

In DC coupled systems, PV power is injected to a DC bus through a charge controller. The main objective of the PV source is to maintain the battery bank charged. The capacity of the charge controller and the battery charge/inverter limit the PV generation. These systems have the advantage of being able to charge the battery bank even when the AC grid is not formed. In addition, the energy to charge the battery bank generated by the photovoltaic source is only affected by the efficiency of the charge controller. In the other hand, the rated capacity of the charge controller is lower of grid-tie PV inverters, making necessary more electronic power units. Also, the rated capacity of the battery charge/inverters limits the maximum PV energy that can be supplied to the load.

In contrast, AC coupled systems the PV energy is injected to the AC bus trough a grid-tie PV inverter. The main objective of the PV source is to supply the load, acting as a load reduction for the rest of the system. The surplus of PV produced energy is used to charge the battery through the battery charge/inverter. The grid-tie PV inverter are sized according to the peak power of the

PV systems and the battery charge/inverters are only sized according to the battery bank capacity. Charge controllers are not necessary. The grid-tie PV inverter required a grid formed to work, in case of power failure, the PV source cannot be used to charge the battery bank.

The hybrid coupled systems combines the two architectures. Photovoltaic energy is injected to the AC bus through grid-tie PV inverters to supply the load and to the DC bus through charge controllers to keep battery charged. These kinds of systems increase the versatility but also the complexity of the system making necessary an energy management system to control all the energy sources. Figure 9 shows the schematic diagram of each architecture.

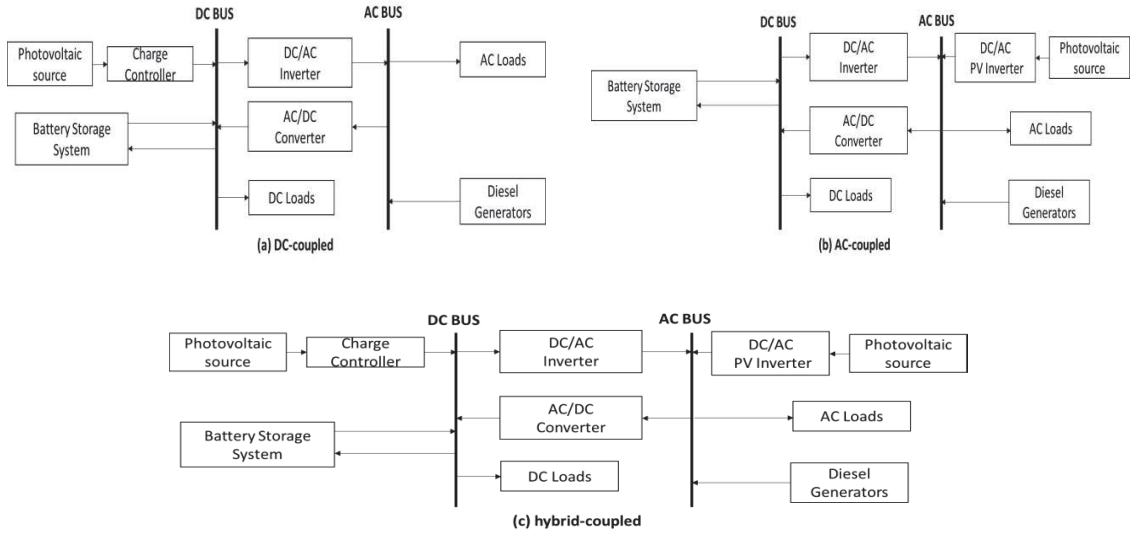

FIGURE 9. STAND-ALONE PV-DIESEL WITH BATTERY CONFIGURATIONS. (A) DC-COUPLED (B) AC COUPLED (C) HYBRID COUPLED.

PV-Battery system and PV-Battery-Diesel system are considered in this work as DC-coupled system and PV-diesel system is considered as AC-coupled system.

4.3.1. PHOTOVOLTAIC ARRAY MODEL

In literature, it can be found many analytical models to estimate the hourly generate power of a PV panel. Some models are complex taking account all the non-linearity's associated to the physical model of a PV module [42]. These models are suitable to evaluate the behavior of all the variables (voltage, current, power) of the system with precision. Other models are simple and only consider parameters that can be found on the module datasheet. In [43], the hourly generated power of the PV system (P_{pv}) is calculated considering the global solar irradiation on the plane of

the array ($G(\beta,\alpha)$) and the cell's temperature (T_{cell}) by Eq.4.40. A derating factor (f_{pv}) is used to account the losses due to dust, shading, wiring loss and mismatch and natural degradation of the solar module.

$$P_{pv}(t) = N_{pv} \times P_{pv_{stc}} \times \frac{G(\beta,\alpha)(t)}{G_{stc}} \times \left(1 + \frac{\alpha_p}{100} \times (T_{cell}(t) - T_{stc})\right) \times f_{pv} \quad (4.40)$$

Where N_{pv} is the number of PV module, P_{pv} is the generated power at the hour *h* of the year, $P_{pv_{stc}}$ is the rated power of the solar module in Standard Test Conditions ($G_{stc} = 1000\,W/m^2$; $T_{stc} = 25\,ºC$; $AM\ 1.5$), $G(\beta,\alpha)$ is the global irradiance on the plane of the array, α_p is the temperature coefficient of maximum power (%/ºC) and T is the cell temperature in Celsius.

Cell temperature (T_{cell}) should not be confused with the ambient temperature (T_{amb}) being calculated according to [43] by:

$$T_{cell}(t) = T_{amb} + G(\beta,\alpha)(t) * \left(\frac{NOCT-20}{800}\right) \quad (4.41)$$

Where NOCT is the nominal operation cell temperature which can be found on the module datasheet. In this model, ambient temperature is considered constant and equal to the average ambient temperature each month.

4.3.2. BATTERY MODEL

In a hybrid renewable energy system, the battery bank is used to store surplus electrical energy, to regulate the system voltage and to supply power to load in case of low solar conditions. Lead-acid batteries are usually employed in hybrid solar energy system due their reliability, low cost and low maintenance. Most battery models are focus on three different characteristics: The battery state of charge, the terminal voltage of the battery bank and the battery lifetime [42]. The battery model, used in this work, is an adapted version of the proposed by [44], expressing the equations in function of the energy instead of current of battery system each hour. In the model, the maximum amount of energy that the battery bank can provide, $E_{bat,\max\_d}(t)$, or be charged in one-time step, $E_{bat,\max\_c}(t)$, is given by

$$E_{bat,\max\_d}(t) = \max[0, \min[E_{max}, (SOC(t) - SOC_{min})]] \quad (4.42)$$

$$E_{bat,\max\_c}(t) = \max[0, \min[E_{max}, (SOC_{max} - SOC(t))]] \quad (4.43)$$

Where, E_{max} is the maximum flow of energy to charge or discharge the battery bank (kWh) to avoid overheating, typically between 10% and 20% of SOC_{max}. The state of charge of the battery bank at time step t is denoted by $SOC(t)$, expressed in kWh, and SOC_{max} and SOC_{min} are the maximum and minimum state of charge of the battery (kWh) respectively. The maximum and minimum SOC of the battery is calculated by

$$SOC_{max} = E_{bat,n} \quad (4.44)$$

$$SOC_{min} = E_{bat,n} \times (1 - DOD_{max}) \quad (4.45)$$

Where, $E_{bat,n}$ is the nominal capacity of the battery bank at a given capacity rate, C_{rate}, (usually C_{10} is selected) and DOD_{max} is the maximum deep of discharge of the battery bank, which is set as input at the beginning of the design. The DOD is correlated to the number of full cycles the battery if capable of during its lifecycle. Figure 10 shows the curve service life in cycle vs DOD for a valve regulated lead-acid (VRLA) battery series from the manufacturer HOPPEKE [44].

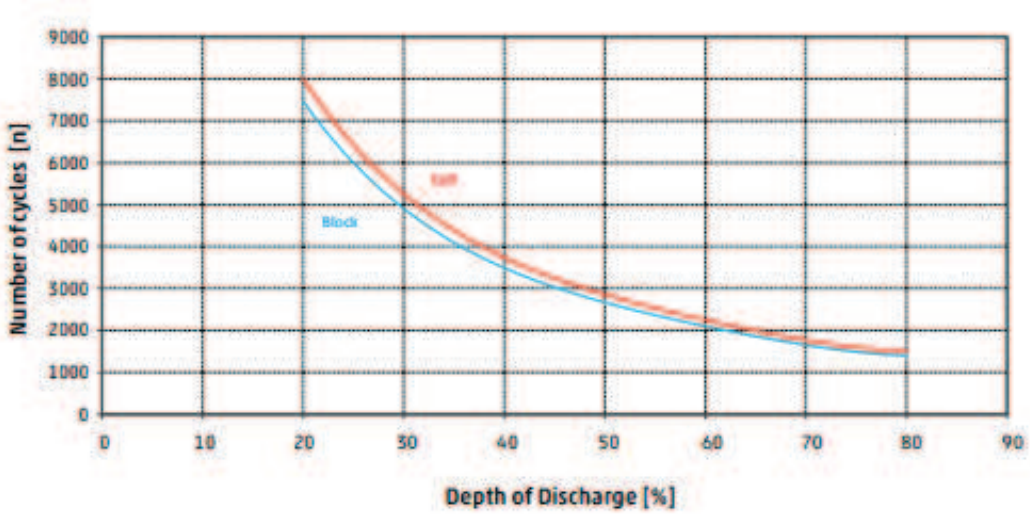

FIGURE 10. SERVICE LIFE IN CYCLES AND DEPTH OF DISCHARGE FOR A VRLA BATTERY FROM HOPPEKE [44].

The maximum flow of energy to fully charge or discharge the battery bank, denoted by E_{max}, is obtained as the ratio between the battery bank nominal capacity (kWh), denoted by $E_{bat,n}$, and the capacity rate, denoted by C_{rate}, in hours (usually C_{10} or C_5 is selected).

$$E_{max} = \frac{E_{bat,n}}{C_{rate}} \quad (4.46)$$

SOC for the next step can be calculated as follows:

$$SOC(t+1) = \begin{cases} SOC(t) \times (1-\sigma) + E_{bat}(t) \times \eta_{bat\_c} & charging \\ SOC(t) \times (1-\sigma) - E_{bat}(t) \times \eta_{bat_d} & discharging \end{cases} \quad (4.47)$$

Where, σ is the self-discharge coefficient, η_{bat_c} and η_{bat_d} are the charge and discharge efficiency of the battery. Usually, the discharge efficiency is assumed to be 1 and the charge efficiency equal to the round-trip efficiency, typically 0.85-0. $E_{bat}(t)$ is the energy that the battery bank provides or is charged at time-step t. $E_{bat}(t)$ varies according to the dispatch strategy as it is explained on the next section.

The nominal capacity of the battery bank is given by

$$E_{bat,n} = N_{b_s} \times N_{b_p} \times E_{bcell,nom} \quad (4.48)$$

Where, N_{b_s} and N_{b_p} are the number of batteries in series and the number of batteries in parallel respectively and $E_{bcell,nom}$ is the nominal capacity of one battery cell in kWh. The number of battery cells in series depends on the voltage of each battery cells and the DC voltage of the system.

$$N_{b_s} = \frac{V_{dc_{sist}}}{V_{dc_{bc}}} \quad (4.49)$$

The DC voltage system ($V_{dc_{sist}}$) is an input of the model and it is usually 12, 24 or 48V, being the former more suitable for large systems. The nominal voltage of each battery cell ($V_{dc_{bc}}$) can be found on the datasheet of the manufacturer.

In the optimization model developed in this work, the variable parameter used is the number of battery cell in parallel, N_{b_p}, as the number of battery cell in series is set with the voltage DC system selected.

The total number of batteries is then calculated as:

$$N_{b_T} = N_{b_p} \times N_{b_s} \quad (4.50)$$

In this model, the battery and DC/AC converter efficiencies are constant. Also, temperature effects on the battery are not considered. In the beginning of the time horizon, the batteries are fully charged.

4.3.3. DIESEL GENERATOR MODEL

In hybrid PV-Diesel energy systems, the diesel genset can have two different operation modes depending the energy dispatch strategy selected [5]:

- Continuous genset operation: The genset(s) always is used for grid generation. Diesel generators establish the grid voltage and frequency and the function of the PV generator is to reduce the fuel usage acting as a load reduction. The genset must operate over 30% of its rated capacity to ensure grid stability. However, in this mode of operation, high level of irradiance and low load could lead to an inacceptable operation point for the genset. Therefore, it is necessary a control system to protect the diesel generator(s) from low loading. In systems without energy storage, the PV power must be dumped to maintain the genset(s) operating over its minimum operation point. These losses can be reduced by splitting the total diesel generator capacity into several units and having a diesel manager system controlling the amount working unit required to supply the load at a suitable power ratio.
- Intermittent genset operation: In this mode of operation, it is imposed an on/off control. The grid can be formed by the genset or the bi-directional battery inverter. The system can operate only from the PV generator and storage. Usually, the genset is only used as backup operating only when the load power exceeds the combined capacity of the storage a PV generator.

The operation cost of the diesel generators depends greatly on its consumption of fuel and this value varies depending on the manufacturer. However, the fuel consumption of the diesel generator, FC_G, in liters, can be modeled in terms of the diesel generator output power by [45][46]:

$$FC_{DG} = f_0 \times w_{DG} + f_1 \times P_{DG} \quad (4.51)$$

Where P_{DG} and w_{DG} are the output power and the rated power of the diesel generator respectively, and f_0, f_1 are coefficients of the fuel consumption curve respectively. These coefficients can be obtained using a linear regression technique assuming the fuel consumption curve is a straight line where f_0 is the curve intercept coefficient and f_1 is the fuel curve slope. Typical values for these two coefficients are f_0 = 0.246 l/kW h and f_1 = 0.08145 l/kW h [46]. In this model, the extra consumption of fuel when the generator start is assumed negligible.

4.3.4. POWER DISPATCH STRATEGY

In literature, many power dispatch strategies can be found [5][47]. In this work two power dispatch strategies are highlighted:

Load following: If the power load cannot be supplied by the battery bank and the renewable energy sources, the Diesel generator runs at a rate that produces only enough power to meet the net load. The battery bank is only charged by the renewable energy sources as the photovoltaic generator. Load following tends to be optimal in systems with a lot of renewable power, when the renewable power output sometimes exceeds the load.

Cycle charging strategy: If the batteries cannot meet the net load, the Diesel generator runs at full power (or at a rate not exceeding the maximum energy that the batteries are capable of absorbing) and charge the batteries with any surplus power. If a SOC set point is applied, the Diesel generator will continue running until the batteries reach this SOC set point.

The power dispatch strategy to be selected in the model depends on the architecture of the system considered. Four architectures are considered: diesel only, diesel-PV battery-less, PV with battery backup, and diesel-PV with battery backup. Each dispatch strategy for each architecture is now explained in detail.

4.3.4.1. DIESEL ONLY SYSTEM

In this model, the diesel generation units are the only source of energy to supply the load.

The following items summarize the key characteristics of the dispatch strategy used on this model.

- A maximum number of DG units allowable, $N_{DG,max}$, is set as input parameter.
- The number DG unit required in each time step can be calculated as

$$N_{on}(t) = \min(N_{DG,max}, \left\lceil \frac{P_L(t)}{w_{DG}} \right\rceil) \quad (4.52)$$

  Where, $N_{on}(t)$ is the minimum number of DG units of nominal power w_{DG} required to supply the load, $P_L(t)$. The "ceil function", $\lceil \cdot \rceil$, is used to round up the result obtained to the nearest integer.

- In this model, all the diesel generator units have the same nominal capacity.
- The DG units must work over the minimum load ratio defined, δ_{min}, otherwise the DG units must turn off and the load cannot be supplied.
- Only AC loads are considered.

The following algorithm describes the dispatch strategy used on the Diesel-only model

1. The load hourly year profile is generated for the location.
2. The maximum number of DG units and the nominal power of each DG unit is introduced.
3. If $P_L(t) \geq N_{DG,max} \times w_{DG}$ then the diesel generation is not enough to supply the load. All DG units works at its maximum load ratio and the energy not supplied (ENS) and the power failure time (TFT) is accounted. Then go to step 6. Else go to step 4.
4. The diesel generation supplies the load and the number of DG units required and the load ratio of DG units is calculated. If $\delta(t) \leq \delta_{min}$ go to step 5, else go to step 6.
5. The DG unit cannot operate under the minimum load ratio then the DG unit turn off and the energy not supplied (ENS) and the power failure time (PFT) is accounted.
6. The fuel consumption, $FC_{DG}(t)$, is calculated by Eq. 4.51
7. Increase the time-step ($t = t + 1$)
8. If $t \leq 8760$ and return to step 3. Else **END.**

Table 7 summarizes the algorithm showing the equations used each step for the dispatch strategy for Diesel only systems.

TABLE 7. DIESEL ONLY SYSTEM DISPATCH STRATEGY AND EQUATIONS.

STEP	DESCRIPTION	EQUATIONS.
1	Upload the load profile data for the location	$P_L(t)$
2	Upload the technical and economic information of the model. Initialize variables.	$N_{DG,max}; w_{DG};\ \delta_{min}; f_0; f_1$ $FC_{DG} = 0\ ; ENS = 0; PFT = 0;$ $P_{DG} = 0;\ N_{on} = 0;\quad \delta = 0\ ;$ $t = 1$
3	$P_L(t) \geq N_{DG,max} \times w_{DG}$ Diesel generation is not enough to supply the load Else go to step 4.	$N_{on}(t) = N_{DG,max};\ \delta(t) = 1;$ $P_{DG}(t) = N_{on}(t) \times w_{DG};$ $ENS(t) = P_L(t) - P_{DG}(t);$ $PFT = PFT + 1$
4	$P_L(t) < N_{DG,max} \times w_{DG}$ && $\delta(t) \geq \delta_{min}$ The diesel generation supply the load and the DG unit can operate over the minimum load ratio. Go to step 6. Else go to step 5.	$P_{DG}(t) = P_L(t);$ $N_{on}(t) = \left\lceil \frac{P_{DG}(t)}{w_{dg}} \right\rceil;$ $\delta(t) = \frac{P_{DG}(t)}{N_{on}(t) \times w_{DG}}$
5	$P_L(t) < N_{DG,max} \times w_{DG}$ && $\delta(t) < \delta_{min}$ The DG unit cannot operate under the minimum load ratio then the DG unit turn off.	$N_{on}(t) = 0; \delta(t) = 0;$ $P_{DG}(t) = 0; ENS(t) = P_L(t);$ $PFT = PFT + 1;$
6	Calculate Fuel Consumption.	$FC_{DG}(t) = N_{on}(t) \times w_{dg} \times f_0 + f_1 \times P_{DG}(t)$
7	Increase time.	$t = t + 1$
8	If $t \leq 8760$ go to step 3. Else **END**	

In Figure 11, the flowchart of the diesel-only dispatch strategy is presented.

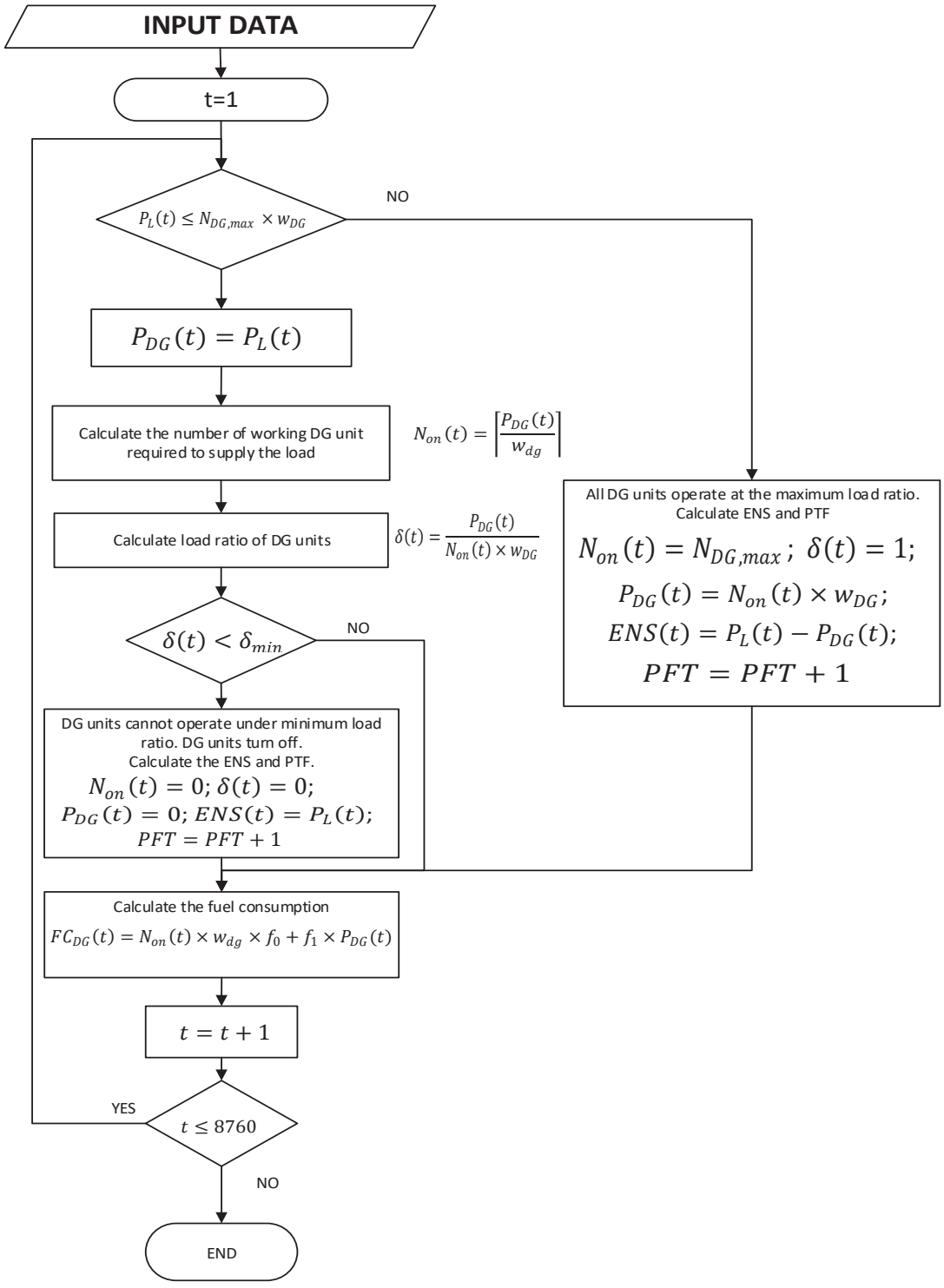

FIGURE 11.- FLOWCHART DIESEL-ONLY DISPATCH STRATEGY.

4.3.4.2. DIESEL-PV SYSTEM

In this architecture, the micro-grid has two AC sources (Diesel units and PV generators). The diesel generation sets the voltage and frequency parameters of the grid, and the other sources (photovoltaic) synchronize to that grid in voltage and frequency. The PV generator supplies a fraction of the load demand, consequently reducing the amount of energy required from the DG genset and therefore reducing the fuel usage.

The following items summarize the key characteristics of the dispatch strategy used on this model.

- At least one diesel generator unit must be "on" and operating over the minimum load ratio $\delta_{min}(t)$ in each time step. The PV inverters requires at least one diesel generator working to deliver the energy from the PV array.
- The PV generation is prioritized over the diesel generation. The diesel generator must supply the deficit of power to supply the load, $\Delta_L(t)$, each time step where

$$\Delta_L(t) = P_L(t) - P_{pv}(t) \times \eta_{inv} \tag{4.53}$$

- If ($\Delta_L(t) \leq \delta_{min} \times w_{DG}$) a control system reduces the energy output of the PV generator to maintain at least one diesel generator operating over the minimum load ratio. The surplus energy of the PV generator is wasted. The energy wasted is accounted.
- If $P_L(t) \leq \delta_{min} \times w_{DG}$ then the diesel generators cannot operate over the minimum load ratio then are turning off, and the load cannot be supplied.
- The number of diesel generators ($N_{on}(t)$) is calculated in each time-step.
- This model considers that all diesel units have the same nominal power capacity.
- Only AC loads are considered.

The following algorithm describes the dispatch strategy used on the Diesel-PV model without batteries.

1. The load, irradiance and temperature hourly year profile are generated for the location.
2. The number of photovoltaic modules, the maximum number of DG units and the technical information of each element of the system is introduced.

3. The PV power output for time-step *t* is calculated using Eq.4.40.
4. The net load power is calculated for each time-step using Eq. 4.53
5. If $\Delta_L(t) \geq N_{DG,max} \times w_{DG}$, the diesel and PV generation is not enough to supply the load. All DG units works at their maximum load ratio and the energy not supplied is accounted. Go to step 9, else.
6. If $P_L(t) < \delta_{min} \times w_{DG}$, the diesel generator cannot operate under the minimum load ratio, then is turned off. The PV inverter turn off since they need at least one DG unit to forming the grid. Therefore, all the PV energy produced is wasted. The demand cannot be supplied and the total Energy Not Supplied (ENS) and the power failure time (PFT) and the PV energy wasted (EW) is accounted. Go to step 9, else
7. If $\Delta_L(t) < \delta_{min} \times w_{DG}$, one DG unit works at the minimum ratio to supply energy to the load and the PV source provides the deficit of energy. The excess of PV power produced is wasted ($EW(t)$). Go to step 9, else.
8. The DG units can provide the deficit of energy to supply the load working over the minimum load ratio. The number of required DG unit and its load ratio is calculated.
9. The fuel consumption $FC_{DG}(t)$, is calculated by Eq. 4.51.
10. Increase the time-step ($t = t + 1$).
11. If $t \leq 8760$ and return to step 3. Else **END**.

Table 8 summarizes the algorithm showing the equations used each step for the dispatch strategy for Diesel-PV battery-less systems.

TABLE 8. DIESEL-PV SYSTEM DISPATCH STRATEGY AND EQUATIONS.

STEP	DESCRIPTION	EQUATIONS.
1	The load, irradiance and temperature hourly year profile are generated for the location	$P_L; G; T$
2	The number of photovoltaic modules, the maximum number of DG units and the technical information of each element of the system is introduced.	$N_{DG,max}; w_{DG};\ \delta_{min}; f_0; f_1$ $N_{pv}; P_{pv_{stc}}; G_{stc}; \alpha_p; NOCT; T_{stc}; f_{pv}; \eta_{inv}$ $FC_{DG} = 0\ ; ENS = 0;$ $PFT = 0;\ EW = 0$ $P_{DG} = 0; N_{on} = 0; \delta = 0; \Delta_L = 0; t = 1;$
3	Calculate the PV power output	$P_{pv}(t) = N_{pv} \times P_{pv_{stc}} \times \frac{G(t)}{G_{stc}} \times \left(1 + \frac{\alpha_p}{100} \times (T(t) - T_{stc})\right) \times f_{pv}$
4	Calculate the net load power	$\Delta_L(t) = P_L(t) - P_{pv}(t) \times \eta_{inv};$
5	$\Delta_L(t) \geq N_{DG,max} \times w_{DG}$ The diesel and PV generation are not enough to supply the load. Go to step 9.	$N_{on}(t) = N_{DG,max};\ \delta(t) = 1;$ $P_{DG}(t) = N_{on}(t) \times w_{DG};$ $ENS(t) = \Delta_L(t) - P_{DG}(t);$ $PFT = PFT + 1$
6	$P_L(t) < \delta_{min} \times w_{DG}$ The diesel generator cannot operate under the minimum load ratio, then is turned off. All the PV energy produced is wasted. Go to step 9.	$N_{on}(t) = 0;\ \delta(t) = 0;$ $P_{DG}(t) = 0; ENS(t) = P_L(t);$ $EW(t) = P_{PV}(t); PFT = PFT + 1$
7	$\Delta_L(t) < \delta_{min} \times w_{DG}$ One DG unit operates at its minimum load ratio. The excess of PV power produced is wasted. Go to step 9.	$N_{on}(t) = 1; \delta(t) = \delta_{min};$ $P_{DG}(t) = N_{on}(t) \times \delta(t) \times w_{DG};$ $EW(t) = P_{PV}(t) - \frac{(P_L(t) - P_{DG}(t))}{\eta_{inv}};$
8	$\Delta_L(t) \geq \delta_{min} \times w_{DG}$ Calculate the number of working DG unit required to supply the net load and calculate the load ratio of DG units.	$P_{DG}(t) = \Delta_L(t); N_{on}(t) = \left\lceil \frac{P_{DG}(t)}{w_{dg}} \right\rceil;$ $\delta(t) = \frac{P_{DG}(t)}{N_{on}(t) \times w_{DG}};$
9	Calculate Fuel Consumption.	$FC_{DG}(t) = N_{on}(t) \times w_{dg} \times f_0 + f_1 \times P_{DG}(t)$
10	Increase time.	$t = t + 1$
11	If $t \leq 8760$ go to step 3. Else **END**	

In Figure 11, the flowchart of the Diesel-PV strategy is presented.

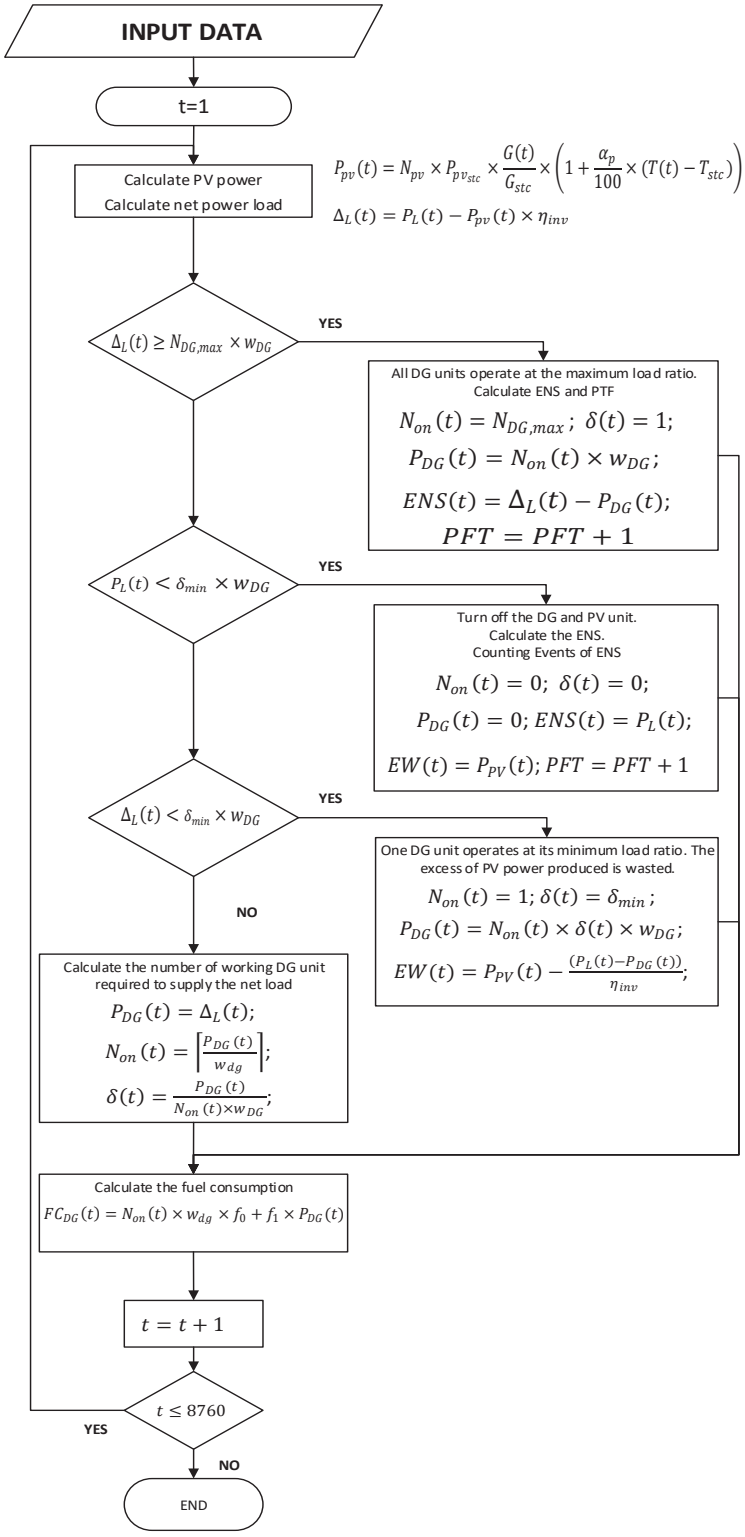

FIGURE 12. FLOWCHART DIESEL-PV DISPATCH STRATEGY.

4.3.4.3. DIESEL-PV WITH BATTERY STORAGE SYSTEM

In this architecture, the grid can be formed either from the diesel unit or from a master inverter. The DC-coupled configuration is considered in this work. The diesel generation is only required when the energy produced by the photovoltaic source and the energy backup in the battery bank is lower than the demanded load.

The following items summarize the key characteristics of the dispatch strategy used in this work to model PV-Diesel with battery storage systems.

- The system is considered DC-coupled.
- The load following strategy is adopted. The diesel generators are only used to supply the load when there is insufficient power from the PV source and the battery bank. Only the minimum DG unit required operates in every time step.
- All DG units must operate over the minimum load ratio (δ_{min}) defined otherwise the DG unit must turn off.
- All DG unit has the same nominal power capacity and operates at the equilibrium point at the same load ratio.
- When the diesel unit are operating, the PV generation prioritizes the charge of the battery bank over the load.
- Only AC loads are considered.
- A maximum number of DG units are considered.

The following algorithm describes the dispatch strategy used on the Diesel-PV-battery model.

1. The load, irradiance and temperature hourly year profile are generated for the location.
2. The number of photovoltaic modules, the number of batteries in parallel, the maximum number of DG units and the technical information of each element of the system is introduced.
3. The maximum energy that the battery can provide or be charged, at the time-step t, is calculated using Eq. 4.42 and 4.43 respectively.

4. The PV power output for time-step t is calculated using Eq.4.40.

5. The difference between PV power generated and load demanded, $\Delta_{L1}(t)$, is calculated

6. If $\Delta_{L1}(t) \leq 0$, then the PV source can supply the load.

   6.1 If the difference between PV power generated and load demanded is lower than the maximum amount of energy that the battery can be charged ($|\Delta_{L1}(t)| \leq E_{bat.max,c}(t) \times \eta_{INV}$), the excess of PV power generated, if any, is used to charge the battery bank and the SOC of the battery is updated. Go to step 10.

   6.2 Else, the battery bank is charged by, $E_{bat,\max\_c}(t)$, and the excess of photovoltaic energy not used to supply the load and charge the battery bank is wasted. The SOC of the battery bank is updated. The energy wasted ($EW(t)$) is accounted. Go to step 10.

7. If $\Delta_{L1}(t) > 0$, the photovoltaic source is insufficient to supply the load.

   7.1 If $\Delta_{L1}(t) < E_{bat,\max,d}(t) \times \eta_{INV}$, the battery bank discharge to supply the lack of energy. The SOC of the battery is updated. Go to step 10.

   7.2 Otherwise, diesel generation is required.

8. The diesel generation is necessary. The photovoltaic energy is used to charge the battery bank and the diesel generation is used to supply the load. The energy stored in the battery bank and energy generated by the diesel unit is used to supply the load at night.

   8.1 **Case 1:** $P_L(t) < \delta_{min} \times w_{DG}$. Since the DG units cannot operate under the minimum load ratio, δ_{min}, all DG units must turn off. The generated PV energy and the energy available in the battery bank are used to supply the load, while the energy not supplied (ENS) and the power time failure (PTF) is accounted.

   8.2 **Case 2:** $P_L(t) \geq \delta_{min} \times w_{DG}$ && $P_{pv}(t) > 0$. The photovoltaic energy is used to charge the battery bank. The diesel generation supplies the load.

      8.2.1 **Case 2.1:** $P_{pv}(t) \geq E_{bat.max,c}(t)$. The battery bank charges at its maximum ratio and the excess of energy is used to supply the load with the diesel generation.

8.2.1.1 **Case 2.1.1:** $P_L(t) > \left(P_{pv}(t) - E_{bat}(t)\right) \times \eta_{inv} - P_{DG}(t)$. The diesel generation is not sufficient to supply the load, the energy not supplied is accounted.

8.2.1.2 **Case 2.1.2**: $\delta(t) < \delta_{min}$. If the load ratio of the DG unit is lower than the minimum load ratio allowed, then just one DG unit works operating at the minimum load ratio and the excess of PV energy generated is wasted.

8.2.2 **Case 2.2** $P_{pv}(t) \leq E_{bat.max,c}(t)$. All photovoltaic energy is used to charge the battery bank.

8.2.2.1 **Case 2.2.1**: $P_L(t) > P_{DG}(t)$ The DG is insufficient to supply the load, the energy not supplied is accounted.

8.3 **Case 3**: ($P_L(t) \geq \delta_{min} \times w_{DG}$ && $P_{pv}(t) \leq 0$). At night, the battery bank and the DG units are used to supply the load.

8.3.1 **Case 3.1**: ($P_L(t) - E_{bat.max,d}(t) \times \eta_{inv} \geq \delta_{min} \times w_{DG}$). Battery bank is discharged at maximum rate and DG units generates the remaining energy necessary to supply the load.

8.3.1.1 **Case 3.1.1:** ($P_L(t) \geq P_{DG} + E_{bat}(t) \times \eta_{inv}$). The diesel generation and the energy provided by the battery bank is not sufficient to supply the load, the energy not supplied is accounted.

8.3.2 **Case 3.2**: ($P_L(t) - E_{bat.max,d}(t) \times \eta_{inv} < \delta_{min} \times w_{DG}$). Just one DG unit works operating at the minimum load ratio. The battery bank provides the insufficient energy to supply the load.

9. The fuel consumption $FC_{DG}(t)$, is calculated by Eq. 4.51

10. Increase the time-step ($t = t + 1$). If $t \leq 8760$ and return to step 3. Else END.

11. The Table 9 summarizes the algorithm showing the equations used each step for the dispatch strategy for Diesel-PV with battery backup systems.

TABLE 9.

DIESEL-PV WITH BATTERY BACKUP SYSTEM DISPATCH STRATEGY AND EQUATIONS.

STEP	DESCRIPTION	EQUATIONS.
1	The load, irradiance and temperature hourly year profile are generated for the location	$P_L; G; T$
2	The number of photovoltaic modules, the maximum number of DG units and the technical information of each element of the system is introduced.	$N_{DG,max}; w_{DG};\ \delta_{min}; f_0; f_1$ $N_{pv}; P_{pv_{stc}}; G_{stc}; \alpha_p; NOCT; T_{stc}; f_{pv}; \eta_{inv}$ $N_{bp}; E_{bcell,nom}; V_{dc_{sist}}; V_{dc_{bc}}; \sigma; \eta_{bat,d}; \eta_{bat,c}; C_{rate}$; DOD_{max} $FC_{DG} = 0$; $ENS = 0; PFT = 0;\ EW = 0$ $P_{DG} = 0; N_{on} = 0; \delta = 0; \Delta_{L1} = 0; \Delta_{L2} = 0; \Delta_{bat} = 0$ $t = 1;\ SOC(1) = SOC_{max}$
3	Calculate the maximum energy that the battery can provide or be charged.	$E_{bat,\max,d}(t) = \max[0, \min[E_{max}, (SOC(t) - SOC_{min})]];$ $E_{bat,\max,c}(t) = \max[0, \min[E_{max}, (SOC_{max} - SOC(t))]];$
4	Calculate the PV power output	$P_{pv}(t) = N_{pv} \times P_{pv_{stc}} \times \frac{G(t)}{G_{stc}} \times \left(1 + \frac{\alpha_p}{100} \times (T(t) - T_{stc})\right) \times f_{pv};$
5	Calculate the difference between PV power generated and load demanded	$\Delta_{L1}(t) = P_L(t) - P_{pv}(t) \times \eta_{inv};$
6.1	$\Delta_{L1}(t) \leq 0$ && $\lvert\Delta_{L1}(t)\rvert \leq E_{bat.max,c}(t) \times \eta_{INV}$ The excess of PV power generated, if any, is used to charge the battery bank and the SOC of the battery is updated. Go to step 10.	$E_{bat}(t) = P_{pv}(t) - \frac{P_L(t)}{\eta_{INV}};$ $SOC(t+1) = SOC(t) \times (1 - \sigma) + E_{bat}(t) \times \eta_{bat,c};$
6.2	$\Delta_{L1}(t) \leq 0$ && $\lvert\Delta_{L1}(t)\rvert > E_{bat.max,c}(t) \times \eta_{INV}$ The battery bank charges by the maximum amount possible and the excess of photovoltaic energy not used to supply the load and charge the battery bank is wasted. The SOC of the battery bank is updated. Go to step 10.	$E_{bat}(t) = E_{bat.max,c}(t);$ $SOC(t+1) = SOC(t) \times (1 - \sigma) + E_{bat}(t) \times \eta_{bat,c};$ $EW(t) = P_{pv}(t) - \frac{P_L(t)}{\eta_{INV}} - E_{bat}(t);$
7.1	$\Delta_{L1}(t) > 0$ && $\Delta_{L1}(t) < E_{bat,\max,d}(t) \times \eta_{INV}$ The battery bank discharges to supply the lack of energy. The SOC of the battery is updated. Go to step 10.	$E_{bat}(t) = \frac{P_L(t)}{\eta_{INV}} - P_{pv}(t);$ $SOC(t+1) = SOC(t) \times (1 - \sigma) - E_{bat}(t) \times \eta_{bat,d};$
7.2	$\Delta_{L1}(t) > 0$ && $\Delta_{L1}(t) < E_{bat,\max,d}(t) \times \eta_{INV}$ Diesel generation is required. Go to step 8	

TABLE 9. (CONTINUED)

DIESEL-PV WITH BATTERY BACKUP SYSTEM DISPATCH STRATEGY AND EQUATIONS.

8	The diesel generation is necessary. The photovoltaic energy is used to charge the battery bank and the diesel generation is used to supply the load. At night, the load is supplied by a combination of the DG and energy from the battery bank.	
8.1	$P_L(t) < \delta_{min} \times w_{DG}$ DG unit cannot operate under the minimum load ratio, δ_{min}, all DG unit must turn off. The PV energy generated and the energy available in the battery bank is used to supply the load. Go to step 10.	$N_{on}(t) = 0;\ \delta(t) = 0;$ $P_{DG}(t) = 0; E_{bat}(t) = E_{bat.max,d};$ $SOC(t+1) = SOC(t) \times (1-\sigma) - E_{bat}(t) \times \eta_{bat\_d};$ $ENS(t) = P_L(t) - \left(P_{pv}(t) + E_{bat}(t)\right) \times \eta_{inv};$ $PFT = PFT + 1$
8.2	$P_L(t) \geq \delta_{min} \times w_{DG}$ && $P_{pv}(t) > 0$ At day, the photovoltaic energy is used to charge the battery bank. The diesel generation supplies the load.	
8.2.1	$P_{pv}(t) \geq E_{bat.max,c}(t)$ The battery bank charges at its maximum ratio and the DG and the excess of PV energy is used to supply the load.	$E_{bat}(t) = E_{bat.max,c}(t);$ $SOC(t+1) = SOC(t) \times (1-\sigma) + E_{bat}(t) \times \eta_{bat,c};$ $P_{DG}(t) = \min(N_{dg,max} * w_{dg}, P_L(t) - (P_{pv} - E_{bat}(t)) \times \eta_{inv})$ $N_{on}(t) = \left\lceil \frac{P_{DG}(t)}{w_{dg}} \right\rceil; \delta(t) = \frac{P_{DG}(t)}{N_{on}(t) \times w_{DG}};$
8.2.1.1	$P_L(t) > \left(P_{pv}(t) - E_{bat}(t)\right) \times \eta_{inv} - P_{DG}(t)$ The diesel generation is not sufficient to supply the load, the energy not supplied is accounted. Go to step 9.	$ENS(t) = P_L(t) - \left(P_{pv}(t) - E_{bat}(t)\right) \times \eta_{inv} - P_{DG}(t)\ PFT = PFT + 1;$
8.2.1.2	$\delta(t) < \delta_{min}$ One DG unit works operating at the minimum load ratio and the excess of PV energy generated is wasted. Go to step 9.	$N_{on}(t) = 1; \delta(t) = \delta_{min};$ $P_{DG}(t) = N_{on}(t) \times \delta(t) \times w_{DG};$ $EW(t) = P_{pv}(t) - E_{bat}(t) - \frac{P_L(t) - P_{dg}(t)}{\eta_{inv}};$
8.2.2	$P_{pv}(t) < E_{bat.max,c}(t)$ All photovoltaic energy is used to charge the battery bank.	$E_{bat}(t) = P_{pv}(t);$ $P_{DG}(t) = \min(N_{dg,max} * w_{dg}, P_L(t))$ $SOC(t+1) = SOC(t) \times (1-\sigma) + E_{bat}(t) \times \eta_{bat,c};$ $N_{on}(t) = \left\lceil \frac{P_{DG}(t)}{w_{dg}} \right\rceil; \delta(t) = \frac{P_{DG}(t)}{N_{on}(t) \times w_{DG}};$
8.2.2.1	$P_L(t) > P_{DG}(t)$ The DG is insufficient to supply the load, the energy not supplied is accounted.	$ENS(t) = P_L(t) - P_{DG}(t)$ $PFT = PFT + 1$

TABLE 9. (CONTINUED)

DIESEL-PV WITH BATTERY BACKUP SYSTEM DISPATCH STRATEGY AND EQUATIONS.

8.3	$(P_L(t) \geq \delta_{min} \times w_{DG}$ && $P_{pv}(t) = 0)$ At night. The battery bank and the DG units are used to supply the load.	
8.3.1	$P_L(t) - E_{bat.max,d}(t) \times \eta_{inv} \geq \delta_{min} \times w_{DG}$ Battery bank is discharged at maximum rate and DG units generates the remaining energy necessary to supply the load.	$E_{bat}(t) = E_{bat.max,d}(t);$ $P_{DG}(t) = \min(N_{dg,max} * w_{dg}, P_L(t) -$ $E_{bat}(t) \times \eta_{inv})$ $SOC(t+1) = SOC(t) \times (1-\sigma) -$ $E_{bat}(t) \times \eta_{bat,d};$ $N_{on}(t) = \left\lceil \frac{P_{DG}(t)}{w_{dg}} \right\rceil; \delta(t) = \frac{P_{DG}(t)}{N_{on}(t) \times w_{DG}};$
8.3.1.1	$(P_L(t) \geq P_{DG} + E_{bat}(t) \times \eta_{inv})$ The diesel generation and the energy provided by the battery bank is not sufficient to supply the load, the ENS and PTF is accounted.	$ENS(t) = P_L(t) - P_{DG}(t) - E_{bat}(t) \times \eta_{inv}$; $PFT = PFT + 1$
8.3.2	$(P_L(t) - E_{bat.max,d}(t) \times \eta_{inv} < \delta_{min} \times w_{DG})$ Just one DG unit works operating at the minimum load ratio. The battery bank provides the insufficient energy to supply the load.	$N_{on}(t) = 1; \delta(t) = \delta_{min};$ $P_{DG}(t) = N_{on}(t) \times \delta(t) \times w_{DG};$ $E_{bat}(t) = \frac{P_L(t) - P_{DG}(t)}{\eta_{inv}}$ $SOC(t+1) = SOC(t) \times (1-\sigma) -$ $E_{bat}(t) \times \eta_{bat,d};$
9	Calculate Fuel Consumption.	$FC_{DG}(t) = N_{on}(t) \times w_{dg} \times f_0 +$ $P_{DG}(t) \times f_1$
10	Increase time. If $t \leq 8760$ go to step 3. Else **END**	$t = t + 1$

In Figure 12, the flowchart of the Diesel-PV with battery backup dispatch strategy is presented.

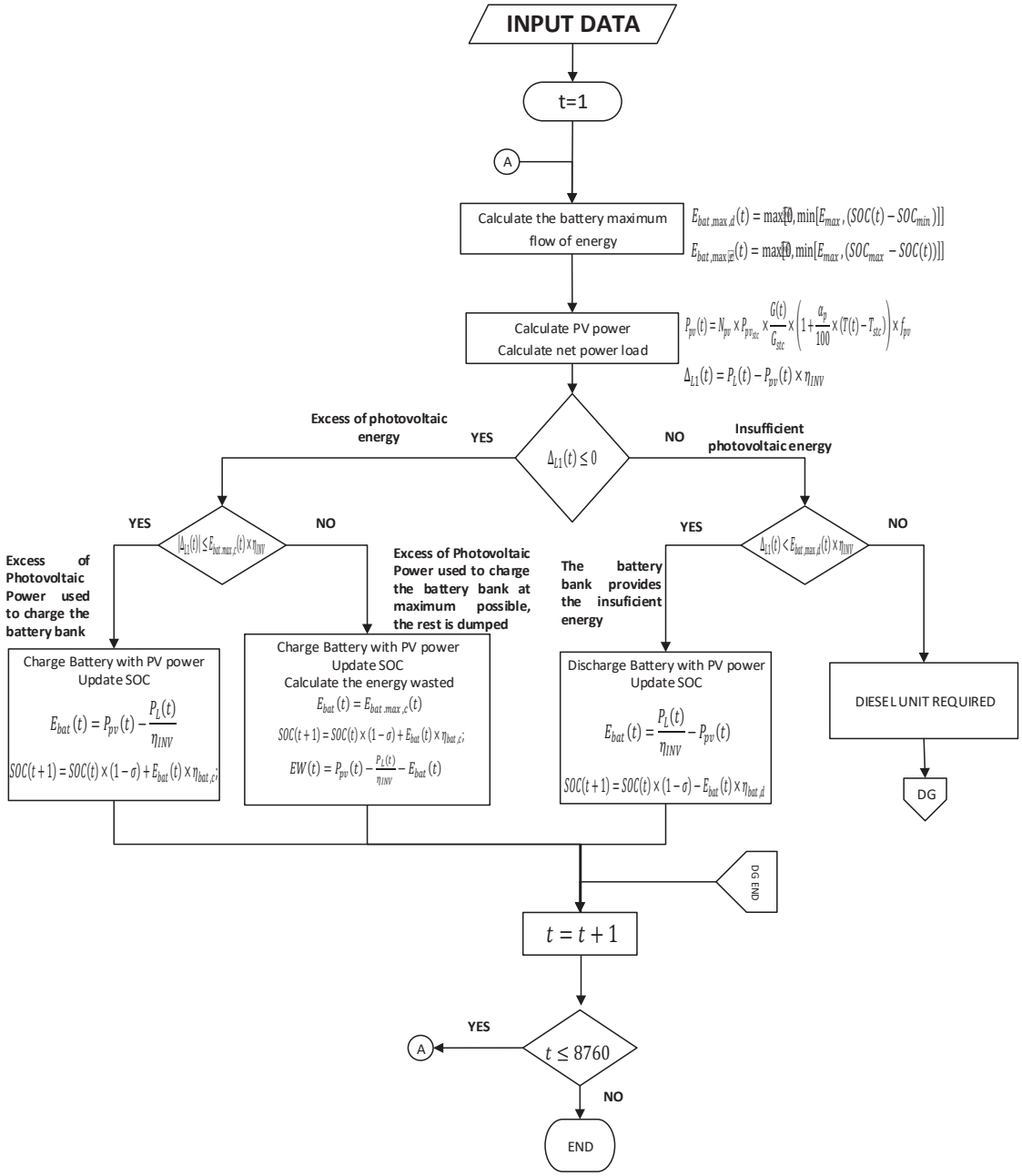

FIGURE 13. (A) FLOWCHART DIESEL-PV WITH BATTERY BACKUP DISPATCH STRATEGY, PART 1.

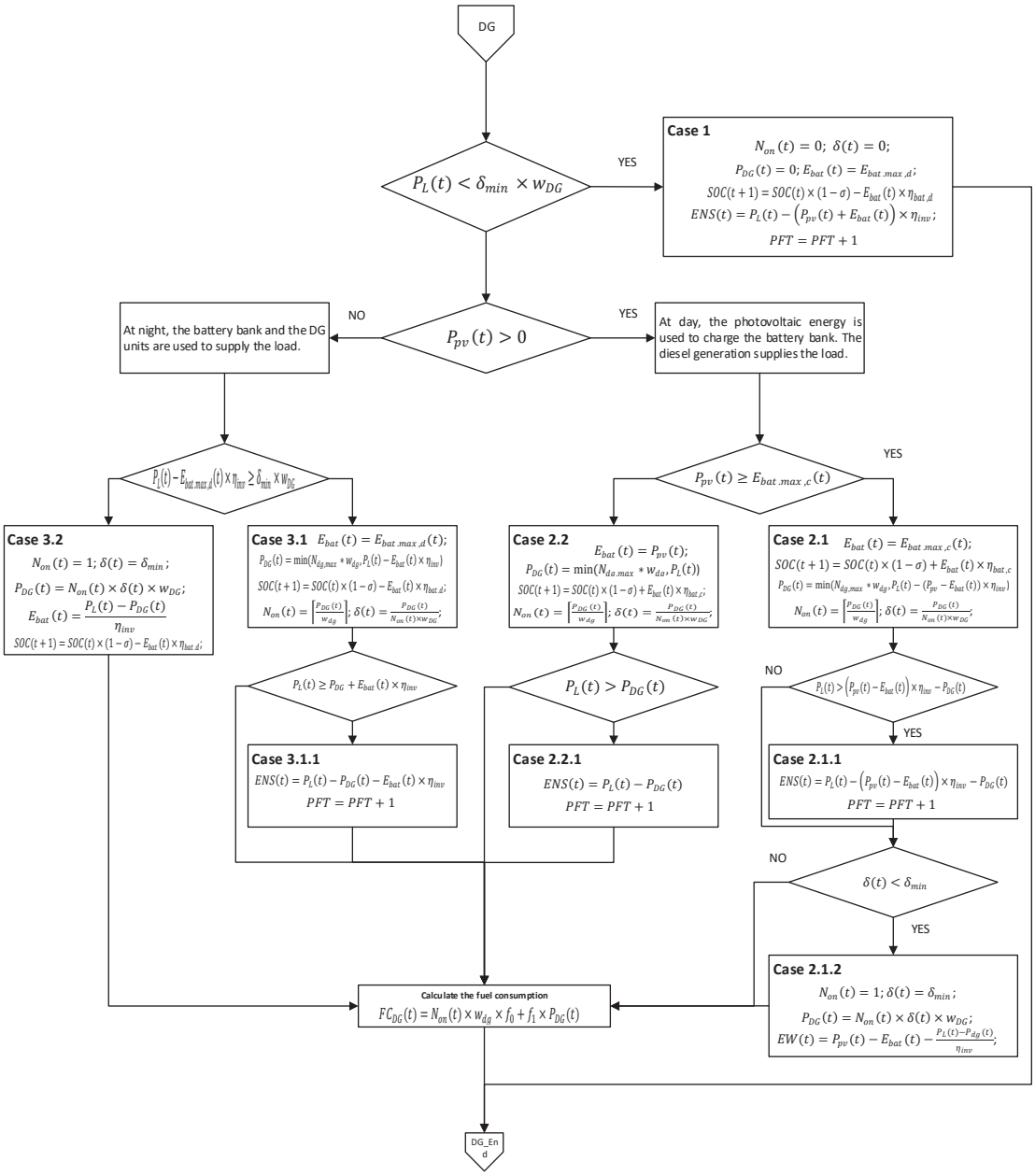

FIGURE 12. (B) FLOWCHART DIESEL-PV WITH BATTERY BACKUP DISPATCH STRATEGY, PART 2.

4.3.4.4. PV WITH BATTERY BACKUP

This system is a sub-case of the Diesel-PV and Battery backup system when the number of DG units is equal to zero. The load is only supplied by a combination energy produced by the PV sources and energy from the battery bank.

The following items summarize the key characteristics of the dispatch strategy used in this work to model PV with battery storage systems.

- The system is considered DC-coupled.
- Only AC loads are considered.
- The photovoltaic source can produce more energy than the energy that the system demands, the excess of energy generated by the photovoltaic source is used to charge the battery, otherwise is wasted. The photovoltaic energy wasted (EW) is accounted.
- When the system demands more energy than the sum of the energy produced by the photovoltaic system and the maximum amount of energy that the battery bank can provide, then the load cannot be fully supplied. The energy not supplied (ENS) is accounted.

The following algorithm describes the dispatch strategy used on the PV-battery model.

1. The load, irradiance and temperature hourly year profile are generated for the location.
2. The number of photovoltaic modules, the number of batteries in parallel, the maximum number of DG units and the technical information of each element of the system is introduced.
3. The maximum energy that the battery can provide or be charged, at the time-step t, is calculated using Eq. 4.42 and 4.43 respectively.
4. The PV power output for time-step t is calculated using Eq.4.40.
5. The difference between PV power generated and load demanded, $\Delta_{L1}(t)$, is calculated
6. If $\Delta_{L1}(t) \leq 0$, then the PV source can supply the load.
   6.1 If and $|\Delta_{L1}(t)| \leq E_{bat.max,c}(t) \times \eta_{INV}$, the excess of PV power generated, if any, is used to charge the battery bank and the SOC of the battery is updated. Go to step 10.
   6.2 Else, the battery bank is charged by $E_{bat,\max\_c}(t)$, and the excess of photovoltaic energy not used to supply the load and charge the battery bank is wasted. The SOC of the battery bank is updated. The energy wasted ($EW(t)$) is accounted. Go to step 10.

7. If $\Delta_{L1}(t) > 0$, the photovoltaic source is insufficient to supply the load.

   7.1 If $\Delta_{L1}(t) < E_{bat,\max,d}(t) \times \eta_{INV}$, the battery bank discharge to supply the lack of energy. The SOC of the battery is updated. Go to step 10.

   7.2 Otherwise, the load cannot be fully supplied, and the energy not supplied (ENS) is accounted. The battery bank discharge by the maximum amount possible and the SOC is updated.

8. Increase the time-step ($t = t + 1$)

9. If $t \leq 8760$ and return to step 3. Else **END**.

Table 10 summarizes the algorithm showing the equations used each step for the dispatch strategy for PV with battery backup systems.

TABLE 10. PV WITH BATTERY BACKUP SYSTEM DISPATCH STRATEGY AND EQUATIONS.

STEP	DESCRIPTION	EQUATIONS.
1	The load, irradiance and temperature hourly year profile are generated for the location	$P_L; G; T$
2	The number of photovoltaic modules, the maximum number of DG units and the technical information of each element of the system is introduced.	$N_{pv}; P_{pv_{stc}}; G_{stc}; \alpha_p; NOCT; T_{stc}; f_{pv}; \eta_{inv}$ $E_{bcell,nom}; V_{dc_{sist}}; V_{dc_{bc}}; \sigma; \eta_{bat,d}; \eta_{bat,c}; C_{rate}; DOD_{max}$ $ENS = 0; PFT = 0;\ EW = 0$ $\Delta_{L1} = 0;\ t = 1;\ SOC(1)$
3	Calculate the maximum energy that the battery can provide or be charged.	$E_{bat,\max,d}(t) = \max[0, \min[E_{max}, (SOC(t) - SOC_{min})]];$ $E_{bat,\max,c}(t) = \max[0, \min[E_{max}, (SOC_{max} - SOC(t))]];$
4	Calculate the PV power output	$P_{pv}(t) = N_{pv} \times P_{pv_{stc}} \times \frac{G(t)}{G_{stc}} \times \left(1 + \frac{\alpha_p}{100} \times (T(t) - T_{stc})\right) \times f_{pv};$
5	Calculate the difference between PV power generated and load demanded	$\Delta_{L1}(t) = P_L(t) - P_{pv}(t) \times \eta_{inv};$
6.1	$\Delta_{L1}(t) \leq 0$ && $\lvert\Delta_{L1}(t)\rvert \leq E_{bat.max,c}(t) \times \eta_{INV}$ The excess of PV power generated, if any, is used to charge the battery bank and the SOC of the battery is updated. Go to step 8.	$E_{bat}(t) = P_{pv}(t) - \frac{P_L(t)}{\eta_{INV}};$ $SOC(t+1) = SOC(t) \times (1 - \sigma) + E_{bat}(t) \times \eta_{bat,c};$
6.2	$\Delta_{L1}(t) \leq 0$ && $\lvert\Delta_{L1}(t)\rvert > E_{bat.max,c}(t) \times \eta_{INV}$ The battery bank charges by the maximum amount possible, $E_{bat,\max,c}(t)$, and the excess of photovoltaic energy not used to supply the load and charge the battery bank is wasted. The SOC of the battery bank is updated. Go to step 8.	$E_{bat}(t) = E_{bat.max,c}(t);$ $SOC(t+1) = SOC(t) \times (1 - \sigma) + E_{bat}(t) \times \eta_{bat,c};$ $EW(t) = P_{pv}(t) - \frac{P_L(t)}{\eta_{INV}} - E_{bat}(t);$
7.1	$\Delta_{L1}(t) > 0$ && $\Delta_{L1}(t) < E_{bat,\max,d}(t) \times \eta_{INV}$ The battery bank discharges to supply the lack of energy. The SOC of the battery is updated. Go to step 8.	$E_{bat}(t) = \frac{P_L(t)}{\eta_{INV}} - P_{pv}(t);$ $SOC(t+1) = SOC(t) \times (1 - \sigma) - E_{bat}(t) \times \eta_{bat,d};$
7.2	$\Delta_{L1}(t) > 0$ && $\Delta_{L1}(t) < E_{bat,\max,d}(t) \times \eta_{INV}$ The load cannot be fully supplied, and the energy not supplied (ENS) is accounted. The battery bank discharge by the maximum amount possible and the SOC is updated.	$E_{bat}(t) = E_{bat,\max,d}(t);$ $SOC(t+1) = SOC(t) \times (1 - \sigma) - E_{bat}(t) \times \eta_{bat,d};$ $ENS(t) = P_L(t) - (P_{pv}(t) + E_{bat.max,d}(t)) \times \eta_{inv};$
8	Increase time.	$t = t + 1$

9	If $t \leq 8760$ go to step 3. Else **END**	

In Figure 13 the flowchart of the PV with battery backup dispatch strategy is presented.

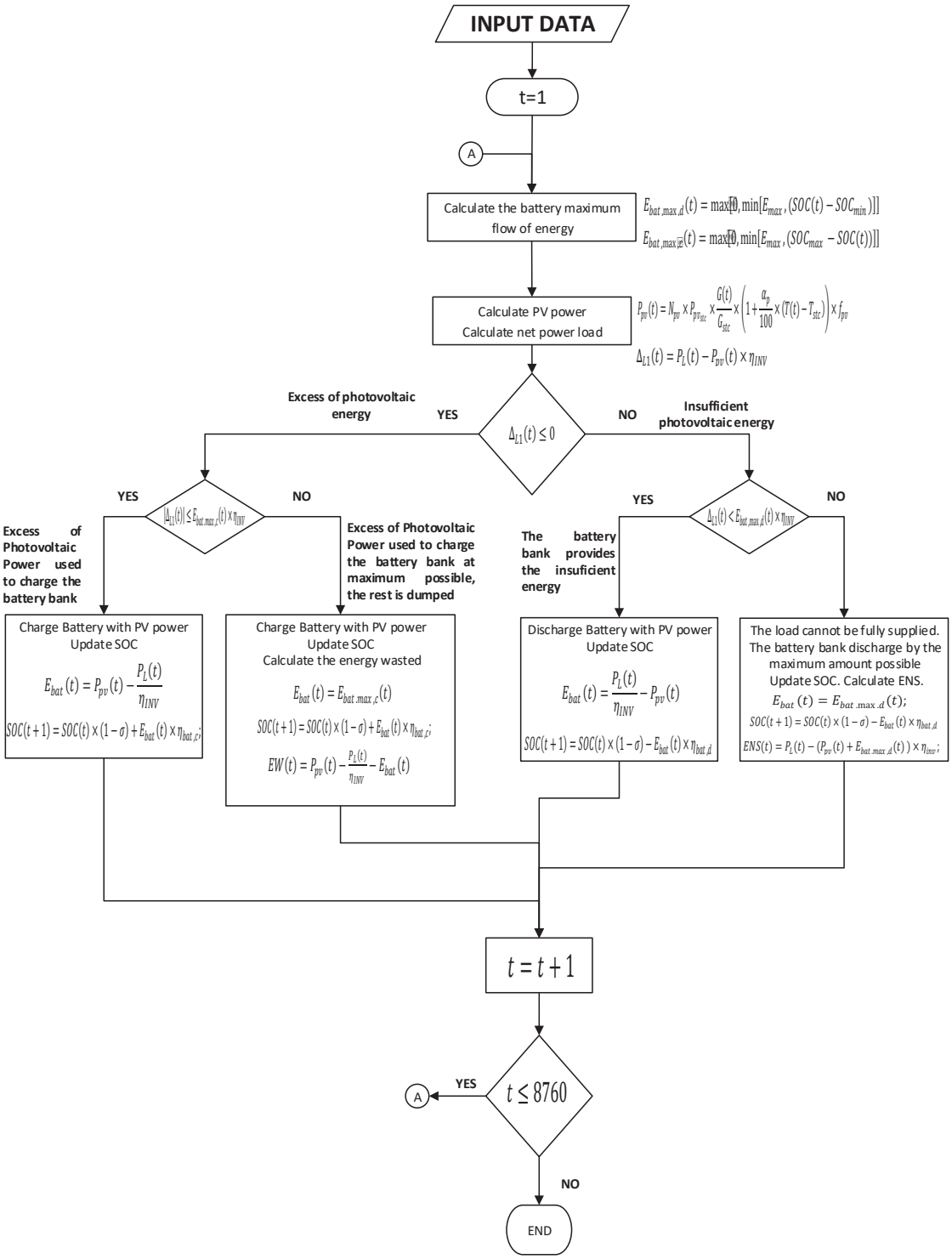

FIGURE 14. FLOWCHART PV WITH BATTERY BACKUP DISPATCH STRATEGY.

4.3. ECONOMIC AND RELIABILITY INDICATORS

This section describes the economic and reliability factor considered to evaluate the best combination of components to supply the load in an off-grid hybrid renewable energy system.

4.3.1. ECONOMIC INDICATORS

An economic analysis is required to determine the optimum cost and benefit ratio of HRES. These systems generally require high capital investment, even though they have low operation and maintenance (O&M) costs and less fuel costs in comparison with systems relaying only on fossil fuels. In literature, many economic based sub-models to evaluate HRES can be found in [15]. In this study, the annualized Cost of the system (ACS) and the Cost of Energy (LCOE) are considered as the economic criteria to evaluate the feasibility of this hybridized system configuration.

The annualized cost of the system (ACS) is the sum of the annualized capital cost (CC), the annualized replacement cost (RC) and the annualized cost of maintenance (OM) [12][48]–[50]. In [48], the annualized cost of the system is defined as

$$ACS = \sum_{i=1}^{N_c}(CC_i + RC_i) \times CRF(i_r, R) + O\&M_i) \qquad (4.54)$$

Where N_c is the number of components, in this study three (PV modules, battery bank, DG unit) and the subscript "i" is used to describe the cost of each component. The capital recovery factor, $CRF(i_r, R)$, can be defined as a ratio used to calculate the present value of an annuity (a series of equal annual cash flows) in function of the real interest rate, i_r, and the life time of the project, R [48]. The capital recovery factor is calculated by

$$CRF(ir, R) = \frac{i_r \times (1+i_r)^R}{(1+i_r)^R - 1} \qquad (4.55)$$

The real interest rate is used to convert between one-time costs and annualized costs. By defining the real discount rate, the inflation rate effect is factored out of the economic analysis. All costs, therefore, become real costs, which are in defined in terms of constant dollars [39]. The real interest rate is calculated by

$$i_r = \frac{i_n - i_f}{1+i_f} \qquad (4.56)$$

Where i_n and i_f are the nominal interest rate and expected annual inflation rate respectively.

The capital cost for each component is described by

$$CC_{pv} = c_{pv} \times N_{pv} \times P_{pv_{stc}} \quad (4.57)$$

$$CC_{bat} = c_{bat} \times N_{bat} \times E_{bcell,nom} \quad (4.58)$$

$$CC_{DG} = c_{DG} \times N_{DG} \times w_{DG} \quad (4.59)$$

Where c_{pv} is the cost per Watt peak installed of photovoltaic power in [USD/W_p], this cost includes: the cost of the module, the electronic power equipment required (charge controller and inverter) and the installation cost (engineering, transportation, balance of system equipment as cable, mounting rack, electrical protection, etc.). c_{pv} varies according to the project location and site conditions, it can range from 3-10 USD/Wp. The cost per unit of battery system, c_{bat}, in [USD/Wh], includes the average cost of the battery cell and the installation cost of the battery system. The parameter c_{DG} in [USD/kW] is the cost per unit of diesel generation installed, also includes the cost of the diesel generator unit and the associated installation costs.

The replacement cost is calculated for each element. The replacement cost of the photovoltaic system is assumed null, as the photovoltaic modules have a life cycle superior to the life time of the project and it is assumed in this model that the charge controllers and inverters do not need replacement during the life time of the project. The replacement cost of the battery system and the DG unit can be calculated as

$$RC_{bat} = \gamma_{bat} \times CC_{bat} \times K_{bat}(i_r, L_{pv}, y_i) \quad (4.60)$$

$$RC_{DG} = \gamma_{DG} \times CC_{DG} \times K_{DG}(i_r, L_{DG}, y_i) \quad (4.61)$$

Where γ_{bat} and γ_{DG} are de-rate factors of the initial capital cost invested for the battery system and the diesel genset respectively, as some cost necessary during the installation are no longer needed during the replacement (civil works, battery rack, electrical protections, fuel tank, etc.). $K_i(i_r, L_i, y_i)$ is the single payment present worth [48], which is defined by

$$K_i(i_r, L_i, y_i) = \sum_{n=1}^{y_i} \frac{1}{(1+i_r)^{n \times L_i}} \quad (4.62)$$

Where L and y, are the useful life time and the number of replacements of the component during the life time of the project, respectively. The number of replacements of each component is a function of useful lifetime of the component and the lifetime of the project, R.

$$y_i = \left\lfloor \frac{R}{Li} \right\rfloor \tag{4.63}$$

The fixed-mount PV systems do not have moving parts, so operating and maintenance costs consist of regular cleaning and monitoring of performance, the annual operation and maintenance cost can be estimated as a percentage of the PV system total investment, ρ_{pv}, usually between 1%-2% [51].

$$O\&M_{PV} = \rho_{pv} \times CC_{pv} \tag{4.64}$$

In a similar way, the annual operation and maintenance cost for the battery system can be calculated as percentage of the total investment cost of the battery system. This cost can vary according to the technology of the battery bank. For example, the cost of operation and maintenance for vented lead-acid batteries is higher than maintenance-free sealed lead acid batteries or Li-ion batteries. The percentage of the total investment cost, ρ_{bat}, can vary between 1-3%.

$$O\&M_{bat} = \rho_{bat} \times CC_{bat} \tag{4.65}$$

The operation and maintenance cost for the diesel system components is divided in two values: a fixed cost, expressed as a percentage of the diesel initial investment, ρ_{DG} ; and a variable cost associated to the cost of fuel, f_C, in [$/gal], and the annual fuel consumption. The annual operation and maintenance cost of the diesel system can be calculated by

$$O\&M_{DG} = \rho_{DG} \times CC_{DG} + f_C \times \sum_{t=1}^{8760} FC(t) \tag{4.66}$$

The cost of energy (COE) can be defined as the average cost per kWh of useful electrical energy produced by the system [52]. It can be obtained as the ratio between the annualized cost of the system and the effective load served in one year. The economic model assumes that the yearly effective load served is constant over the lifetime of the project.

The COE can be calculated as

$$COE = \frac{ACS}{\sum_{t=1}^{8760}(E_L(t) - ENS(t))} \quad (4.67)$$

In this work, the COE is used as main criteria for the economic evaluation of the different possible combination in the HRE off-grid projects. Nevertheless, the ACS is calculated and presented in each possible solution.

4.3.2. RELIABILITY INDICATORS

The dependency on nature and unpredictability of solar resources has a great impact on energy production which leads to unreliable power supply during cloudy days. A system is reliable if it can supply the required power to the electrical load within a specific time period. In literature, several reliability indicators to evaluate the performance of HRES can be found [15], [53].

The loss of power supply probability (LPSP) is the most widely used method to evaluate the reliability in hybrid system, therefore is selected, in this work, as reliability criteria. The LPSP be calculated as the ratio of power supply deficit to the electric load demand during a certain period of time (normally a year). A ratio equal to zero means all load demand, during the period of time, is served by system [53]. The LPSP is given by

$$LPSP = \frac{\sum_{t=1}^{8760} ENS(t)}{\sum_{t=1}^{8760} E_L(t)} \quad (4.68)$$

A method that takes into account the weight of reliability in the economic sub-model is to include a component of cost of electricity interruptions or cost of load (C_{loss}) [48]. Cost of electricity interruptions can be estimated in different ways. For example, looking at the customer's willingness to pay for an expansion or at production losses at industries affected, or at the level of compensations, which makes shortages acceptable. In [48], for 2009, the cost ranges from 5-40 USD$/kWh for industrial users and 2-12 USD$/kWh for domestic users. In Colombia, the cost of electricity shortage is calculated monthly by the UPME for grid-tie systems and varies according to the percentage of load not served (LPSP). Table 11 shows the cost of electricity lost in Colombia, for March 2018, converted to USD using a TRM of 2800 COP/USD.

TABLE 11. COST OF ELECTRICITY LOST IN SIN IN COLOMBIA

GROUP	USD/KWH	CONDITION
CRO1	0.45466786	< 1.5%
CRO2	0.82421429	1.5 %< LPSP<5 %
CRO3	1.445475	5 % < LPSP< 90 %
CRO4	2.86226786	LPSP< 90 %

Source: UPME, March 2018. [54]

The cost of electricity lost for non-interconnected zone can vary with respect the reference cost and could be difficult to estimate, as depends on the wiliness of users to pay for a more robust system. The cost of electricity not supply (C_{loss}) in [USD/kWh] is as input parameter in the economic model. The annualized cost of energy not supplied can be calculated as

$$AC_{loss} = C_{loss} \times \sum_{t=1}^{8760} ENS(t) \quad (4.69)$$

The $LPSP$ and the AC_{loss} is calculated for each possible combination considered during the sizing methodology.

4.3.3. FISCAL INCENTIVES

Under Colombian renewable energy law, new clean energy projects will receive up to 50% tax credits, but they can only be applied during the first five years. In this work, when the fiscal incentives are considered, it is assumed that the company will receive the 50% of the tax credit equally distributed over the first 5 years of the project. In general, investment tax credits can be calculated as

$$i = \sum_{j=1}^{5} i_j = 0.5 \quad (4.70)$$

$$i_1 = i_2 = i_3 = i_4 = i_5 = 0.1 \quad (4.71)$$

In a similar way, it is assumed that the effect of depreciation is equally distributed each year and the useful life for accelerated depreciation purposes is five years. Then

$$d = \sum_{j=1}^{5} d_j = 1 \qquad (4.72)$$

$$d_1 = d_2 = d_3 = d_4 = d_5 = 0.2 \qquad (4.73)$$

Assuming an effective corporate tax income rate of 33% and under the previous consideration, the tax reduction factor Δ for the purpose of this work is given by

$$\Delta = \frac{1}{(1-t)} \times \left[1 - t \times \left(\sum_{j=1}^{T1} \frac{i_j}{(1+i_r)^j} + \sum_{j=1}^{T2} \frac{d_j}{(1+i_r)^j}\right)\right] \qquad (4.74)$$

$t =$ effective corporate tax income rate

$T1 =$ maximum number of years to apply the investment tax credit

$T2 =$ useful life of the power generating facility for accelerated depreciation purposes (in year) = 5

$i =$ investment tax credit

$d =$depreciation factor expressed as percentage of investment cost over T2 year.

The fiscal incentives granted by the Colombia Law 1715 only apply to not conventional energy sources installation and its components. In this way, the incentive tax factor only applies to the capital cost of photovoltaic and battery components. Therefore, Eq 4.54 is reformulated as

$$ACS_{adj} = \left[\left(CC_{pv} + CC_{bat}\right) \times \Delta + CC_{DG} + RC_{bat} + RC_{DG}\right] \times CRF(i_r, R) + O\&M_{pv} + O\&M_{bat} + O\&M_{DG} \quad (4.75)$$

4.4. OPTIMIZATION TECHNIQUES

4.4.1. PARTICLE SWARM OPTIMIZATION

The particle swarm optimization (PSO) is an evolutionary agent-based technique which simulates the social behavior of how a swarm moves in search of food. This method considers a swarm of p particles, where each particle´s position represents a possible solution in the design problem [12]. At each iteration, particle move towards an optimum solution, through its present velocity, its personal best solution $(pbest)$ obtained by themselves so far and the global best solution $(gbest)$ obtained by all particles. The basic concept of PSO is shown in Fig 14.

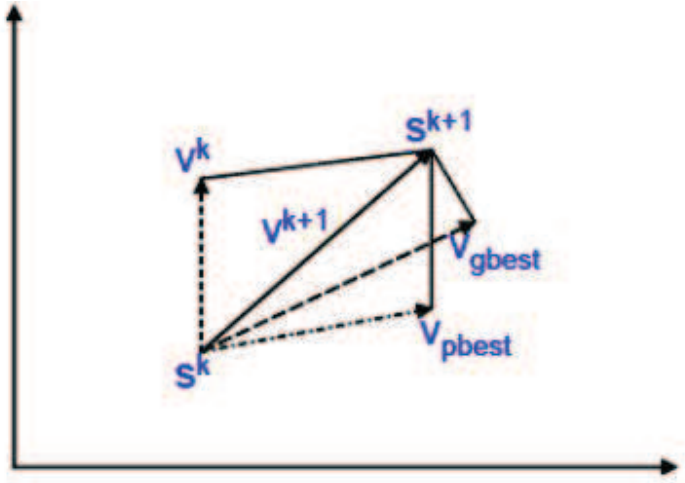

FIGURE 15. CONCEPT OF MODIFICATION OF A SEARCHING POINT BY PSO [55].

The position and the velocity of each particle is updated using equations 4.74 and 4.75 at each iteration[56].

$$v_i = w \times v_{i-1} + c_1 \times R_1 \times (pbest_{i-1} - s_{i-1}) + c_2 \times R_2 \times (gbest_{i-1} - s_{i-1}) \quad (4.76)$$

$$s_i = s_{i-1} + v_i \quad (4.77)$$

where s_i and v_i are the current position and velocity of particles. R_1 and R_2 are two uniformly distributed random numbers in the ranges (0,1). c_1 and c_2 are the acceleration coefficients that pull each particle towards the personal best $(pbest)$ and the global best $(gbest)$ positions respectively and are often set to be 2.0 and w is the inertia weight factor.

The success of PSO depends on values taken by the inertia weight. Without the first term of Eq. 4.74, the search will be reduced to a local search. If the inertia weight takes large values (other terms of this equation are almost omitted), the algorithm keeps exploring new spaces and then the convergence is delayed. Therefore, the inertia weight must be adjusted for a better exploration-exploitation trade-off [57]. This work uses a time-varying inertia weight adaptation described in [57] to update the inertia weight factor at each iteration.

$$w = (w_{max} - w_{min}) \times \frac{(Iter_{max} - it)}{Iter_{max}} + w_{min} \qquad (4.78)$$

where the value of w is linearly decreased from an initial value (w_{max}) to a final value (w_{min}) and $Iter_{max}$ and t denotes the maximum number of iterations and the current iteration respectively.

PSO technique is frequently used for optimization of stand-alone renewable energy systems due its advantages [20], [22], [55], [58], [59]. These advantages include code simplicity, ease of use, high convergence speed and minimum storage requirements, in addition to slightly less dependence on the initial population compared to other algorithms, making it a strong convergent algorithm [60]. The main parameters of the PSO algorithm used are presented in Table 12. Figure 15 summarizes the PSO structure in hybrid system sizing [13].

TABLE 12. MAIN PARAMETERS OF PSO ALGORITHM

$Iter_{max}$	Maximum number of iterations
$nPop$	Population Size
w	Inertia Coefficient
w_{max}	Inertia Coefficient max
w_{min}	Inertia Coefficient min
c_1	Personal Acceleration Coefficient
c_2	Social Acceleration Coefficient

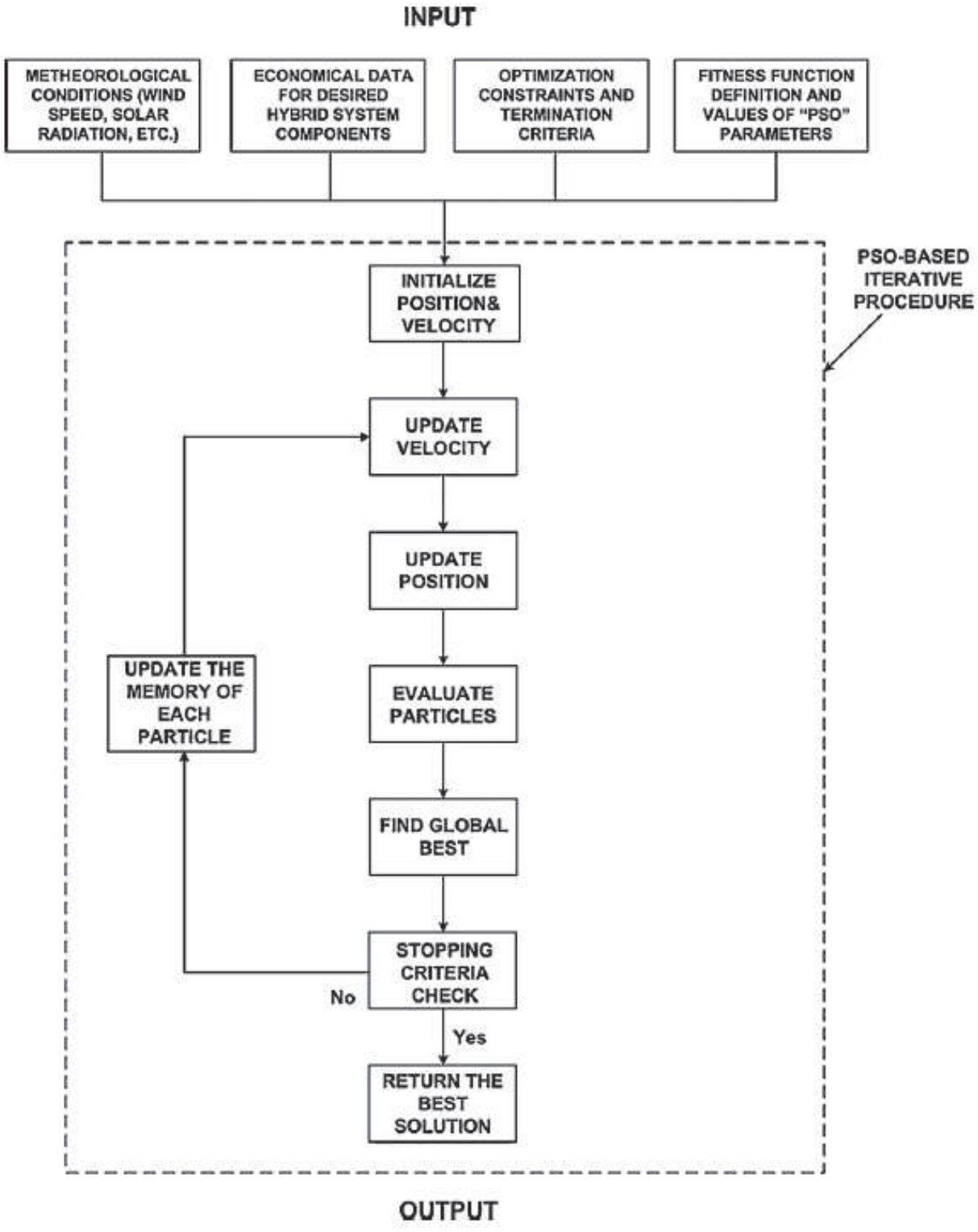

FIGURE 16. FLOWCHART PSO [13].

4.5. MODELS DESCRIPTION

This section describes the PSO models developed in this work. Four models are developed depending on the system configuration: Diesel only, Diesel-Photovoltaic, Photovoltaic-with energy storage, and Diesel-Photovoltaic with energy storage. Also, the following MATLAB sub-models are described: Irradiance, load profile, photovoltaic power generation and 4 load flow sub models according the system configuration. These functions were developed in this work as were required in the optimization models.

4.5.1. SUB-MODELS.

This section describes the sub-model developed in this project which are required to complete the main optimization models. For each sub-model describe a MATLAB function is created.

4.5.1.1. IRRADIANCE FUNCTION

The function routine ***"irradiance.m"*** is created. This routine generates an array with a one-year hourly resolution average irradiance over the plane for an arbitrary inclined surface. The calculation methodology used in this routine is described section 4.2.1. Figure 16 shows the flowchart of the function.

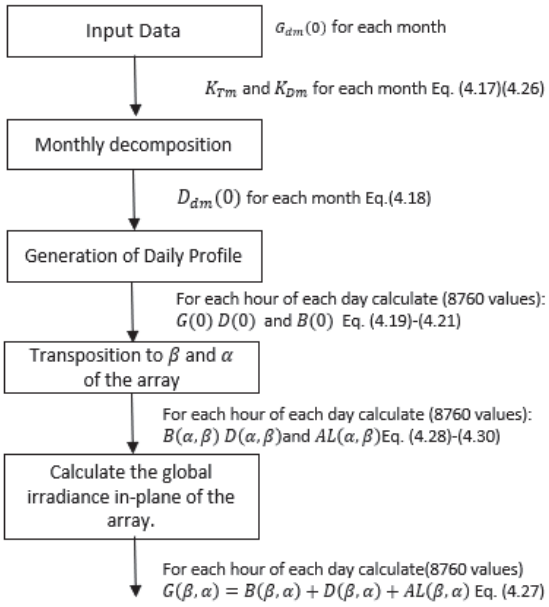

FIGURE 17. FLOWCHART IRRADIANCE FUNCTION.

The worksheet ***"input_irradiance"*** in the Excel file ***"data.xls"*** is created to fill the input data required. In addition, the Excel file ***"meteo_output.xls"*** is generated containing the hourly and monthly data of the direct, diffuse and global irradiance over the horizontal and over the plane of the array for the input parameters employed.

4.5.1.2. LOAD PROFILE FUNCTION

A MATLAB routine is developed to generate the hour resolution long-year electrical demand array. Three functions are created, each for the three approaches as described in section 4.2.2: ***"Loadprofile1.m", "Loadprofile2.m"*** and ***"Loadprofile3.m"***. Figures 17 shows the flowcharts of load profile functions.

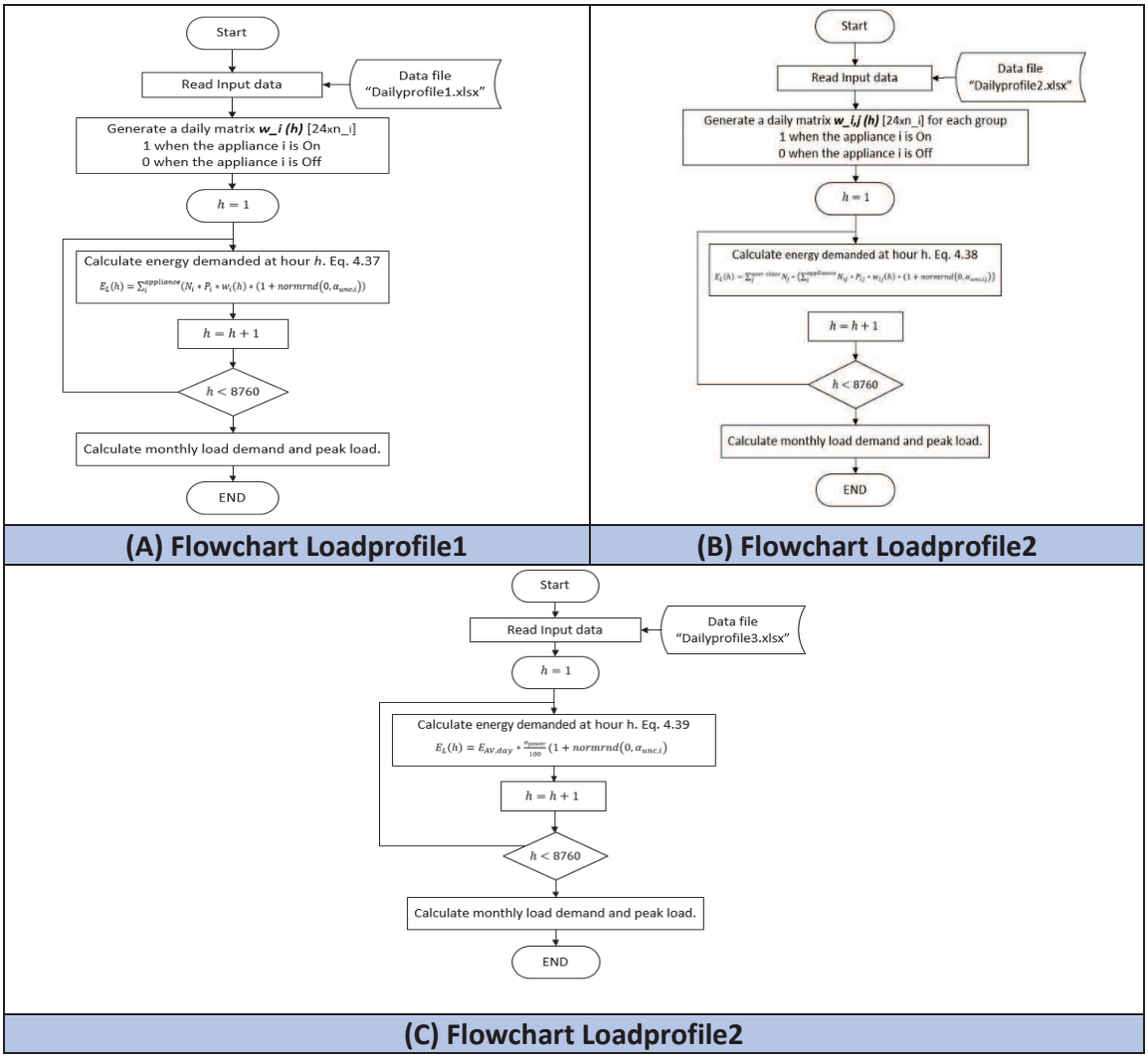

FIGURE 18. FLOWCHART LOAD PROFILE FUNCTION: (A) LOADPROFILE1 (B) LOADPROFILE2 (C) LOADPROFILE3

Excel templates: ***"DailyProfile1.xlsx"***, ***"DailyProfile2.xlsx"*** and ***"DailyProfile3.xlsx"***; are created to simplify the introduction of the input data needed for each load demand estimation approach. The daily load profile values obtained by these functions can be show graphically.

4.5.1.3. PHOTOVOLTAIC POWER FUNCTION.

The MATLAB function generates an array with a one-year hourly resolution photovoltaic generation in kWh. The calculation method is described in Section 4.3.1 where Eq. 4.40. is used to calculate the photovoltaic production for each hour. The temperature of the cell is calculated based on the monthly average ambient temperature and the irradiance over the plane of the array. The ***"pvpower.m"*** is developed. Figures 18 shows the flowchart of pvpower function.

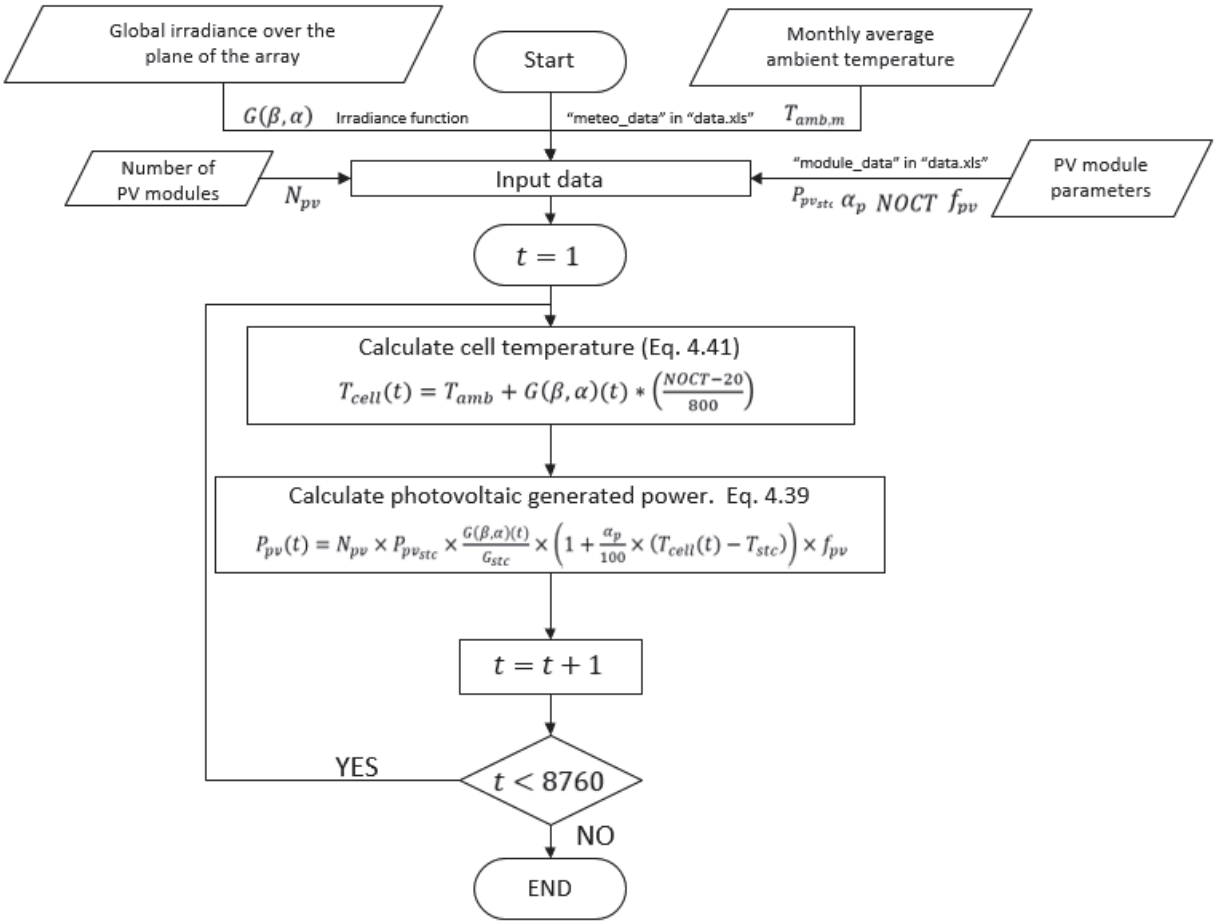

FIGURE 19. FLOWCHART PVPOWER FUNCTION

The global irradiance over the plane and the monthly average ambient temperature are obtained as result of the irradiance function. The rest of the inputs can be filled out at the worksheet ***"module_data"*** of the ***"data.xls"*** file to therefore be read by the MATLAB routine.

4.5.1.4. SYSTEM SUB-MODEL

A sub-model is developed for each of the four-architecture described in this work in section 4.3.4. The objective of each sub model is to calculate the Annualized Cost of System for an off-grid network for a given set of input parameters. The input data required by each model can be fill out in the Excel template "data.xls". This model also calculates the LPSP, the ENS and the LCOE for a given configuration. Figure 19, 20, 21 and 22 describe the flowchart of each sub-model.

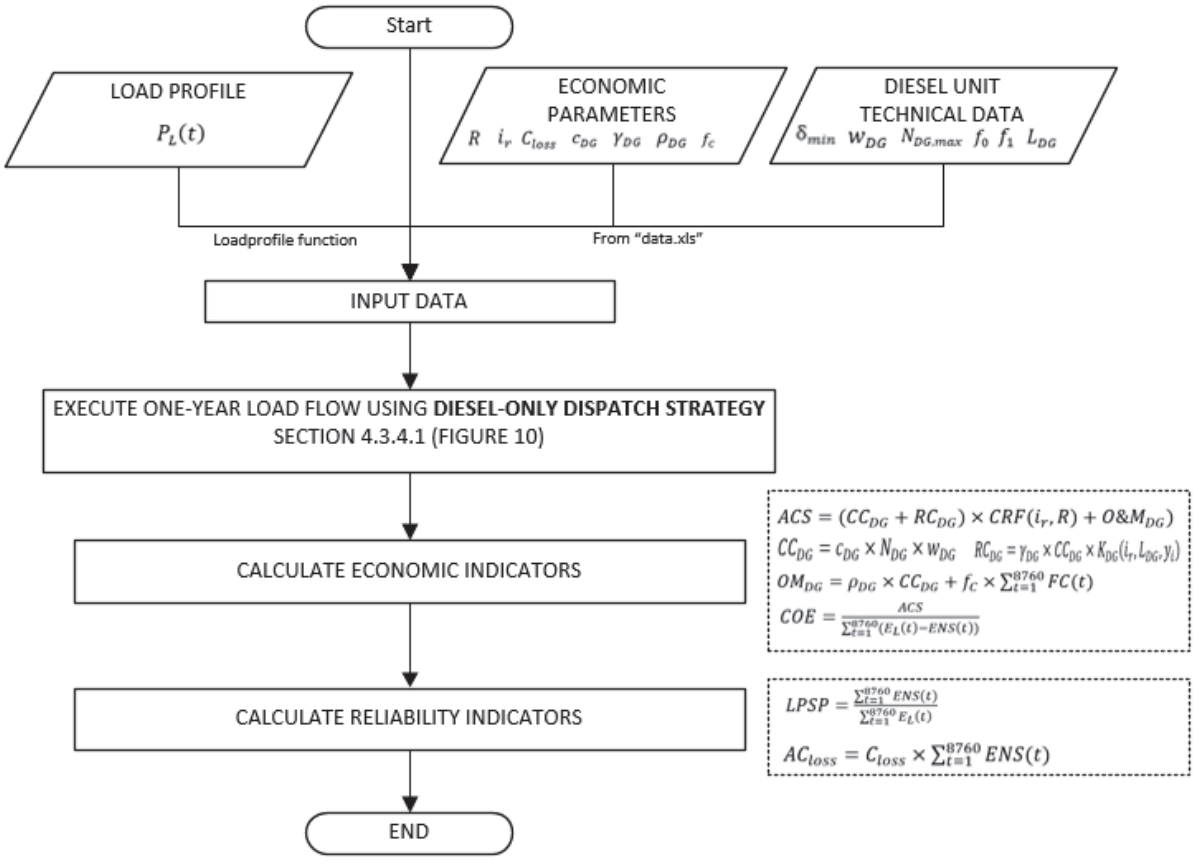

FIGURE 20. FLOWCHART DG ONLY SUB-MODEL

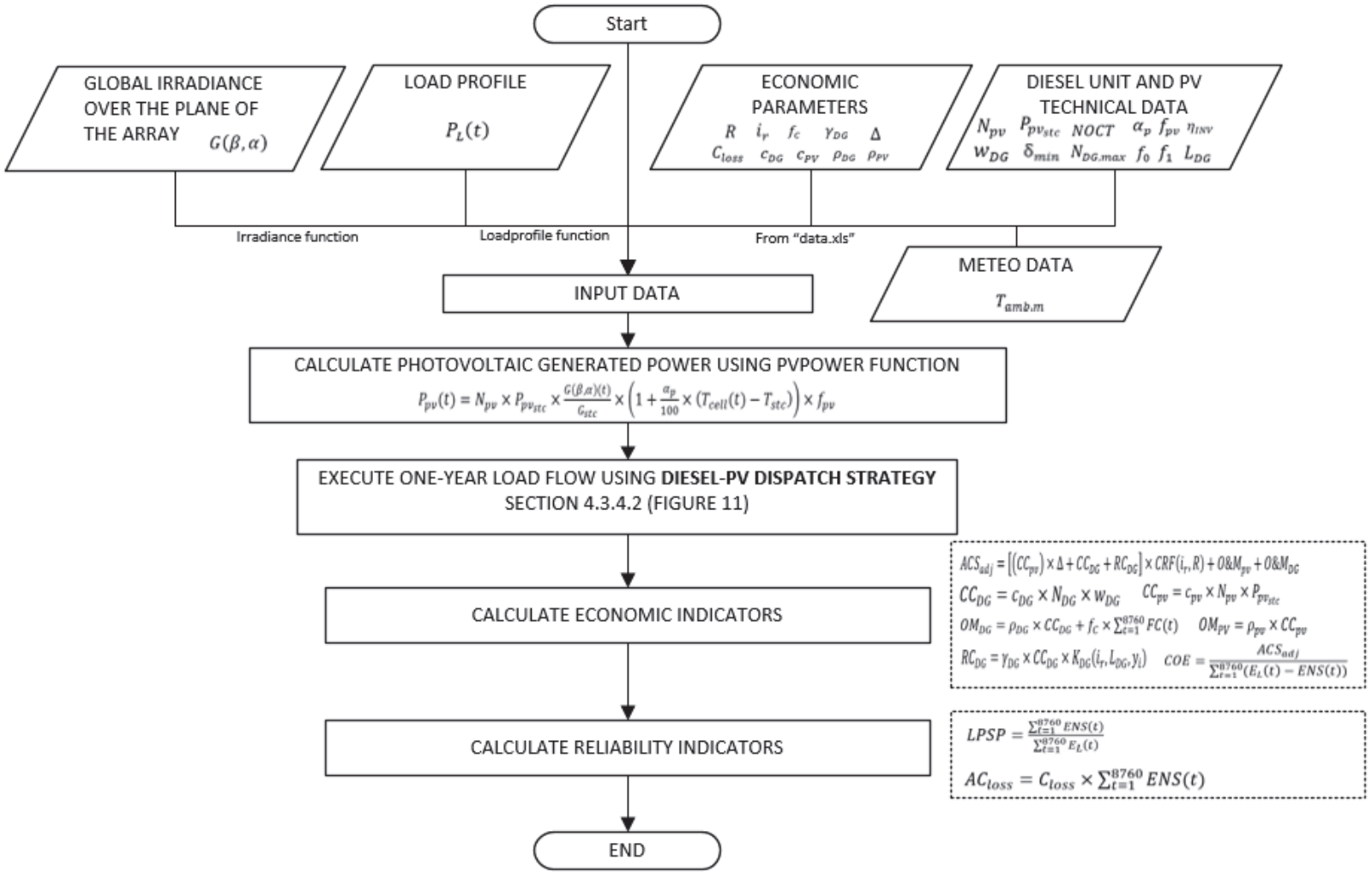

FIGURE 21. FLOWCHART DG-PV SUB-MODEL

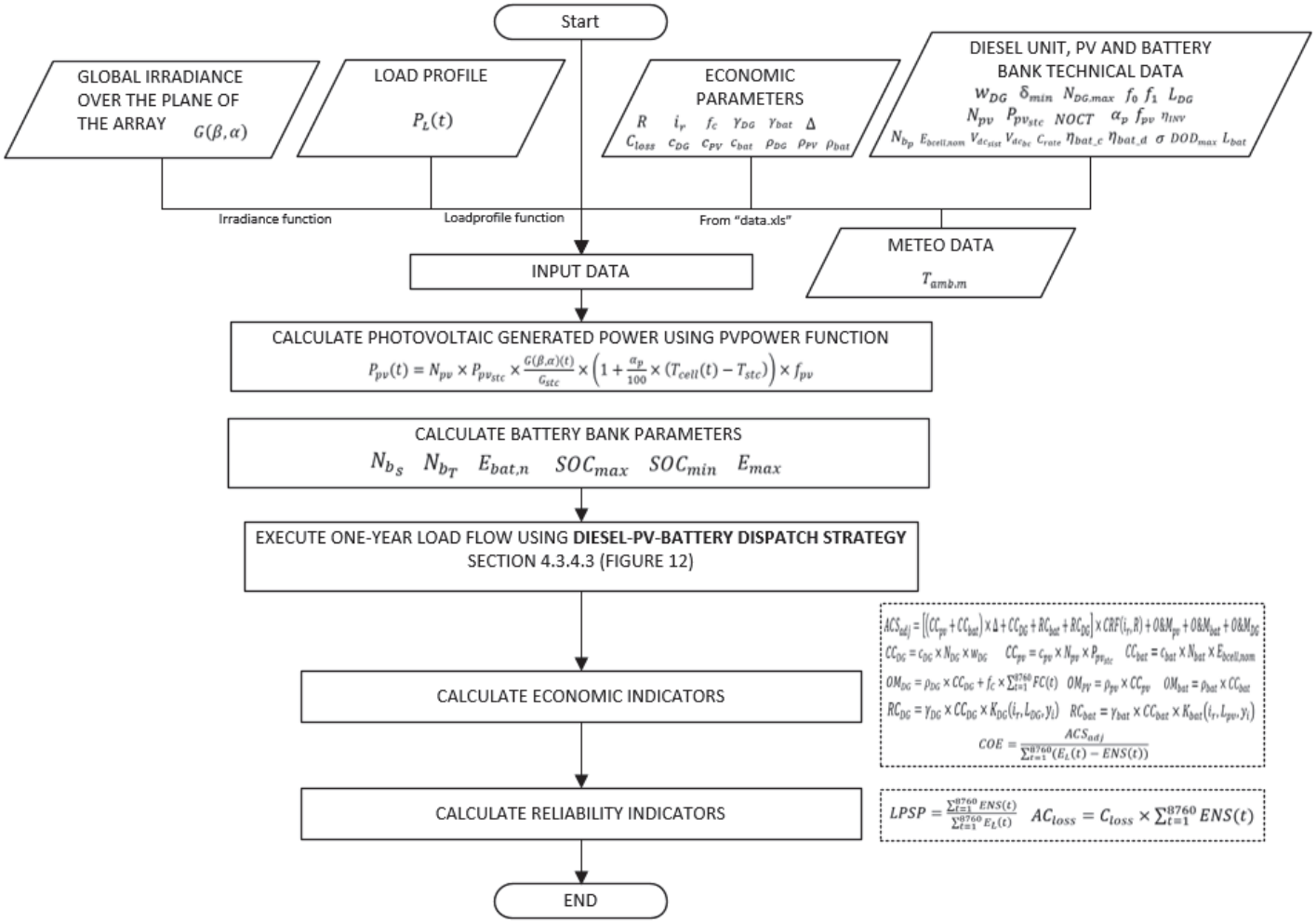

FIGURE 22. FLOWCHART DG-PV-BATTERY SUB-MODEL

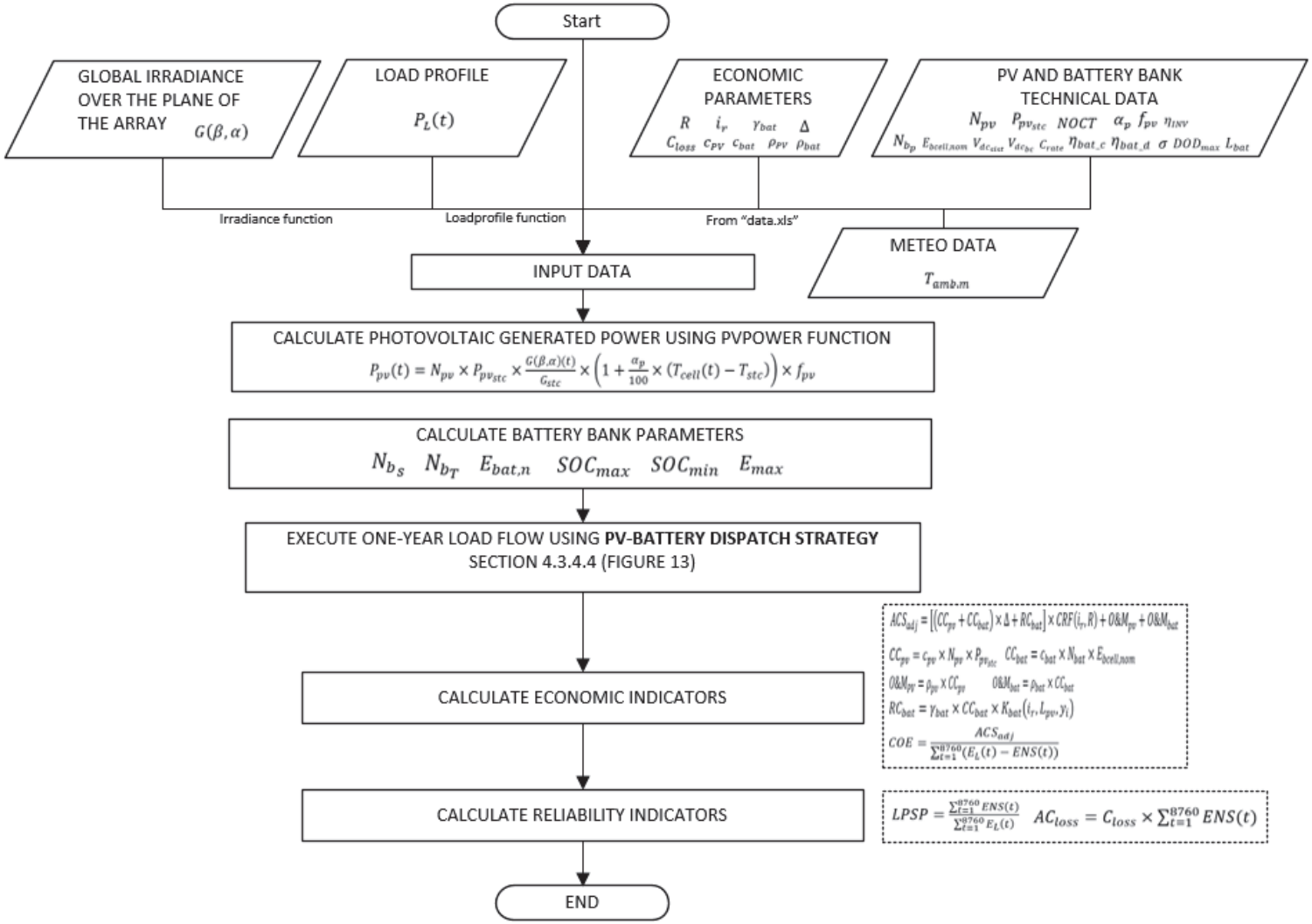

FIGURE 23. FLOWCHART PV-BATTERY SUB-MODEL

4.5.2. PROBLEM FORMULATION

This work aims to develop an optimization model for sizing an energy system to supply the energy demand on an off-grid location. The optimization of these systems could be complex, since many variables are naturally stochastic depends mostly on the characteristic of the solar resource and the load profile of the selected location. Four system architecture are considered on this work as previous sections describes. In this work, each system architecture considered is evaluated independently. The objective is to minimize the total cost of the solution and maximize the reliability of the supply.

As result of the optimization problems the following information is obtained.

- Most cost convenient system architecture.
- Amount of photovoltaic modules and therefore the total photovoltaic power in kWp.
- Amount of diesel generation units and the total diesel energy power in kWp.
- Amount of battery cell required and total capacity of the energy storage system in kWh.
- Energy flow in the system showing the different states of the system according to the dispatch strategy described in this work.
- Discriminated cost of each technology in terms of initial capital required and O&M cost.
- Annualized cost of energy (COE) of the best solution.
- Amount and cost of energy not supply and LPSP.

This section describes the model developed in this work. First, the input parameters are described, then the objective function is presented and lastly the flowchart of the model is explained.

4.5.2.1 INPUT DATA

First, the meteorological and load profile data required by the respectively sub-model is necessary. Second, the technical data of each component of the system must be supplied. Then, parameters related to the economical evaluation are required. Table 13 describes the input data required by the main model. Some input parameters can be not required according to the system architecture to be evaluated.

TABLE 13. INPUT PARAMETERS.

Meteorological Inputs					
ϕ	Latitude degrees north reference in decimal format				
L_{loc}	Longitude of the location East positive				
ΔT_{gmt}	Local time zone				
β	Tilt of the inclined plane [0-90°]				
α	Surface azimuth angle [0S 90W]				
ρ	Ground reflection factor				
$G_{dm}(0)$	Average daily horizontal global irradiation of a month				
Load Profile Inputs					
Load profile sub-model 1		**Load profile sub-model 2**		**Load profile sub-model 3**	
i	Description of the electrical appliance	i	Description of the electrical appliance	$E_{AV,day}$	Average energy demanded in a day
N_i	Number of electrical appliances	j	User class	α_{power}	Percentage of daily demand
P_i	Nominal power of each electrical appliance	N_j	Number of user class		
h_i	Daily overall time each appliance is in use	N_{ij}	Number of electrical appliances for user class		
w_i	Period during the day when each appliance can be used	P_{ij}	Nominal power of each electrical appliance and each user class		
		w_{ij}	Period during the day when each appliance can be used for each user class		
Technical Inputs					
Diesel model		**Photovoltaic model**		**Battery model**	
$N_{DG,max}$	Maximum number of DG unit	$P_{pv_{stc}}$	Rated power of the solar module in STC	$V_{dc_{bc}}$	Battery Voltage
δ_{min}	Minimum load ratio allowed	η_{INV}	Inverter Efficiency	$V_{dc_{sist}}$	DC system voltage (Vdc_sist)
L_{DG}	Lifecycle [Years]	α_P	Pmax Temperature Coefficient [%/°C]	C_{rate}	Capacity Rate [h]
ρ_{DG}	Fixed OM value as percentage of the diesel initial investment	$NOCT$	NOCT [°C]	η_{bat_c}	Charge efficiency
f_0	Fuel Curve intercept coefficient	f_{PV}	Photovoltaic derating factor	η_{bat_d}	Discharge efficiency
f_1	Fuel curve slope coefficient			σ	Self-Discharge rate
				L_{bat}	Lifecycle [years]
				DOD_{max}	Maximum Depth of Discharge
Economic Inputs					
R	Time of the project [years]				
i_r	Real interest rate [%]				
c_{loss}	Cost of energy loss [USD/kWh]				
Δ	Fiscal Incentive Factor				
f_C	Fuel Cost [USD/l]				
δ_{DG}	De-rate factors of the initial capital cost invested				
c_{DG}	Cost per unit installed for each component				
c_{PV}	Cost per Wp installed [USD/Wp]				
ρ_{PV}	Fixed OM factor as ratio of the PV CC				
δ_{bat}	Factor of the initial capital cost invested for the battery bank				
ρ_{bat}	Fixed OM value as percentage of the battery bank initial investment				

The components of the position particle depend on the architecture of the system. The **decision variables** of the problem are represented as each component of the position particle. Table 14 describes structure of the position particle for each of the four architectures considered in this work.

TABLE 14. POSITION PARTICLE STRUCTURE

SYSTEM ARCHITECTURE	POSITION PARTICLE
Diesel-only	$[w_{DG}]$
Photovoltaic-Diesel	$[N_{pv}, w_{DG}]$
Photovoltaic-battery	$[N_{pv}, N_{b_p}, E_{bcell,nom}]$
Diesel-photovoltaic-Battery	$[N_{pv}, w_{DG}, N_{b_p}, E_{bcell,nom}]$

Each component of the position particle is limited by a lower and upper boundary; in this way the problem can be framed reducing the processing time. The number of PV modules, N_{pv}, and the number of battery cells in parallel, N_{b_p}, are integer values, and DG unit nominal power in kW, w_{DG}, and the battery cell nominal capacity in kWh, $E_{bcell,nom}$, are restricted to a list of elements in the ***"Elements database"*** worksheet in the ***"Data.xls"*** file. Since the PSO algorithm employs real values in each iteration, it is required a correction step where each component of the position particle is converted to the nearest possible value permitted. Table 15 shows the main parameters used in the PSO algorithm developed.

TABLE 15. MAIN PARAMETERS OF PSO ALGORITHM DEVELOPED

Symbol	Description
N_{pv_l}	Lower bound number of PV module
w_{DG_l}	Lower bound nominal power of Diesel
$N_{b_{p_l}}$	Lower bound number of Battery cell in parallel
E_{bcell,nom_l}	Lower bound nominal capacities of battery cell kWh
N_{pv_u}	Upper bound number of PV modules
w_{DG_u}	Upper bound nominal power of Diesel unit in kW
$N_{b_{p_u}}$	Upper bound number of Battery cell in parallel
E_{bcell,nom_u}	Upper bound nominal capacity of battery cell kWh
$Iter_{max}$	Maximum number of iterations
$nPop$	Population Size
w	Inertia Coefficient
w_{max}	Inertia Coefficient maximum
w_{min}	Inertia Coefficient minimum
c_1	Personal Acceleration Coefficient
c_2	Social Acceleration Coefficient

4.5.2.2. OBJECTIVE FUNCTION

The objective of this work and thus the PSO algorithm developed is sizing hybrid power generation systems (solar-diesel) battery-backed, in non-interconnected zones, which minimizes the total cost of the solution and maximize the reliability of supply. To minimize the total cost of the system, it is used the Eq. 4.67 described in section 4.4.1 using the annualized cost of the system adjusted by the fiscal incentives as defined in Eq. 4.75 resulting:

$$COE_{adj} = \frac{ACS_{adj}}{\sum_{t=1}^{8760}(E_L(t) - ENS(t))} \quad (4.79)$$

$$COE_{adj} = \frac{\left[(CC_{pv} + CC_{bat}) \times \Delta + CC_{DG} + RC_{bat} + RC_{DG}\right] \times CRF(i_r, R) + O\&M_{pv} + O\&M_{bat} + O\&M_{DG}}{\sum_{t=1}^{8760}(E_L(t) - ENS(t))} \quad (4.80)$$

On cases where one or more the sources of generation are not considered in the system architecture, the economic parameters associated to those sources are equal to zero.

In this work, the reliability is treated as an economic indicator through the annualized cost of energy not supplied described in Eq.4.69. So, to maximize reliability of the system, it is necessary to minimize the annualized cost of energy not supplied. Either way, for each iteration the LPSP is calculated and showed.

As both, the economic and reliability indicators are calculated in terms of the annualized cost of energy, it is possible to treat the PSO developed in this work as a single objective problem. In Eq.4.81 both economic and reliability indicators are combined.

$$Cost = \frac{ACS_{adj} + AC_{loss}}{\sum_{t=1}^{8760}\left(E_L(t) - ENS(t)\right)} \quad (4.81)$$

The objective in the PSO algorithm developed in this work is to minimize the function Cost described by Eq. 4.81 regardless the architecture of the system considered.

4.5.2.3. MODEL DESCRIPTION

This method considers a swarm of p particles, where each particle´s position represents a possible solution in the design problem [12]. The position particle structure depends on the system architecture selected and is described in Table 14.

First, each particle is initialized with random position vectors. Since the PSO algorithm employs real values in each iteration, the components of the position vector are corrected to the nearest possible value permitted. One-year load flow is then computed for each particle, according to the dispatch strategy described in section 4.3.4. The objective function is then evaluated for each particle. The results obtained by each particle are saved as personal best solution $(pbest)$. Also, the best result among all particle is saved as the global best solution $(gbest)$.

Then, a loop starts until the maximum number of iterations is reached. In each step of the loop, the velocity vector and the position vector are updated using Eq. 4.76 and Eq. 4.77 respectively. The components of the position vectors are corrected. Next, the objective function is evaluated for each particle. If the result of each particle is better than its personal best, its personal best is updated. If a result obtained among all particles is better than the previous global best, the global best is updated. When the loop reaches the maximum number of iterations, the particle with the global best solution is presented as the best design option to minimize the system costs and maximize the reliability. At each iteration, the particle with the global best solution is presented.

The flowchart of the PSO algorithm developed in this work is presented in Figure 24.

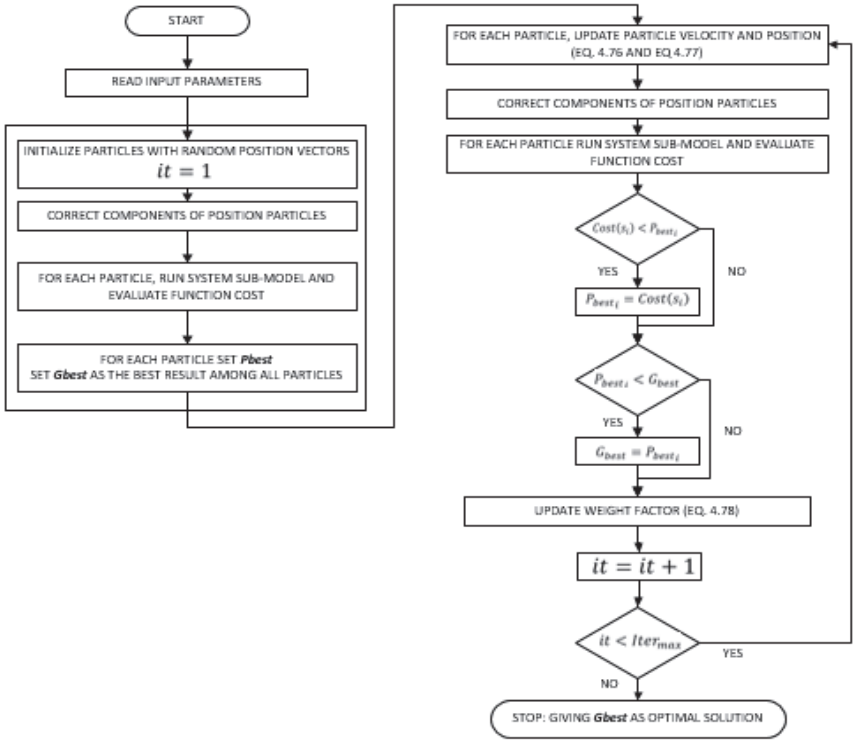

FIGURE 24. FLOWCHART PSO ALGORITHM.

Finally, Figure 25 shows the flowchart of the methodology for sizing HRE system proposed on this work. First, the system architecture must be selected, since the MATLAB routine and the required input data required depends on chosen architecture. Second, the meteorological, technical and economic data must be filled on the "data.xls" file on the selected folder. Third, a daily profile strategy must be selected and then fill the required information on the respectively daily profile input file. Lastly, the *"main"* routine on the folder must be executed. This main routine will use employ the sub-model described on previous sections of this work to obtain a solution of the sizing problem. It is recommended to repeat this process for each system architecture and then compare the results obtained to select the most suitable solution.

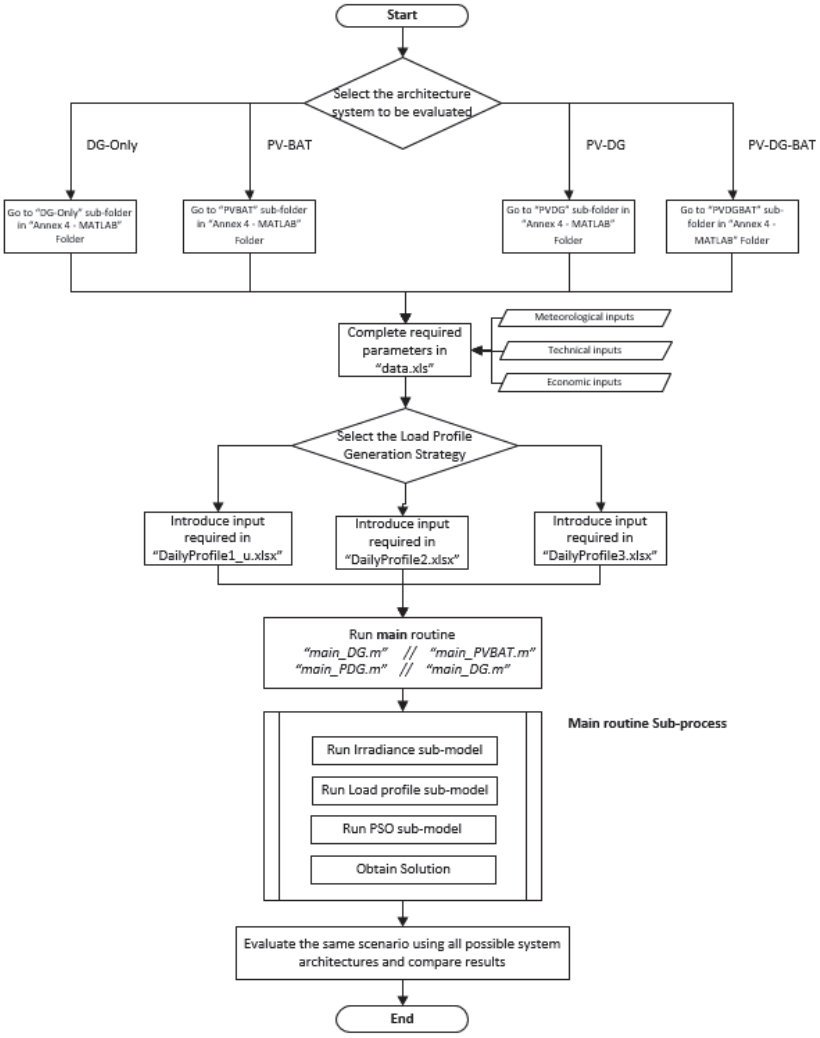

FIGURE 25. SIZING METHODOLOGY FLOWCHART.

CHAPTER V

CASE OF STUDY

In this section, the developed model is applied to optimize the sizing of a hybrid renewable energy solution. Three cases are evaluated, each case using a different load profile estimation approach. Also, each case is evaluated using the following solutions: Diesel only; Solar-diesel; solar-battery and solar-diesel battery solution. The results are compared and discussed. Lastly, the results are contrasted with the results obtained with commercial software HOMER.

5.1. INPUT DATA

5.1.1. IRRADIANCE INPUTS

The monthly average daily global horizontal irradiance, G_{dm}, and the monthly average ambient temperature, $T_{amb,m}$, for the selected location is taken from the platform "Pvplanner" from Solargis. This company provides reliable and accurate solar, weather and solar electricity data that are used in the whole lifecycle of solar power plants. Table 16 shows the input data for the selected location. The output file with the meteorological data from Solargis can be found in the Annex 1 of this work.

The monthly global irradiance over the horizontal and over the plane of the array is calculated using the MATLAB routine developed in this work and then compared with results obtained from Solargis. Table 17 shows the results obtained. The difference can be accounted to the simplicity of the transposition model used in our MATLAB routine, nevertheless the results are good enough for the purpose of this work.

TABLE 16 METEOROLOGICAL INPUT PARAMETERS

Location	Islote de Santa Cruz, Colombia	
Latitude	9.79	
Longitude	-75.859167	
Time Zone (GTM)	-5	
Tilt	10	Plane inclination
Azimuth	0	Plane orientation (South = 0°; West 90°)
GRF	0.2	Ground Reflection Factor (0-1) Default=0.2
Month	Daily sum of global irradiation [Wh/m2]	Average diurnal (24-hour) air temperature [deg. C]
January	5922.6	27.8
February	6271.4	27.6
March	6267.7	27.6
April	5906.7	27.7
May	5367.7	27.9
June	5396.7	28.5
July	5587.1	28.7
August	5538.7	28.5
September	5363.3	28.2
October	5025.8	27.9
November	4970.0	27.8
December	5200.0	28.0
Average	5568.1	28.0

Source: Solargis [61]

TABLE 17 METEOROLOGICAL INPUT PARAMETERS

MONTH	Monthly sum of global horizontal irradiation [kWh/m2] Solargis	Monthly sum of global horizontal irradiation [kWh/m2] Calculated	Deviation [%]	Monthly sum of global tilted irradiation [kWh/m2] Solargis	Monthly sum of global tilted irradiation [kWh/m2] Calculated	Deviation [%]
Jan	183.6	182.0	-0.88%	201.9	198.6	-1.65%
Feb	175.6	174.2	-0.81%	186.9	184.3	-1.41%
Mar	194.3	193.0	-0.68%	198.5	196.2	-1.14%
Apr	177.2	176.1	-0.65%	175	172.9	-1.17%
May	166.4	165.2	-0.70%	160.1	158.8	-0.83%
Jun	161.9	160.8	-0.71%	153.6	152.6	-0.65%
Jul	173.2	172.0	-0.69%	165.3	163.9	-0.84%
Aug	171.7	170.6	-0.65%	167.8	166.1	-1.03%
Sep	160.9	159.8	-0.70%	162	160.1	-1.17%
Oct	155.8	154.4	-0.91%	162.4	159.5	-1.79%
Nov	149.1	147.7	-0.96%	160.5	157.1	-2.13%
Dec	161.2	159.7	-0.93%	177.8	174.1	-2.09%
Year	2030.9	2015.3	-0.77%	2071.8	2044.1	-1.34%

(Source: Own preparation)

Figure 26 shows the daily global profile on the horizontal and on the tilted plane for the first four days of the year calculated for the selected location. The effect of shadows or cloudiness is not considered in this project.

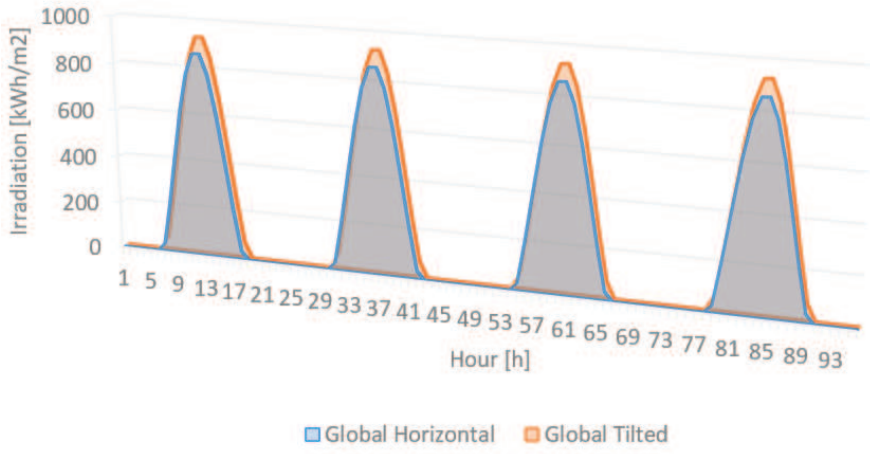

FIGURE 26. DAILY GLOBAL IRRADIATION CALCULATED FOR "ISLOTE DE SANTA CRUZ".

5.1.2. LOAD PROFILE INPUTS

In this section, there are showed the input data for three different scenarios for daily load profile estimation. The first scenario presents the daily load profile of a single user obtained from a load survey. The second scenario shows the daily load profile generated for a community based on a load survey. Lastly, it is presented the daily load profile generated from the average daily load profile data measured.

5.1.2.1 Daily load profile for a single user from a survey

A small rural house is used as an example to test the optimization model developed. Table 18 shows the input data required. Figure 27 shows the resulting daily load profile.

TABLE 18. EXAMPLE OF LOAD ON A RURAL HOUSE WITH UNCERTAINTIES

Electrical Appliance	Qty	Nominal Power [W]	Daily use [h/day]	Functioning Windows 1 $w_{i,1}$		Functioning Windows 2 $w_{i,2}$		Functioning Windows 3 $w_{i,3}$		Uncertainty Factor [%]	Daily energy [Wh/day]
i	N_i	P_i	h_i	h_{start}	h_{stop}	h_{start}	h_{stop}	h_{start}	h_{stop}	α_{unc}	$E_{L,d,i}$
Lamps	2	10	4	19	23	-	-	-	-	20	80
TV	1	75	3	13	14	18	20	-	-	30	225
Radio	1	50	2	8	10	-	-	-	-	10	100
Fan	1	60	2	12	14	-	-	-	-	15	120
Fridge	1	40	24	0	24	-	-	-	-	20	960

(Source: Own preparation)

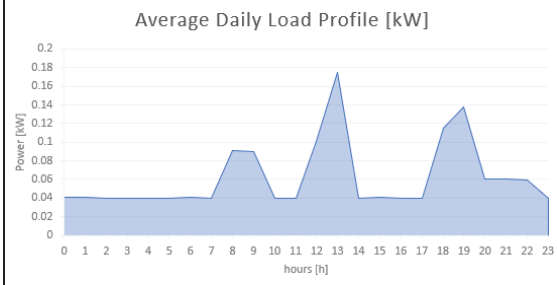

(A) AVERAGE DAILY LOAD PROFILE

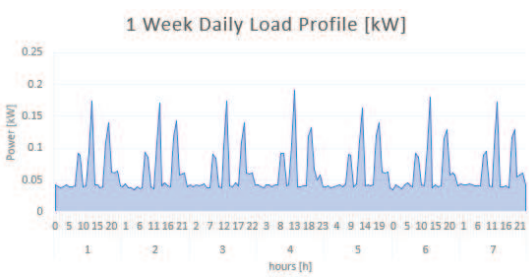

(B) DAILY LOAD PROFILE FOR A WEEK.

FIGURE 27. DAILY LOAD PROFILE CURVES FOR A SINGLE USER

The "LoadProfile1_Data.xlsx" Excel file with the load survey and the array generated with 8760 load demand values per hour of a year can be found in Annex 1.

5.1.2.2 Daily load profile for a community from a survey

In this work, a community with 3 user classes is used as example to model the daily load profile. The input data required by each user class is presented in Table 19. Figure 28 shows the resulting daily load profile generated by the MATLAB routine.

TABLE 19. EXAMPLE OF LOAD ON A RURAL HOUSE WITH UNCERTAINTIES

User class	Qty	Electrical Appliance	Qty	Nominal Power [W]	Daily use [h/day]	Functioning Windows 1 $w_{i,1}$		Functioning Windows 2 $w_{i,2}$		Functioning Windows 3 $w_{i,3}$		Uncertainty Factor [%]
j	N_j	i	N_i	P_i	h_i	h_{start}	h_{stop}	h_{start}	h_{stop}	h_{start}	h_{stop}	α_{unc}
Household_1	50	Lamps	2	10	4	19	23	-	-	-	-	20
		TV	1	75	3	13	14	18	20	-	-	30
		Radio	1	50	2	8	10	-	-	-	-	10
		Fan	1	60	2	12	14	-	-	-	-	15
		Fridge	1	40	24	0	24	-	-	-	-	20
Household_2	30	Lamps	2	10	5	6	8	17	20	-	-	15
		TV	1	75	2	18	20	-	-	-	-	30
		Fridge	1	40	24	0	24	-	-	-	-	0
School	2	Lamps	16	10	6	8	14	-	-	-	-	20
		Lamps	4	20	6	16	22	-	-	-	-	20
		TV	1	75	2	8	9	15	16	-	-	10
		PC	1	150	2	8	10	-	-	-	-	10
		Fridge	1	40	24	0	24	-	-	-	-	0

(Source: Own preparation)

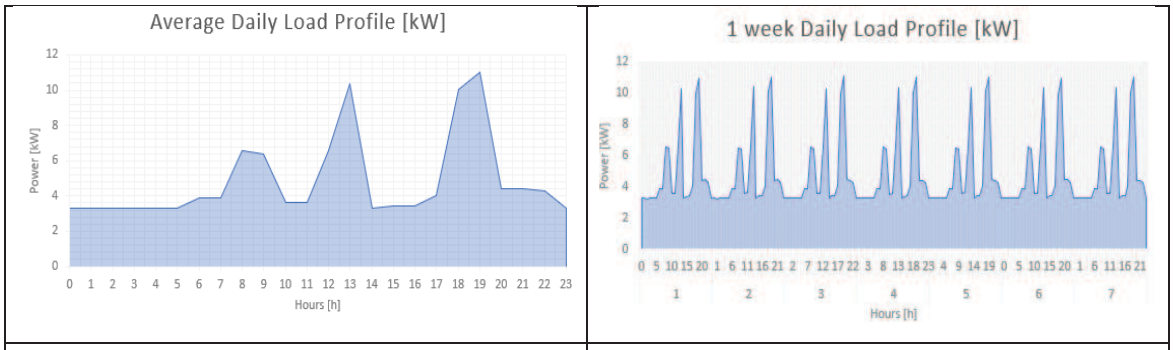

(A) AVERAGE DAILY LOAD PROFILE | **(B) DAILY LOAD PROFILE FOR A WEEK.**

FIGURE 28. DAILY LOAD PROFILE CURVES FOR A COMMUNITY

The "LoadProfile2_Data.xlsx" Excel file with the load survey and the array generated with 8760 load demand values per hour of a year can be found in Annex 1.

5.1.2.3 Daily load profile for a community from measured electrical demand

Lastly, the average daily load profile from the community "Santa Cruz del Islote" in Bolivar, Colombia, is introduced. This rural community is selected to evaluate the optimization model developed in this work. Presently, this community has a Diesel-Solar with battery backup energy system to supply the load. Figure 29 shows the schematic one-line diagram of the generation system in this location.

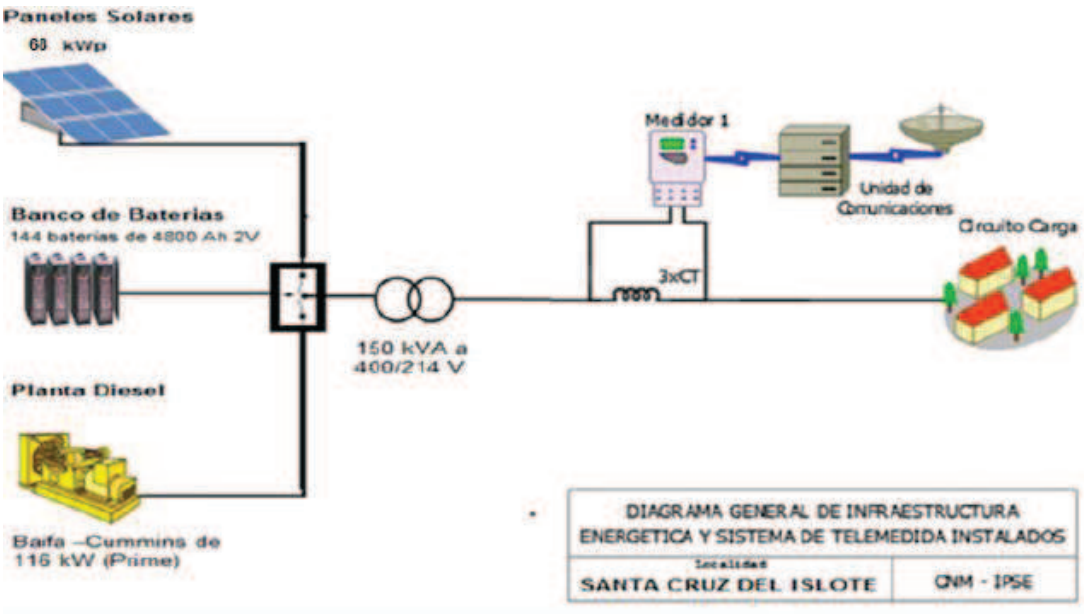

FIGURE 29. SCHEMATIC ONE-LINE DIAGRAM OF "SANTA CRUZ DEL ISLOTE" [62]

The load profile data is obtained from the National Monitoring Center (CNM) of the IPSE (Instituto de Planificación y Promoción de Soluciones Energéticas para las Zonas no Interconectadas)[62]. Figure 30 shows the average daily load profile curve in July 2017 and July 2018 of the location.

FIGURE 30. DAILY LOAD PROFILE CURVE "SANTA CRUZ DEL ISLOTE" JULY 2017-2018 [62]

This information is used as input data to execute the MATLAB routine developed for the third daily load profile estimation approach. Table 20 shows the input data used to generate the daily load profile curve. Figure 31 shows the daily load profile curves generated by the MATLAB routine developed in this work.

TABLE 20. DAILY LOAD PROFILE FOR "SANTA CRUZ DEL ISLOTE" JULY 2018

Hour	Power [%]	Uncertainty factor [%]	Hour	Power [%]	Uncertainty factor [%]
h	α_{power}	α_{unc}	h	α_{power}	α_{unc}
0	7.78	10	12	0.96	10
1	7.68	10	13	2.88	10
2	7.40	10	14	5.67	10
3	7.20	10	15	5.86	10
4	6.34	10	16	3.75	10
5	1.15	10	17	1.54	10
6	0.00	0	18	0.96	10
7	0.00	0	19	6.24	10
8	0.00	0	20	8.65	10
9	0.00	0	21	8.65	10
10	0.00	0	22	8.65	10
11	0.38	10	23	8.26	10
Yearly average daily energy demand [kWh], $E_{AV,day}$					520.5

(Source: Own preparation)

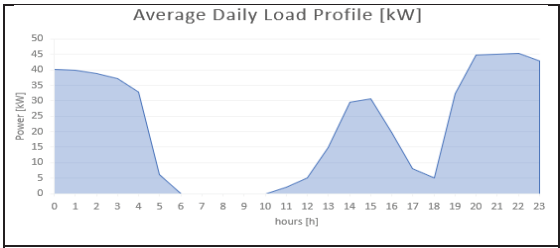

(A) AVERAGE DAILY LOAD PROFILE

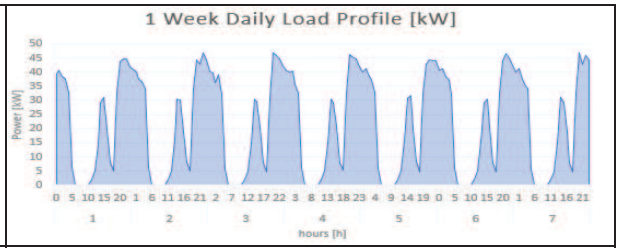

(B) DAILY LOAD PROFILE FOR A WEEK.

FIGURE 31. DAILY LOAD PROFILE CURVES GENERATED FOR "SANTA CRUZ DEL ISLOTE"

The "LoadProfile3_Data.xlsx" Excel file with the load survey and the array generated with 8760 load demand values per hour of a year can be found in Annex 1.

5.1.3. TECHNICAL INPUTS

This section describes the technical inputs required by the photovoltaic, diesel and battery model employed in the optimization model developed in this work.

5.1.3.1 Photovoltaic Module technical data

A monocrystalline PV module of 300 Wp, reference JKM300M-60, from the company JINKO SOLAR, is used. Table 21 shows the technical characteristics of the PV module selected. The cost per Wp installed presented in Table 21 include other costs not related to the price of the PV modules as the cost of charge controller, the PV inverters and the mounting structure. Also, this price includes indirect cost associated to the PV installation as engineering studies costs, logistic costs and certification costs. The cost per Wp presented is taken as reference and is provided by experts consulted in companies of energy sector.

TABLE 21. PV MODULE TECHNICAL INPUTS

Symbol	Description	Value
$P_{pv_{stc}}$	Maximum Power [Wp]	300
V_{mpp}	Maximum Power Voltage [V]	32.6
I_{mpp}	Maximum Power Current [A]	9.21
V_{oc}	Open-circuit Voltage [V]	40.1
I_{sc}	Short-Circuit Current [A]	9.72
η_{pv}	Module Efficiency (%)	18.33
α_P	Power Temperature Coefficient [%/°C]	-0.39
α_V	Voc Temperature Coefficient [%/°C]	-0.29
α_I	Isc Temperature Coefficient [%/°C]	0.05
$NOCT$	NOCT [°C]	45
c_{PV}	Cost per Wp installed [USD/Wp]	2
ρ_{PV}	Fixed OM factor as ratio of the PV CC	0.01
f_{PV}	Photovoltaic derating factor	0.85
η_{INV}	Inverter Efficiency	0.9

In the Diesel-PV architecture, the price per Wp installed is reduced by 25% since charge controllers are not required and grid-tie inverters are usually cheaper than off-grid inverters. The datasheet of this PV module can be found in Annex 1 on the PV module folder.

5.1.3.2 Diesel gen-set technical data

The input data required by the Diesel generation model is presented in Table 22. This information is collected from expert opinions on companies in the energy sector. This information must be validated each time the optimization model is used since can vary depending on the studied case.

TABLE 22. DIESEL MODEL TECHNICAL INPUTS

DIESEL INPUT DATA		
Symbol	Description	Value
$N_{DG,max}$	Maximum number of DG unit	5
δ_{min}	Minimum load ratio allowed	0.3
L_{DG}	Lifecycle [Years]	10
ρ_{DG}	Fixed OM value as percentage of the diesel initial investment [%]	0.1
f_C	Fuel Cost [USD/l]	0.8

Table 23 shows a database of Diesel generation units with the cost per kW and the fuel curve parameters. This table is built using information supplied by the Colombian Regulation Commission of Energy and Gas (CREG- Comisión de Regulación de Energía y Gas) in [63]. The cost per kW presented in Table 23 includes the direct and indirect costs related to the installation of a Diesel plant in non-interconnected zones.

TABLE 23. DIESEL GEN-SET UNITS DATABASE

DG POWER [kW]	Cost per kW installed [USD/kW]	De-rate factors of the initial capital cost invested [%]	1/2 Load 1 Hour in liters	Full Load 1 Hour in liters	f0 [L/kWh]	f1 [L/kWh]
10	2,724.09	31.83	1.4	2.6	0.020	0.240
20	1,697.26	32.43	3.4	6.05	0.037	0.265
25	1,540.12	31.63	3.6	6.4	0.032	0.224
30	1,934.44	23.00	6.8	10.96	0.088	0.277
40	1,654.09	23.71	8.69	15.12	0.056	0.321
50	1,434.92	25.12	9.825	16.63	0.060	0.272
60	1,343.75	25.26	10.96	18.14	0.063	0.239
70	1,788.83	18.13	11.43	19.77	0.044	0.238
80	1,686.08	18.56	11.9	21.4	0.030	0.237
100	1,723.40	17.24	12.85	23.06	0.026	0.204
125	1,587.11	17.92	18.9	34.4	0.027	0.248
150	1,572.63	17.55	22.3	41.2	0.022	0.252
200	1,373.73	19.32	29.11	54.43	0.019	0.253

(Source: Own preparation)

5.1.3.3 Battery bank technical data

In this work, there are only considered vented lead-acid battery banks. This kind of battery cells are often selected for large energy storage banks due the low cost, low maintenance and high cycle stability. Table 24 shows the input data required by the battery bank. The battery bank charge and discharge efficiency and the self-discharge ratio is taken from [64]. The maximum depth of discharge is set in 0.5 since the battery bank can accomplish 3000 cycles during its life service according the datasheet. Other values as maintenance cost, ρ_{bat}, and the fraction of reposition cost, δ_{bat}, are set according recommendation of experts in the energy sector.

TABLE 24. BATTERY BANK TECHNICAL INPUTS

BATTERY BANK INPUT DATA		
Symbol	**Description**	**Value**
$V_{dc_{bc}}$	Battery Voltage [V]	2
$V_{dc_{sist}}$	DC system voltage [V]	48
C_{rate}	Capacity Rate [h]	5
η_{bat_c}	Charge efficiency	0.9
η_{bat_d}	Discharge efficiency	1
σ	Self-Discharge rate	0.000083
L_{bat}	Lifecycle [years]	10
δ_{bat}	Factor of the initial capital cost invested for the battery bank	0.7
ρ_{bat}	Fixed OM factor as ratio of the battery bank initial investment	0.02
DOD_{max}	Maximum Depth of Discharge	0.5

(Source: Own preparation)

The main characteristics and price of the battery cells of the reference used in this work are presented in Table 25. The information was obtained from inquiries to local companies.

The datasheet of the battery cells reference “sun | power V L Series OPzS bloc” from HOPPECKE can be found in Annex 1 on the battery bank folder.

TABLE 25. BATTERY CELLS DATABASE

Battery cell Capacity [Ah] @ C10	Battery cell Capacity [kWh] @ C10	Battery Cell Voltage [V]	Depth of Discharge	#cycles @ 50% DOD	Maintenance required?	Price per unit [USD]	Price per kWh [USD/kWh]
280	0.56	2	0.5	3000	YES	114.00 €	203.57 €
350	0.7	2	0.5	3000	YES	135.00 €	192.86 €
420	0.84	2	0.5	3000	YES	153.00 €	182.14 €
520	1.04	2	0.5	3000	YES	161.00 €	154.81 €
620	1.24	2	0.5	3000	YES	186.00 €	150.00 €
730	1.46	2	0.5	3000	YES	210.00 €	143.84 €
910	1.82	2	0.5	3000	YES	234.00 €	128.57 €
1070	2.14	2	0.5	3000	YES	303.00 €	141.59 €
1220	2.44	2	0.5	3000	YES	330.00 €	135.25 €

TABLE 25. BATTERY CELLS DATABASE (CONTINUED)

Battery cell Capacity [Ah] @ C10	Battery cell Capacity [kWh] @ C10	Battery Cell Voltage [V]	Depth of Discharge	#cycles @ 50% DOD	Maintenance required?	Price per unit [USD]	Price per kWh [USD/kWh]
1370	2.74	2	0.5	3000	YES	361.00 €	131.75 €
1520	3.04	2	0.5	3000	YES	389.00 €	127.96 €
1670	3.34	2	0.5	3000	YES	426.00 €	127.54 €
1820	3.64	2	0.5	3000	YES	460.00 €	126.37 €
2170	4.34	2	0.5	3000	YES	538.00 €	123.96 €
2540	5.08	2	0.5	3000	YES	664.00 €	130.71 €
2900	5.8	2	0.5	3000	YES	744.00 €	128.28 €
3250	6.5	2	0.5	3000	YES	834.00 €	128.31 €
3610	7.22	2	0.5	3000	YES	906.00 €	125.48 €
3980	7.96	2	0.5	3000	YES	981.00 €	123.24 €
4340	8.68	2	0.5	3000	YES	1,056.00 €	121.66 €
4700	9.4	2	0.5	3000	YES	1,097.00 €	116.70 €

(Source: Own preparation)

5.1.4. SYSTEM INPUTS

The system input parameters are shown in Table 26. The cost of energy lost is assumed in 0.2 USD/kWh. This value depends on the necessities and characteristics of the users of the select location. The interest rate considered in this work in 8.08 % taking as in [65].

TABLE 26. SYSTEM INPUT PARAMETERS

System inputs parameters		
Symbol	**Description**	**Value**
R	Time of the project [years]	20
i_r	Real interest rate [%]	8.08
c_{loss}	Cost of energy loss [USD/kWh]	0.2
Δ	Fiscal Incentive Factor	0.9038

The fiscal incentive factor is calculated using Eq. 4.74 applying the consideration on the investment tax credit, i_j, and the depreciation rate, d_j, indicated on section 4.3.3 of this work and an effective corporate tax income rate of 33%. The resulting incentive factor is given by

$$\Delta = \frac{1}{(1-0.33)} \times \left[1 - 0.33 \times \left(\sum_{j=1}^{T1} \frac{0.1}{(1+0.0808)^j} + \sum_{j=1}^{T2} \frac{0.2}{(1+0.0808)^j}\right)\right] = 0.9038 \qquad (4.82)$$

The parameters for the PSO algorithm and the boundaries for each decision variable are shown in Table 27.

TABLE 27. PSO INPUT PARAMETERS

PSO Input parameters		
Symbol	**Description**	**Value**
N_{PV_l}	Lower bound Number of PV modules	0
w_{DG_l}	Lower bound Nominal power of Diesel	0
$N_{B_{p_l}}$	Lower bound Number of Battery cell in parallel	0
E_{bcell,nom_l}	Lower bound Nominal capacity of battery cell kWh	0
N_{PV_u}	Upper bound Number of PV modules	20000
w_{DG_u}	Upper bound Nominal power of Diesel unit in kW	200
$N_{B_{p_u}}$	Upper bound Number of Battery cell in parallel	10
E_{bcell,nom_u}	Upper bound Nominal capacity of battery cell kWh	9.40
Max_{it}	Maximum number of iterations	50
$nPop$	Population Size	200
w	Inertia Coefficient	1
w_{max}	Inertia Coefficient max	0.9
w_{min}	Inertia Coefficient min	0.5
c_1	Personal Acceleration Coefficient	2.5
c_2	Social Acceleration Coefficient	1.5

5.2. RESULTS AND DISCUSSION

This section presents the results obtained from the evaluation of the three cases of study, each linked to the daily load profile calculated, using the input data described in the previous section. All system architecture described in this work (Diesel, Diesel-PV, Diesel-PV-Battery and PV-Battery) are used to evaluate each case of study. Then, the results are discussed and compared. Lastly, the third case of study is evaluated using HOMER and its results are compared with the results obtained in this work.

5.2.1. STUDY CASE 1 – SINGLE USER.

This case of study is only evaluated with the PV and battery architecture. The diesel generation is rule out due to the low demand of the system and the smallest diesel generator on our database cannot operate over its minimum load ratio. The voltage system is change to 12 V and the upper limits or the number of modules and the nominal capacity of the battery bank are set in 10 and 1.46 respectively.

The resulting system configuration is compounded by 2 PV modules of 300 Wp and a battery bank of 6 batteries with a total nominal capacity of 3.36 kWh. The ACS including the fiscal incentives is 222.699 USD/year and the resulting COE is 0.4117 USD/kWh. The LPSP is zero, it means all the load is supplied effectively and the annualized cost of energy loss (AC_{loss}) is also zero. Furthermore, the function *Cost* coincides with the COE since the annualized cost of energy loss is zero. The parameter of Loss of Photovoltaic Power Generated ($LPVG$) is introduced as the ratio between the total energy wasted by the system (e.g. when the battery is fully charged, and the PV generations surpass the load demand) and the photovoltaic generation in a year. In the best solution, for this case of study, around 35% of the PV energy generated is wasted. The best result is obtained in the first iteration. This is expected since the project is small and there are not many possible combinations to solve the sizing problem. The results are summarized on Table 28.

TABLE 28. RESULTS STUDY CASE 1 SMALL PROJECT – SINGLE USER

System Parameters		
Symbol	**PV-BAT**	**Units**
N_{pv}	2	Units
$P_{pv_{stc}}$	0.6	[kWp]
N_{b_p}	1	Units
N_{b_s}	6	Units
N_{bat}	6	Units
$E_{bcell,nom}$	0.56	[kWh]
$E_{bat,n}$	3.36	[kWh]

Results		
Symbol	**PV-BAT**	**Units**
CC_{pv}	1200	USD
CC_{bat}	684	USD
$O\&M_{pv}$	12	USD/year
$O\&M_{bat}$	13.68	USD/year
RC_{bat}	220.1409	USD
ACS_{adj}	222.699	USD/year
$LPSP$	0	%
COE_{adj}	0.4117	USD/kWh
AC_{loss}	0	USD/year
$LPVG$	35.068	%
$Cost$	0.4117	USD/kWh

The figure 32 shows the daily average energy flow, and the state of charge of the battery in % using the best system configuration resulting. The battery is charged between 6:00 am and midday, and the surplus of PV generation results after 10:00 am when the battery is usually charged. At night, as expected, the load demand is supplied by the battery bank.

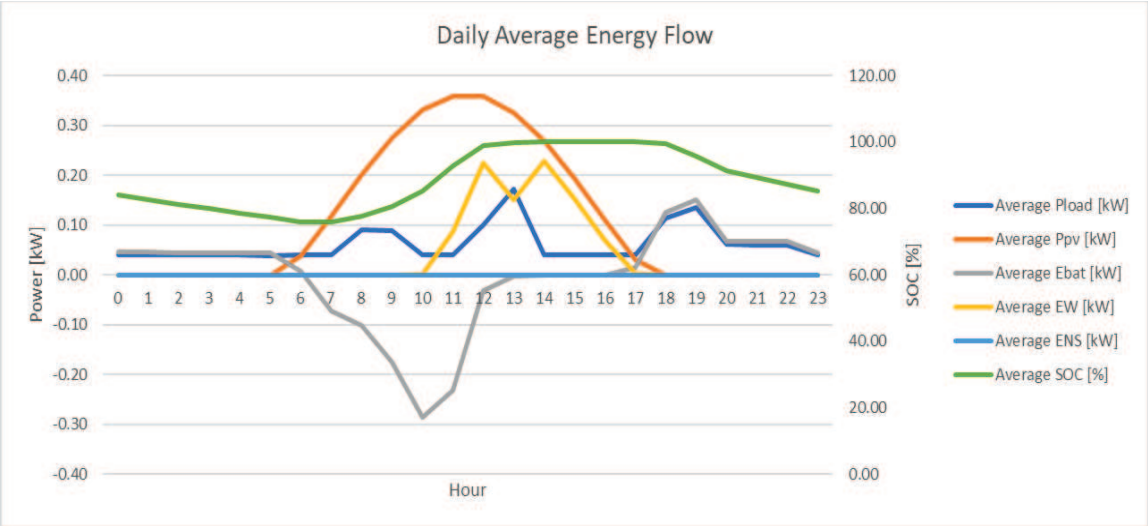

FIGURE 32. AVERAGE ENERGY FLOW AND SOC OF THE BATTERY IN PV-BAT CONFIGURATION FOR STUDY CASE 1.

5.2.2. STUDY CASE 2 - COMMUNITY FROM A SURVEY.

The sizing methodology through the PSO developed in this work is applied to the daily load profile described in section 5.1.2.2 for each system architecture. The uncertainties associated to the load profile are set in zero to compare the different system architectures in equal conditions. The best results were obtained with the PV-BAT configuration achieving a cost of energy of 0.2253 USD/kWh including the cost of the energy lost. The characteristics of the resulting systems and its economic and reliability parameters, after the optimization process, are summarized in Table 29.

TABLE 29. RESULTS STUDY CASE 2

System Parameters					
Parameter	**DG**	**DG-PV**	**DG-PV-BAT**	**PV-BAT**	**Unit**
N_{pv}	-	4	111	111	Units
$P_{pv_{stc}}$	-	1.2	33.3	33.3	[kWp]
w_{DG}	10	10	0	-	[kW]
N_{DG}	2	2	0	-	Units
P_{DG}	20	20	0	-	[kW]
N_{b_p}	-	-	3	1	Units
N_{b_s}	-	-	24	24	Units
N_{bat}	-	-	24	24	Units
$E_{bcell,nom}$	-	-	5.8	5.8	[kWh]
$E_{bat,n}$	-	-	139.2	139.2	[kWh]

TABLE 29 (CONTINUED). RESULTS STUDY CASE 2

Results					
Symbol	**DG**	**DG-PV**	**DG-PV-BAT**	**PV-BAT**	**Unit**
CC_{pv}	-	1800.00	66600.00	66600.00	USD
CC_{DG}	34142.66	34142.66	0.00	-	USD
CC_{bat}	-	-	17856.00	17856.00	USD
$O\&M_{pv}$	-	11600.08	666.00	666.00	USD/year
$O\&M_{DG_f}$	3414.27	3414.27	0.00	-	USD/year
$O\&M_{DG_v}$	8508.15	8185.82	0.00	-	USD/year
$O\&M_{DG}$	11922.42	11580.37	0.00	-	USD/year
$O\&M_{bat}$	-	-	357.12	357.12	USD/year
RC_{DG}	4998.01	4998.01	0.00	-	USD
RC_{bat}	-	-	5746.84	5746.84	USD
FC	12154.50	11694.02	0.00	-	[l]
ACS_{adj}	15932.74	15795.09	9432.79	9432.79	USD/year
$LPSP$	0.00	0.00	0.71	0.71	%
COE_{adj}	0.38	0.37	0.22	0.22	USD/kWh
AC_{loss}	0.00	0.00	59.95	59.95	USD/year
$LPVG$	-	5.80	6.72	6.72	%
$Cost$	0.3755	0.3723	0.2253	0.2253	USD/kWh

A system with 111 PV modules of 300Wp and 24 battery cells for a battery bank capacity of 139.2 kWh achieved the lowest cost of energy. The PV-BAT architecture and the DG-PV-BAT architecture obtained the same results since best solution in the former do not included Diesel genset units.

In the DG-PV system, a reduction on the yearly fuel consumption and therefore in the O&M of the diesel component, was achieved due to the contribution of the PV generation in the energy mix. It is worth to notice that, despite having the same DG component than the DG system, the DG-PV configuration achieved a lower cost of energy than the DG-only system.

The optimization process for each system architecture is shown in Figure 33. At right of Figure 33, a closer view is presented to better appreciation of the slope of the resulting curve. In both figures it can be appreciated, in each iteration, a slight decline in the function cost.

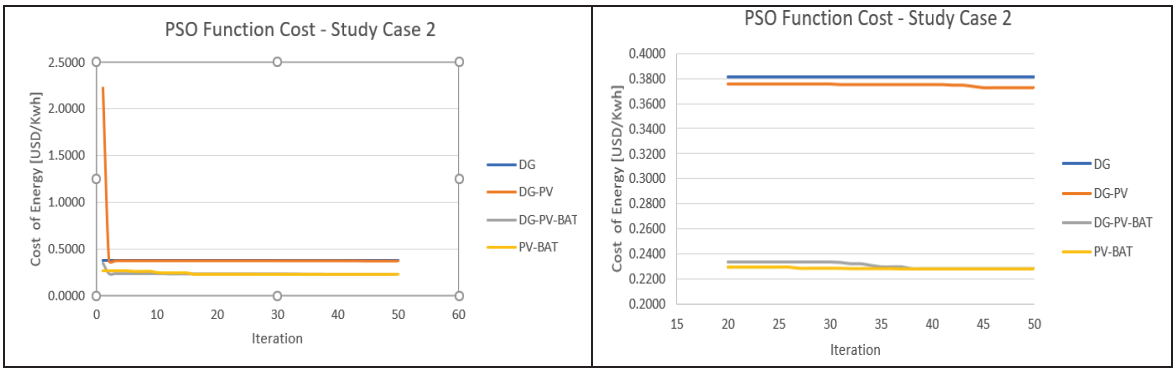

FIGURE 33. OPTIMIZATION PROCESS STUDY CASE 2

Figure 34 shows the daily average energy flow, and the state of charge of the battery in % (if applies) using the best system configuration resulting in each system architecture.

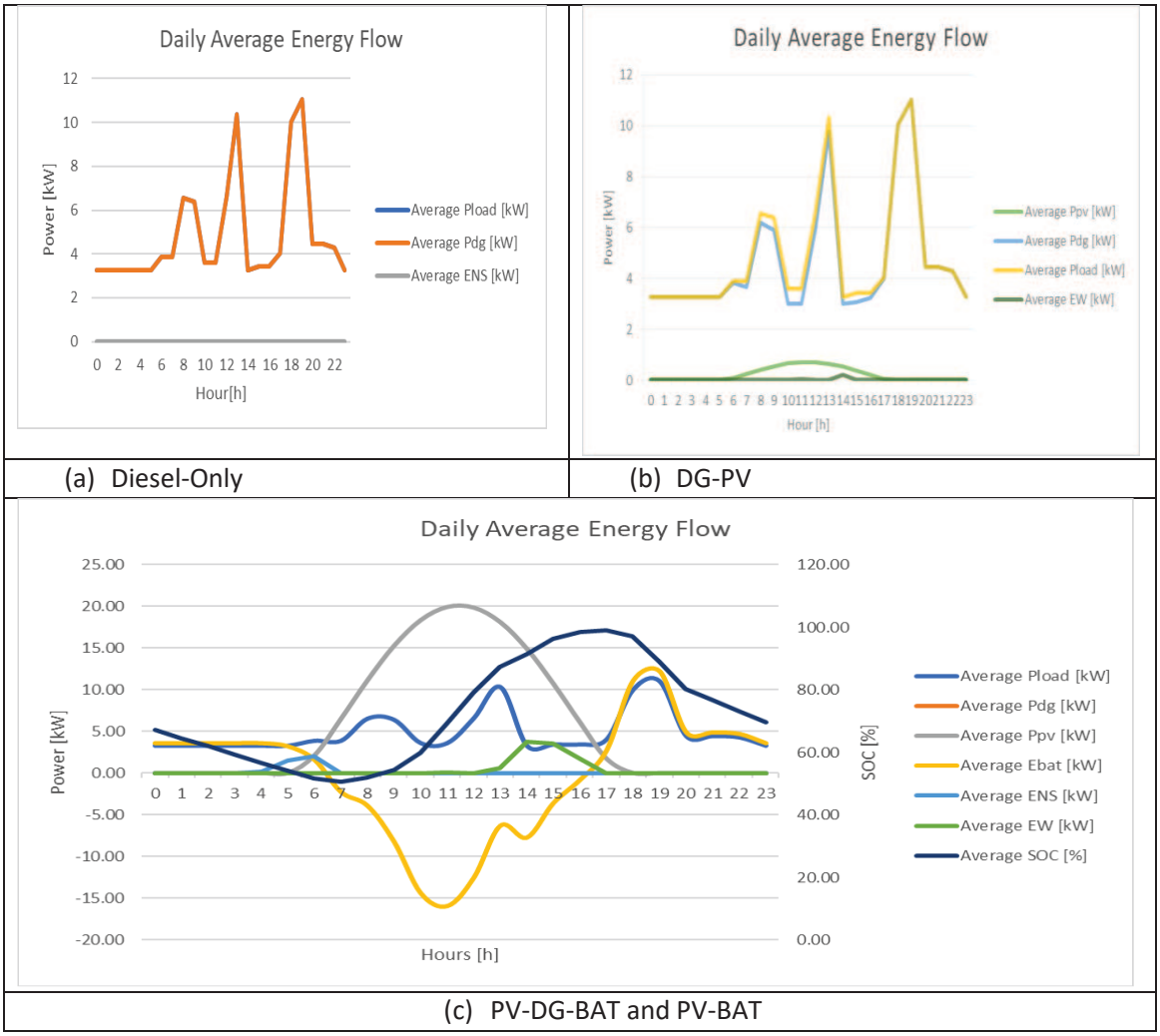

(a) Diesel-Only

(b) DG-PV

(c) PV-DG-BAT and PV-BAT

FIGURE 34. AVERAGE DAILY ENERGY FLOW STUDY CASE 2

In Annex 2, in folder case 2, it can be found the results, graphs and time series for each system architecture for this case of study.

5.2.3. STUDY CASE 3 – COMMUNITY "SANTA CRUZ DEL ISLOTE"

For the study case 3, it is designed an energy system to supply the energy demand of the community of "Santa Cruz del Islote" located in Bolivar, Colombia. The inputs parameters mentioned on Section 5.1 are used. A system composed by 2 diesel generators of 25 kW obtained the lowest cost of energy among all architectures. The results obtained by each system architecture are summarized in Table 30.

The best result was obtained by the DG-PV-BAT architecture. The best cost achieved was 0.2090 USD/kWh being the lowest obtained by a large range, comparing with others system architectures. The second best was obtained by the DG-Only architecture, where the cost function achieved 0.2512 USD/kWh. Both system architectures had the same configuration of DG units, consequently having the same capital cost invested in this item. However, in the DG-PV-BAT configuration, the PV generation with the battery storage systems allows to reduce the cost in fuel consumption therefore reducing the variable component of operation and maintenance of Diesel generation. The worst result was obtained by the PV-BAT configuration, nonetheless, the cost function value was close of the obtained by the DG-Only configuration. A sensibility analysis varying some input parameters on the model could result in a different outcome.

TABLE 30. RESULTS STUDY CASE 3

System Parameters					
Parameters	**DG**	**DG-PV**	**DG-PV-BAT**	**PV-BAT**	**Unit**
N_{pv}	-	0	13	502	Units
$P_{pv_{stc}}$	-	0	3.9	150.6	[kWp]
w_{DG}	25	25	25	-	[kW]
N_{DG}	2	2	2	-	Units
P_{DG}	50	50	50	-	[kW]
N_{b_p}	-	-	1	4	Units
N_{b_s}	-	-	24	24	Units
N_{bat}	-	-	24	96	Units
$E_{bcell,nom}$	-	-	1.04	9.4	[kWh]
$E_{bat,n}$	-	-	24.96	902.4	[kWh]

TABLE 30. RESULTS STUDY CASE 3 (CONTINUED)

Results					
Parameters	**DG**	**DG-PV**	**DG-PV-BAT**	**PV-BAT**	**Unit**
CC_{pv}	-	0	7800.00	301200	USD
CC_{DG}	48257.99	48257.99	48257.99	-	USD
CC_{bat}	-	-	3864.00	105312	USD
$O\&M_{pv}$	-	22.5	78.00	3012	USD/year
$O\&M_{DG_f}$	4825.80	4825.80	4825.80	-	USD/year
$O\&M_{DG_v}$	34277.88	34277.88	26884.74	-	USD/year
$O\&M_{DG}$	39103.68	39103.68	31710.54	-	USD/year
$O\&M_{bat}$	-	-	77.28	2106.2	USD/year
RC_{DG}	7019.48	7019.48	7019.48	-	USD
RC_{bat}	-	-	1243.60	33893.98	USD
FC	48968.40	48968.40	38406.77	-	[l]
ACS_{adj}	44767.37	44767.37	38737.05	46235.11	USD/year
$LPSP$	3.46	3.46	1.25	0.80	%
COE_{adj}	0.2441	0.2441	0.26	0.2489	USD/kWh
AC_{loss}	1314	1314	475.03	843.88	USD/year
$LPVG$	-	0.00	0.00	6.78	%
$Cost$	0.2512	0.2512	0.21	0.2534	USD/kWh

The curves showing the improvement obtained due the optimization process on each system architecture is shown in Figure 35.

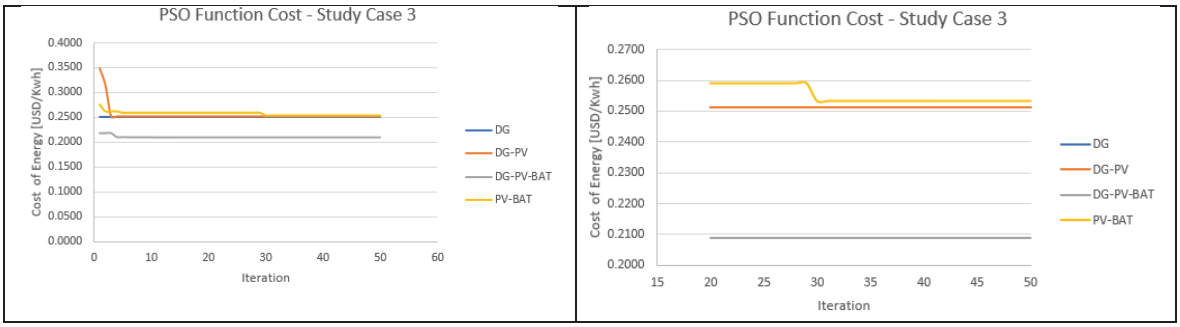

FIGURE 35. OPTIMIZATION PROCESS STUDY CASE 3

Also, the daily average energy flow curves of each system are shown in Figure 36.

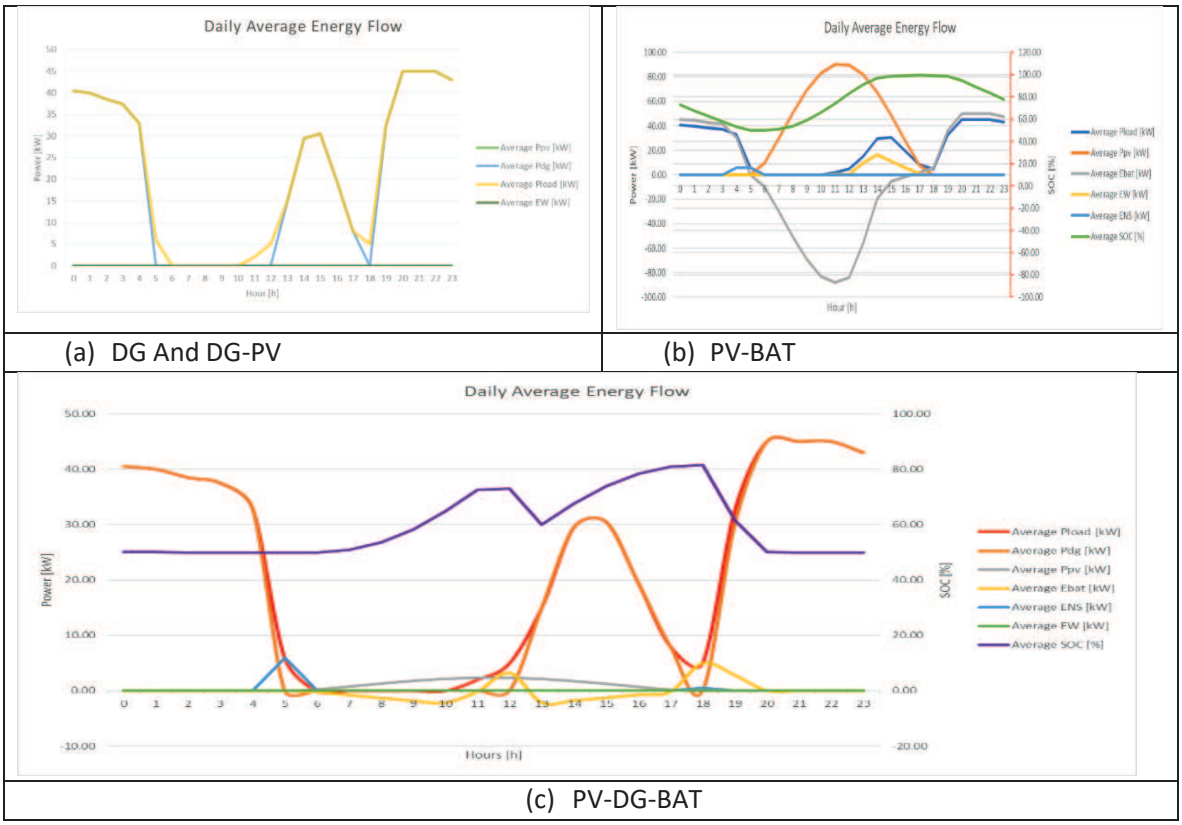

(a) DG And DG-PV

(b) PV-BAT

(c) PV-DG-BAT

FIGURE 36. AVERAGE DAILY ENERGY FLOW STUDY CASE 3

The proposed system resulting from the optimization process is noticeably smaller than the actual hybrid system installed on the island (described on Figure 28). In addition, under the evaluation parameters used in this model, if the capacity of the photovoltaic system is increased, the battery bank has sufficient capacity to satisfy the current load demand of the island. However, it is possible that, due to space restrictions, the capacity of the photovoltaic system cannot be increased.

In the Annex 2, in folder "case 3", it can be found the results, graphs and time series for each system architecture for this case of study.

5.2.3 COMPARISON WITH COMMERCIAL SOFTWARE.

HOMER (Hybrid Optimization Model for Multiple Energy Resources) released on 2000, is the global standard software for optimizing microgrid design in all sectors, from village power and island utilities to grid-connected campuses and military bases [66]. This software tool can model different kind of hybrid energy system integrating renewable energy sources such solar wind, hydro and biomass. This commercial software can cost from 1000$/year.

Among the features HOMER can offer are: examination of all possible combinations of system types in a single run, perform sensibility analysis over selected variables; multiyear evaluation to consider changes on the load profile; cost of fuel or cost of energy; 9 modules that allow simulate microgrid including different sources energies as wind, hydro, biomass, heat power, hydrogen, energy storage among other. Table 31 summarizes the main features of HOMER. A review of 37 computational tools to evaluate and analyses the integration of renewable energy systems into various energy systems can be found in [67]

TABLE 31. HOMER MAIN FEATURES

Sub-model	Description
Irradiation Model	• The global irradiation and its components can be calculated in one-minute resolution. • Only one method can be selected to generate synthetic hourly radiation, the proposed by Graham VA, Hollands KGT (1990). • Allows to import GHI from external sources.
Load profile Model	• Four pre-defined load profiles are available (residential, commercial, industrial and community). • A daily load profile can be defined per month. • The load can be defined as AC or DC.
PV generation Model	• The PV generation can be connected either to the BUS DC (DC-coupling) or AC (AC-coupling). • Calculation using tracking system is available. • A model to calculate the MPPT is available (optimizer DC-DC). • Database with different PV modules and its technical characteristics is available. • The cost of the module can vary depending the capacity of the system. • The inverter and/or charge controller are considered as an individual component on the system.
Battery Storage Model	• Complex battery model is used to calculate the battery energy flow, lifetime and state of charge of the battery. • Different types of battery can be modeled on the system (Li-on, fly-wheel, etc.). • Battery bank of different sizes can be modeled on the same system. • Effects of ambient temperature can be included on the battery model.
Diesel Generation Model	• The lifetime of the DG unit is calculated according the operation hours. • The cost of O&M depends on the fuel cost and on the operation hours. • An auto-sizing tool for DG units is available.
Dispatch Strategy Model	• Six types of dispatch strategies can be defined, including custom strategies developed in MATLAB. • More than one dispatch strategy can be considered on the optimization process. • The capital, replacement and O&M cost of the plant controller can be included in the model.
Optimization model	• Constrains as minimum LPSP or percentage of renewable energy penetration can be defined. • Environmental parameters and costs can be considered in the objective function. • Sensibility analysis can be performed. The variable to realize such analysis must be defined. • Grid-Tie project can be simulated. • Multiyear modeling can be performed to considering, for example, variation on the fuel cost or variation on the load profile. • All architectures run on a single optimization process and more than one result is presented. • Savage recovery cost is included on the calculation of the NPC.
User interface and reports	• An intuitive user interface is available to design the microgrid. • Time series of all variables can be exported to a csv file.

The results obtained on study case 3 are simulated in HOMER using the same inputs parameters. Figure 37 shows the system architecture. The input report generated by HOMER is attached in Annex 3.

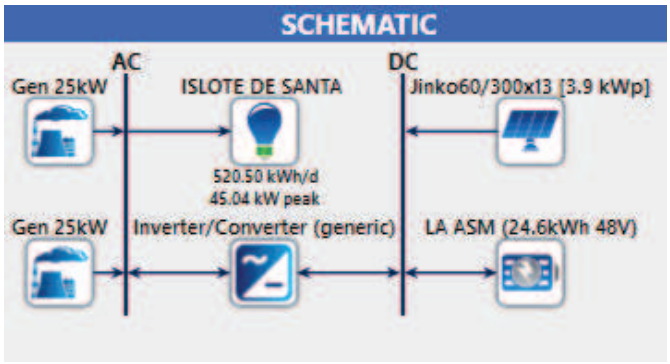

FIGURE 37. SCHEMATIC HYBRID SYSTEM IN HOMER

The dispatch strategy selected in homer is "HOMER Load Following". In this strategy, as it is described by HOMER, whenever a diesel generator operates, it produces only enough power to meet the primary load. Lower priority objectives such as charging the storage energy bank are left to renewable power sources. This strategy differs, from the developed on this work, in that the priority to supply the load is from the DG units, and the renewable energy source seeks to reduce the fuel consumption. In the dispatch strategy developed in this work, the priority to supply the load rely on the photovoltaic energy, then the energy storage on the battery bank and lastly, if required, the diesel generation. HOMER simulation report can be found in Annex 3. Table 32 shows the comparison of the results obtained for the study case 3.

TABLE 32. RESULTS COMPARISON STUDY CASE 3

SYSTEM PARAMETER							
Symbol	**DG-PV-BAT PSO**	**DG-PV-BAT HOMER**	**Unit**	**Symbol**	**DG-PV-BAT PSO**	**DG-PV-BAT HOMER**	**Unit**
CC_{pv}	\$ 7800	\$ 7800	USD	RC_{DG}	\$ 7019	\$ 5212,83	USD
CC_{DG}	\$ 48258	\$ 24129	USD			\$ 2586,75	USD
		\$ 24129	USD	RC_{bat}	\$ 1244	\$ 1345,05	USD
CC_{bat}	\$ 3864	\$ 3864	USD	FC	38406,77	51517,00	[l]
$O\&M_{pv}$	\$ 78	\$ 78	USD/year	ACS_{adj}	\$ 38737	\$ 46748,55	USD/year
$O\&M_{DG_f}$	\$ 4826	\$ 4826	USD/year	$LPSP$	1,25	0,00	%
$O\&M_{DG_v}$	\$ 26885	\$ 23059,07	USD/year	COE_{adj}	\$ 0,258	\$ 0,249	USD/kWh
		\$ 11915,04	USD/year	AC_{loss}	\$ 475	\$ 0	USD/year
$O\&M_{DG}$	\$ 31711	\$ 39800	USD/year	$LPVG$	0,00	0,00	%
$O\&M_{bat}$	\$ 77	\$ 77	USD/year	$Cost$	\$ 0,2090	\$ 0,2461	USD/kWh

The results show a levelized cost of energy 20% higher on the HOMER simulation. This is caused mainly for five reasons:

1. Higher fuel consumption: In the dispatch strategy used by HOMER, the load is supplied mostly by the DG units, increasing the fuel consumption. Figure 38 shows the comparison in the daily average fuel consumption between the two models. A difference on the fuel consumption can be seen between 5:00 and 6:00 am and between 13:00 and 18:00.

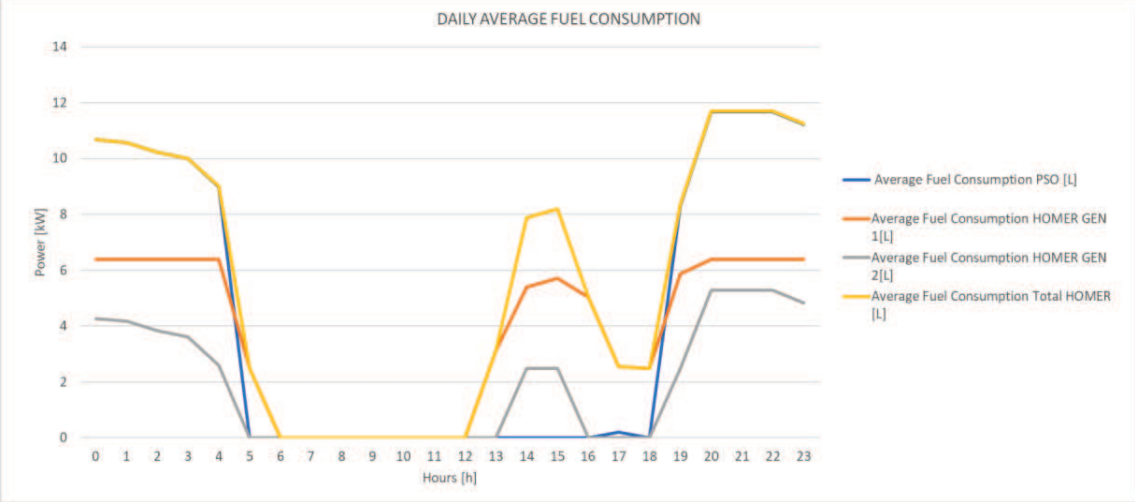

FIGURE 38. AVERAGE DAILY FUEL CONSUMPTION STUDY CASE 3

2. In HOMER, DG units can operate individually at different power rate. Figure 38 shows this condition too.
3. The replacement cost on DG units vary in function of the lifecycle of each DG unit. The lifecycle of DG unit is calculated by HOMER as function of the hours of operation of each unit.
4. Homer simulation does not include tax reduction incentives in the capital cost of the PV and the energy storage system. Despite the values are the same in Table 30, in the calculation of the function Cost, the HOMER's levelized cost of energy equation does not include the tax incentive factor. However, since the system relies mostly in diesel generation, the effect of the tax reduction incentives on the cost of energy is less than 1%, due to a reduction of the initial investment in 1122.07 USD.
5. HOMER considers the salvage value of each component of the installation at the end of the project life.

A main difference between the two models is the dispatch strategy used. On the PSO model developed in this work, a dispatch strategy that prioritize the consumption of renewable energy (directly from Photovoltaic generation or storage on the battery bank). In consequence, the fuel consumption is reduced and therefore, in this study case, a lower cost of energy is achieved.

It is important to notice that the energy storage model and the Diesel generation model used in HOMER are more complex than the used on this work. For instance, HOMER calculate the lifecycle of the battery storage bank according to the state of charge, affecting the energy output and the replacement cost of this component. Figure 39 shows the comparison in the daily average battery bank energy flow and SOC between the two simulations. The charging and discharging windows of the battery bank are different. On HOMER simulation, the battery bank can be charged in hours without irradiance, using the diesel generation, this condition is restricted in the dispatch strategy developed. Also, the SOC of the battery bank in HOMER results is around 67 % in contrast with the PSO model in which the average SOC is 59.45%.

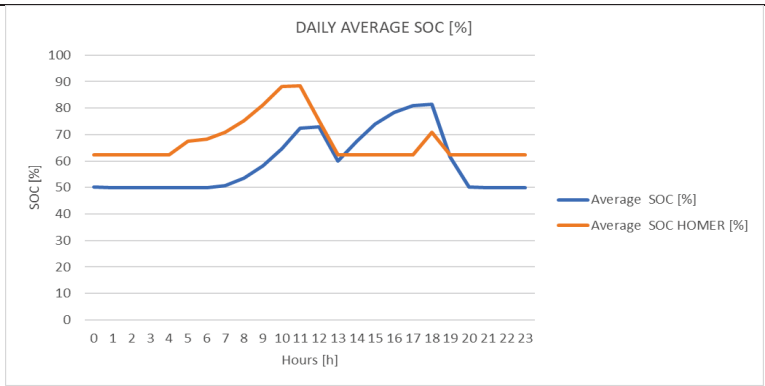

(a) Daily average SOC [%] comparison

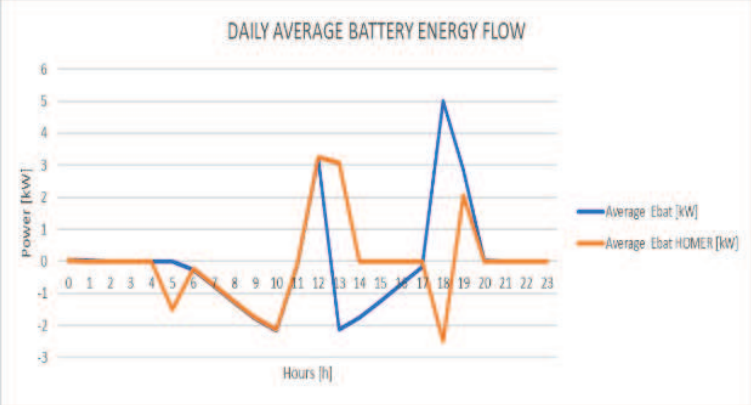

(b) Daily average SOC [%] comparison

FIGURE 39. AVERAGE DAILY BATTERY ENERGY FLOW AND SOC

Lastly, the comparison between the daily average energy flow on both simulations is presented on Figure 40. The effect of the dispatch strategy employed is evident. The dispatch strategy has a critical impact on the economic and reliability evaluation of the system and must be chosen wisely, as it has been demonstrated with this comparison. However, the results obtained are similar in both systems, giving a close reference of an economically efficient design for a hybrid renewable energy system using the dispatch strategy and the algorithm developed.

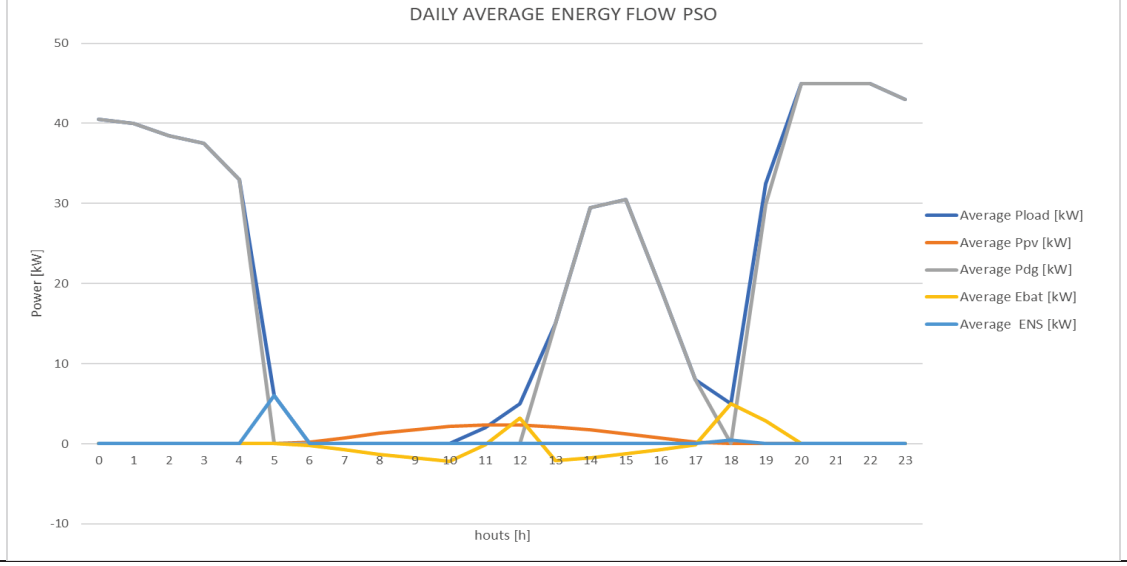

(a) Daily average Energy Flow PSO for Study case 3.

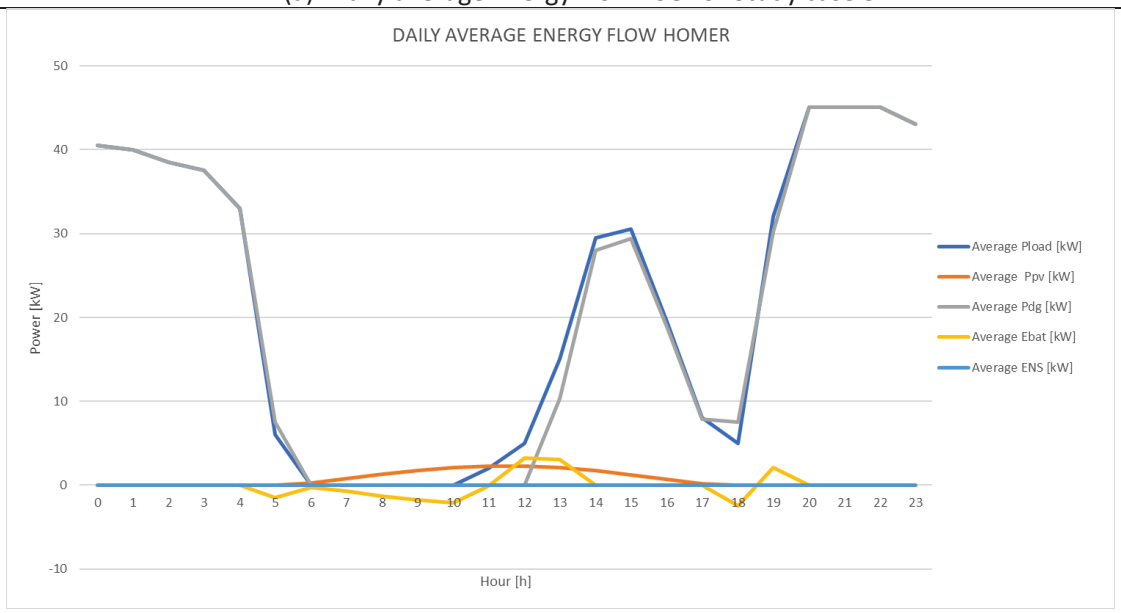

(b) Daily average Energy Flow HOMER for Study case 3.

FIGURE 40. AVERAGE DAILY ENERGY FLOW STUDY CASE 3

CHAPTER VI

CONCLUSIONS AND FUTURE WORK

6.1. CONCLUSIONS

In this work, an optimization methodology was developed and described in detail to help dimension and simulate hybrid renewable energy systems integrated by photovoltaic and diesel generation with energy storage. Four system architectures were considered and described: only diesel, diesel and photovoltaic generation (DG-PV), diesel and photovoltaic generation with energy storage (DG-PV-BAT) and photovoltaic generation with energy storage (PV-BAT).

A PSO algorithm was developed to evaluate the different combinations of components of each system to obtain the most cost-effective solution. This metaheuristic was selected due to advantages such code simplicity, ease of use, high convergence speed. The reliability of the system was included in the objective function of the PSO algorithm through the annual cost of the energy not supplied. Also, a fiscal incentive factor is used to include the financial benefits granted by the Law 1715 of 2014 in Colombia to non-conventional renewable energy source of energy. The results are obtained after simulating the energy flow of the system for one year with one-hour resolution.

To simulate the energy flow of the system, the construction of the following sub-models was required: solar resource estimation, load demand estimation, photovoltaic generation, energy storage, diesel generation and power dispatch strategies. In chapter 4, each model was described in detail. MATLAB was used to program each of these sub-models.

Four dispatch strategies were described in detail, one for each system architecture. The dispatch strategies developed in this work prioritize the use of renewable resource over diesel generation to supply the load. Also, diesel generation cannot be used to charge the battery bank. This condition is based on the fact that, in non-interconnected rural areas, the complications associated to supply the fuel and the maintenance of DG units are commonly underestimated.

Three study cases were evaluated using the optimization methodology developed. The input parameters required by the model were described in detail. On the first and second case, the best solution found was a PV-BAT system. On the third case, a real system is modeled, and the best solution found was a PV-BAT-DG system. In this solution, photovoltaic generation with the battery storage system made it possible to reduce the cost of fuel consumption. Also, it was possible to reduce the operating cost of diesel generation, obtaining a lower annualized cost of Energy. This highlights the advantages of HRE systems over conventional fossil generation to electrification of non-interconnected zones.

Lastly, the system configuration resulting in study case 3 was simulated using the software HOMER. This software is the global standard for optimizing microgrid design and was selected to validate the sizing methodology developed on this work. The levelized cost of energy obtained by HOMER was higher than the obtained by the PSO algorithm. The main difference between the two models was the dispatch strategy used in which HOMER does not always prioritize the use of renewable energy source and the battery bank can be charged by the DG unit. This highlights the fact that, dispatch strategy, has a critical impact on the economic and reliability evaluation of the hybrid system and must be chosen wisely. However, despite the difference on the results, the energy flow curve obtained by both simulations are comparable validating, in this way, the functionality of the methodology developed.

The main features of the sizing methodology developed were: (a) allows the simulation of hybrid renewable systems and the evaluation of its economic and reliability integrated by diesel and photovoltaic generation with energy storage, (b) the dispatch strategy developed prioritize the use of renewable energy among other energy sources, (c) each possible condition of the system, described by the dispatch strategy, can be visualized in a column on the time series output file, (d) fiscal incentives granted by the Law 1715 of 2014 in Colombia are considered on the calculation of the cost of energy using the fiscal incentive factor.

It is expected that this work will help the process of designing hybrid renewable energy systems in non-interconnected areas, thus contributing to the development of these locations and improving the life quality of the population living on these places. Also, it is expected that this work can be used as starting point for further development on this research line.

6.2. FUTURE WORK

After completing this work, the following aspects must be revised or explored toward complementing the outcome of this work:

- Develop a routine to calculate the global irradiance on tilted surfaces and the load profile with one-minute resolution to obtain more precise results. Other methods for estimation of the solar resource must be considered.
- Refine the battery model to calculate the lifecycle and efficiency of this component in function of its state of charge.
- Extend the Diesel generation model to allow the integration of DG units of different nominal capacity and optimize the energy dispatch strategy of the DG gen-set. In addition, a model to estimate the lifecycle of each DG unit and its operation and maintenance cost in function of its hour of operation must be developed.
- Applied the proposed methodology to size real proposal of HRE systems and run sensibility analysis in order to evaluate the most sensitive parameters of the model.
- Evaluate the efficiency of the PSO algorithm developed using others optimization algorithms (heuristic or metaheuristic), and other multi-objective algorithms and compare the results obtained.
- Integrate different dispatch strategies, as cycle charging or economic dispatch, on the optimization process and compare the results obtained.
- Extend the model to include the model of power electronic components (converter/inverter) on the optimization model.
- Extend the model to include on the economic analysis the calculation of the savage value of each component and the degradation on the efficiency due the life cycle of the component.
- Model the dioxide carbon emission impact of each component and include on the objective function the economic benefits of cleaner energy sources.
- Integrate others renewable resources, as wind energy, hydro power and biomass, on the optimization model.
- Extend the model including multi-year evaluation to consider the variation on fuel cost and load demand over the years.
- Extend the model to include constrained simulation.

BIBLIOGRAPHY

[1] U. Unidad de Planeación Minero Energética, "Resumen Ejecutivo: Plan Indicativo de Expansión de Cobertura de Energía Electrica 2013-2017", 2013.

[2] Congreso de la República de Colombia., *Ley 1753 - Plan Nacional de Desarrollo 2014 - 2018.* Colombia: www.secretariasenado.gov.co/senado/basedoc/ley_1753_2015.html, 2015.

[3] C. R. Noriega *et al.*, "FORMULACIÓN DE UN PLAN DE DESARROLLO PARA LAS FUENTES NO CONVENCIONALES DE ENERGÍA EN COLOMBIA (PDFNCE) VOLUMEN 2 – DIAGNÓSTICO DE LAS FNCE EN COLOMBIA", Bogotá, 2010.

[4] A. Castillo Ramírez, "Barreras para la implementación de generación distribuida: dos representantes de países desarrollados vs. un representante de país en desarrollo", vol. 15, núm. 1529, pp. 62–75, 2011.

[5] V. Salas, W. Suponthana, y R. A. Salas, "Overview of the off-grid photovoltaic diesel batteries systems with AC loads", *Appl. Energy*, vol. 157, pp. 195–216, nov. 2015.

[6] IDEAM, "Atlas de Radiación Solar de Colombia". [En línea]. Disponible en: http://www.upme.gov.co/Docs/Atlas_Radiacion_Solar/1-Atlas_Radiacion_Solar.pdf. [Consultado: 06-jun-2016].

[7] S. M. Shaahid y M. A. Elhadidy, "Opportunities for utilization of stand-alone hybrid (photovoltaic + diesel + battery) power systems in hot climates", *Renew. Energy*, vol. 28, pp. 1741–1753, 2003.

[8] S. M. Shaahid y I. El-Amin, "Techno-economic evaluation of off-grid hybrid photovoltaic–diesel–battery power systems for rural electrification in Saudi Arabia—A way forward for sustainable development", Renew. Energy, vol 13, Issue 3, , P 625-633, 2009.

[9] D. Tsuanyo, Y. Azoumah, D. Aussel, y P. Neveu, "Modeling and optimization of batteryless hybrid PV (photovoltaic)/Diesel systems for off-grid applications", *Energy*, vol. 86, pp. 152–163, jun. 2015.

[10] S. B. Jeyaprabha y A. I. Selvakumar, "Optimal sizing of photovoltaic/battery/diesel based hybrid system and optimal tilting of solar array using the artificial intelligence for remote houses in India", *Energy Build.*, vol. 96, pp. 40–52, jun. 2015.

[11] H. Belmili, M. Haddadi, S. Bacha, M. F. Almi, y B. Bendib, “Sizing stand-alone photovoltaic–wind hybrid system: Techno-economic analysis and optimization”, *Renew. Sustain. Energy Rev.*, vol. 30, pp. 821–832, feb. 2014.

[12] R. Luna-Rubio, M. Trejo-Perea, D. Vargas-Vázquez, y G. J. Ríos-Moreno, “Optimal sizing of renewable hybrids energy systems: A review of methodologies”, *Sol. Energy*, vol. 86, núm. 4, pp. 1077–1088, abr. 2012.

[13] O. Erdinc y M. Uzunoglu, “Optimum design of hybrid renewable energy systems: Overview of different approaches”, *Renew. Sustain. Energy Rev.*, vol. 16, núm. 3, pp. 1412–1425, abr. 2012.

[14] A. Ahmad Khan, M. Naeem, M. Iqbal, S. Qaisar, y A. Anpalagan, “A compendium of optimization objectives, constraints, tools and algorithms for energy management in microgrids”, *Renew. Sustain. Energy Rev.*, vol. 58, pp. 1664–1683, may 2016.

[15] R. Siddaiah y R. P. Saini, “A review on planning, configurations, modeling and optimization techniques of hybrid renewable energy systems for off grid applications”, *Renew. Sustain. Energy Rev.*, vol. 58, pp. 376–396, may 2016.

[16] P. Prakash y D. K. Khatod, “Optimal sizing and siting techniques for distributed generation in distribution systems: A review”, *Renew. Sustain. Energy Rev.*, vol. 57, pp. 111–130, may 2016.

[17] S. Mandelli, C. Brivio, E. Colombo, y M. Merlo, “A sizing methodology based on Levelized Cost of Supplied and Lost Energy for off-grid rural electrification systems”, *Renew. Energy*, vol. 89, pp. 475–488, abr. 2016.

[18] A. Haghighat Mamaghani, S. A. Avella Escandon, B. Najafi, A. Shirazi, y F. Rinaldi, “Techno-economic feasibility of photovoltaic, wind, diesel and hybrid electrification systems for off-grid rural electrification in Colombia”, *Renew. Energy*, vol. 97, pp. 293–305, 2016.

[19] S. Ashok, “Optimised model for community-based hybrid energy system”, *Renew. Energy*, vol. 32, núm. 7, pp. 1155–1164, 2007.

[20] A. Maleki y F. Pourfayaz, “Optimal sizing of autonomous hybrid photovoltaic/wind/battery power system with LPSP technology by using evolutionary algorithms”, *Sol. Energy*, vol. 115, pp. 471–483, may 2015.

[21] M. B. Shadmand y R. S. Balog, “Multi-Objective Optimization and Design of Photovoltaic-Wind Hybrid System for Community Smart DC Microgrid”, *IEEE Trans. Smart Grid*, vol. 5, núm. 5, pp. 2635–2643, sep. 2014.

[22] A. Maleki, M. G. Khajeh, y M. Ameri, “Optimal sizing of a grid independent hybrid renewable energy system incorporating resource uncertainty, and load uncertainty”, *Int. J. Electr. Power Energy Syst.*, vol. 83, pp. 514–524, dic. 2016.

[23] R. Hernández Sampieri, C. Fernández Collado, y P. Baptista Lucio, *Metodología de la investigación*. McGraw Hill, 2006.

[24] M. Jimenez, C. J. Franco, y I. Dyner, “Diffusion of renewable energy technologies: The need for policy in Colombia”, *Energy*, vol. 111, pp. 818–829, sep. 2016.

[25] B. K. Sovacool, “The importance of comprehensiveness in renewable electricity and energy-efficiency policy”, *Energy Policy*, vol. 37, núm. 4, pp. 1529–1541, 2009.

[26] Solargis, “Solargis Solar Resource Database Description and Accuracy”, 2016.

[27] A. (Antonio) Luque y S. Hegedus, *Handbook of photovoltaic science and engineering*. Wiley, 2011.

[28] T. Khatib y W. Elmenreich, “A Model for Hourly Solar Radiation Data Generation from Daily Solar Radiation Data Using a Generalized Regression Artificial Neural Network”.

[29] C. Demain, M. Journée, y C. Bertrand, “Evaluation of different models to estimate the global solar radiation on inclined surfaces”, 2013.

[30] R. Moretón, E. Lorenzo, A. Pinto, J. Muñoz, y L. Narvarte, “From broadband horizontal to effective in-plane irradiation: A review of modelling and derived uncertainty for PV yield prediction”, *Renew. Sustain. Energy Rev.*, vol. 78, pp. 886–903, oct. 2017.

[31] M. Collares-Pereira y A. Rabl, “The average distribution of solar radiation-correlations between diffuse and hemispherical and between daily and hourly insolation values”, *Sol. Energy*, vol. 22, núm. 2, pp. 155–164, ene. 1979.

[32] J. K. Page, “The estimation of monthly mean values of daily short wave irradiation on vertical and inclined surfaces from sunshine records for latitudes 60 N to 40 S”, University of Sheffield, 1976.

[33] D. G. Erbs, S. A. Klein, y J. A. Duffie, “Estimation of the diffuse radiation fraction for hourly, daily and monthly-average global radiation”, *Sol. Energy*, vol. 28, núm. 4, pp. 293–302, ene. 1982.

[34] M. H. MACAGNAN, E. LORENZO, y C. JIMENEZ, “SOLAR RADIATION IN MADRID”, *Int. J. Sol. Energy*, vol. 16, núm. 1, pp. 1–14, may 1994.

[35] R. Moretón, E. Lorenzo, A. Pinto, J. Muñoz, y L. Narvarte, “From broadband horizontal to effective in-plane irradiation: A review of modelling and derived uncertainty for PV yield prediction”, *Renew. Sustain. Energy Rev.*, vol. 78, pp. 886–903, oct. 2017.

[36] M. Richter, J. Kalisch, T. Schmidt, E. Lorenz, y K. De Brabandere, “Best Practice Guide On Uncertainty in PV Modelling”.

[37] J. A. Duffie y W. A. Beckman, *Solar engineering of thermal processes*. Wiley, 2013.

[38] S. Mandelli, M. Merlo, y E. Colombo, “Novel procedure to formulate load profiles for off-grid rural areas”, *Energy Sustain. Dev.*, vol. 31, pp. 130–142, abr. 2016.

[39] “HOMER - Hybrid Renewable and Distributed Generation System Design Software”. [En línea]. Disponible en: https://www.homerenergy.com/index.html. [Consultado: 02-abr-2018].

[40] “Centro Nacional de Monitoreo -INFORME MENSUAL DE LOCALIDADES SIN - TELEMETRIA DE LAS ZNI”, 2017. [En línea]. Disponible en: http://190.216.196.84/cnm/no_telemetria.php?v1=no_telemetria/INFORME LOCALIDADES SIN TELEMETRÍA ZNI DICIEMBRE 2017.pdf. [Consultado: 02-abr-2018].

[41] M. D. A. Al-Falahi, S. D. G. Jayasinghe, y H. Enshaei, “A review on recent size optimization methodologies for standalone solar and wind hybrid renewable energy system”, *Energy Convers. Manag.*, vol. 143, pp. 252–274, 2017.

[42] H. Yang, W. Zhou, L. Lu, y Z. Fang, “Optimal sizing method for stand-alone hybrid solar–wind system with LPSP technology by using genetic algorithm”, *Sol. Energy*, vol. 82, núm. 4, pp. 354–367, abr. 2008.

[43] A. Y. Hatata, G. Osman, y M. M. Aladl, “An optimization method for sizing a solar/wind/battery hybrid power system based on the artificial immune system”, *Sustain. Energy Technol. Assessments*, vol. 27, pp. 83–93, jun. 2018.

[44] “Vented lead-acid batteries for cyclic applications”.

[45] A. Mohammed, J. Pasupuleti, T. Khatib, y W. Elmenreich, “A review of process and operational system control of hybrid photovoltaic/diesel generator systems”, *Renew. Sustain. Energy Rev.*, vol. 44, pp. 436–446, abr. 2015.

[46] A. M. Ameen, J. Pasupuleti, y T. Khatib, “Simplified performance models of photovoltaic/diesel generator/battery system considering typical control strategies”, *Energy Convers. Manag.*, vol. 99, pp. 313–325, jul. 2015.

[47] J. L. Bernal-Agustín y R. Dufo-López, “Simulation and optimization of stand-alone hybrid renewable energy systems”, *Renew. Sustain. Energy Rev.*, vol. 13, núm. 8, pp. 2111–2118, oct. 2009.

[48] A. Kashefi Kaviani, G. H. Riahy, y S. M. Kouhsari, “Optimal design of a reliable hydrogen-based stand-alone wind/PV generating system, considering component outages”, *Renew. Energy*, vol. 34, núm. 11, pp. 2380–2390, nov. 2009.

[49] A. H. Fathima y K. Palanisamy, “Optimization in microgrids with hybrid energy systems – A review”, *Renew. Sustain. Energy Rev.*, vol. 45, pp. 431–446, may 2015.

[50] A. Chauhan y R. P. Saini, “A review on Integrated Renewable Energy System based power generation for stand-alone applications: Configurations, storage options, sizing methodologies and control”, *Renew. Sustain. Energy Rev.*, vol. 38, pp. 99–120, oct. 2014.

[51] J. Hernández-Moro y J. M. Martínez-Duart, “Analytical model for solar PV and CSP electricity costs: Present LCOE values and their future evolution”, *Renew. Sustain. Energy Rev.*, vol. 20, pp. 119–132, 2013.

[52] J. Zhang, L. Huang, J. Shu, H. Wang, y J. Ding, “Energy Management of PV-diesel-battery Hybrid Power System for Island Stand-alone Micro-grid”, *Energy Procedia*, vol. 105, pp. 2201–2206, may 2017.

[53] S. Sinha y S. S. S. Chandel, “Review of recent trends in optimization techniques for solar photovoltaic–wind based hybrid energy systems”, *Renew. Sustain. Energy Rev.*, vol. 50, pp. 755–769, oct. 2015.

[54] “Costo Incremental Operativo de Racionamiento de Energía, Proyecciones de Demanda, UPME”. [En línea]. Disponible en:

http://www.siel.gov.co/Inicio/Demanda/ProyeccionesdeDemanda/tabid/97/Default.aspx. [Consultado: 24-abr-2018].

[55] M. Amer, A. Namaane, y N. K. M'Sirdi, "Optimization of Hybrid Renewable Energy Systems (HRES) Using PSO for Cost Reduction", *Energy Procedia*, vol. 42, pp. 318–327, ene. 2013.

[56] N. Bigdeli, "Optimal management of hybrid PV/fuel cell/battery power system: A comparison of optimal hybrid approaches", *Renew. Sustain. Energy Rev.*, vol. 42, pp. 377–393, 2015.

[57] S. Kessentini y D. Barchiesi, "Particle Swarm Optimization with Adaptive Inertia Weight", *Int. J. Mach. Learn. Comput.*, vol. 5, núm. 5, pp. 368–373, oct. 2015.

[58] N. Ghorbani, A. Kasaeian, A. Toopshekan, L. Bahrami, y A. Maghami, "Optimizing a Hybrid Wind-PV-Battery System Using GA-PSO and MOPSO for Reducing Cost and Increasing Reliability", *Energy*, dic. 2017.

[59] H. Borhanazad, S. Mekhilef, V. Gounder Ganapathy, M. Modiri-Delshad, y A. Mirtaheri, "Optimization of micro-grid system using MOPSO", *Renew. Energy*, vol. 71, pp. 295–306, nov. 2014.

[60] T. Tezer, R. Yaman, y G. Yaman, "Evaluation of approaches used for optimization of stand-alone hybrid renewable energy systems", *Renew. Sustain. Energy Rev.*, vol. 73, pp. 840–853, 2017.

[61] "Solargis :: pvPlanner". [En línea]. Disponible en: https://solargis.info/pvplanner/#tl=Google:hybrid&bm=satellite. [Consultado: 05-nov-2018].

[62] "CNM-IPSE". [En línea]. Disponible en: http://www.ipse.gov.co/. [Consultado: 05-nov-2018].

[63] Comisión de Regulación de Energía y Gas, "METODOLOGÍA PARA REMUNERAR LAS ACTIVIDADES DE GENERACIÓN, DISTRIBUCIÓN Y COMERCIALIZACIÓN DE ENERGÍA ELÉCTRICA EN ZONAS NO INTERCONECTADAS", Colombia, 2014.

[64] H. Yang, W. Zhou, L. Lu, y Z. Fang, "Optimal sizing method for stand-alone hybrid solar–wind system with LPSP technology by using genetic algorithm", *Sol. Energy*, vol. 82, núm. 4, pp. 354–367, abr. 2008.

[65] A. Castillo-Ramírez, D. Mejía-Giraldo, y J. D. Molina-Castro, “Fiscal incentives impact for RETs investments in Colombia”, 2017.

[66] “HOMER Pro - Microgrid Software for Designing Optimized Hybrid Microgrids”. [En línea]. Disponible en: https://www.homerenergy.com/products/pro/index.html. [Consultado: 08-nov-2018].

[67] D. Connolly, H. Lund, B. V. Mathiesen, y M. Leahy, “A review of computer tools for analysing the integration of renewable energy into various energy systems”, *Appl. Energy*, vol. 87, núm. 4, pp. 1059–1082, 2010.